DOCTORAATSPROEFSCHRIFT

2007 | Faculteit Wetenschappen

Design of Low Band Gap Polymers: An Effort to Broaden the Optical Response of the Active Layer in Plastic Solar Cells

Proefschrift voorgelegd tot het behalen van de graad van
Doctor in de Wetenschappen, richting scheikunde, te verdedigen door:

Kristof Colladet

Promotor: prof. dr. Dirk Vanderzande

D/2007/2451/7

universiteit hasselt

"Polymer chemistry is one of the most attractive branches of materials science. The macromolecular character makes various unique physical and chemical properties realizable. The realization of each specific property requires an interdisciplinary approach in a wide range of fundamental sciences." – K. Fukui

Table Of Contents

Chapter One

Band Gap Control in Conjugated Polymers

Abstract: *This chapter includes a historical background and a general introduction to the field of conjugated polymers. Further, in the framework of low band gap polymers, a comprehensive overview of "band gap engineering" is given followed by an overview of thiophene based low band gap polymers. Finally, since all the polymers in this work were developed to serve in plastic solar cells, a more detailed explanation of this application will be given at the end of this chapter.*

1.1 Organic conductive polymers: a historical background

1.1.1 Three generations of polymeric materials

Polymeric materials in the form of wood, bone, skin and fibers have been used by man since prehistoric time. Mankind gradually invented techniques to modify these materials, e.g. to make leather from hides, do dye fibers, to prepare paints and glues. Although organic chemistry as a science dates back to the 1700s, the development of polymer science has only occurred during the last 80 years. According to Rånby the polymeric materials developed since can be divided into four generations[1]. The first generation are polymeric materials introduced on the market before 1950. These are simple plastics like polystyrene,

poly(vinyl chloride) or PVC, polyacrylates and polymethacrylates, the first synthetic fibers of aliphatic polyamides or nylon and many more. The second generation, introduced in 1950-65, are polymers of better properties as construction materials, e.g. high-density polyethylene, isotactic polypropylene, polycarbonates and linear polyesters for fibers and films. They have higher mechanical strength and higher softening temperature than the first generation materials. Since 1965 a third generation of specialty polymers have been synthesized and brought on the market. They are usually of more complex chemical structure, have high mechanical strength, very high softening temperature and high chemical resistance. Some commercial examples include Kevlar®, Teflon® and Kraton®.

1.1.2 The fourth generation of polymeric materials – electrically conducting polymers

Since their discovery in 1977[2], by Alan J. Heeger, Alan G. MacDiarmid and Hideki Shirakawa, for which they were awarded the Nobel Prize in chemistry in 2000, a new generation of polymeric materials has been developed: the organic semiconductors, i.e. polymers with electric conductivity. The earliest work on semiconducting polymers was focused on doping semiconducting polymers to form conductors; this work developed much of our understanding of the mechanisms of electrical transport and methods for synthesis of semiconducting polymers. Despite that progress, the field languished because few practical applications were developed beyond electrostatic coatings[3]. Within the last fifteen years, however, a number of potentially lucrative applications, such as flat-panel displays[4] and photovoltaic devices[5,6], have emerged. These applications can take advantage of the unique features of semiconducting polymers relative to vacuum-deposited inorganic materials. For example, their ability to be coated into thin films over large areas in the ambient using simple techniques, such as screen and inkjet printing, provides practical advantages for

displays and photovoltaic cells, both of which are cost-driven applications[7-9]. Further the power of synthetic chemistry allows one to readily tune the HOMO-LUMO gap of semiconducting polymers providing a tool to tailor the optical and electrical properties of light emitting diodes and photovoltaic cells. In addition, polymeric materials have the promise of enabling mechanically flexible electronics. Thus, as with most electronic materials, the needs of industry help drive scientific development.

1.2 Conjugated polymers as semiconductors

1.2.1 Electronic structure of conjugated polymers

The distinguishing feature of all conjugated polymers is the unsaturated carbon-based alternating single and double bond structure of the polymer backbone, the so-called conjugated carbon chain. Some common conjugated polymers are listed inn Figure 1-1.

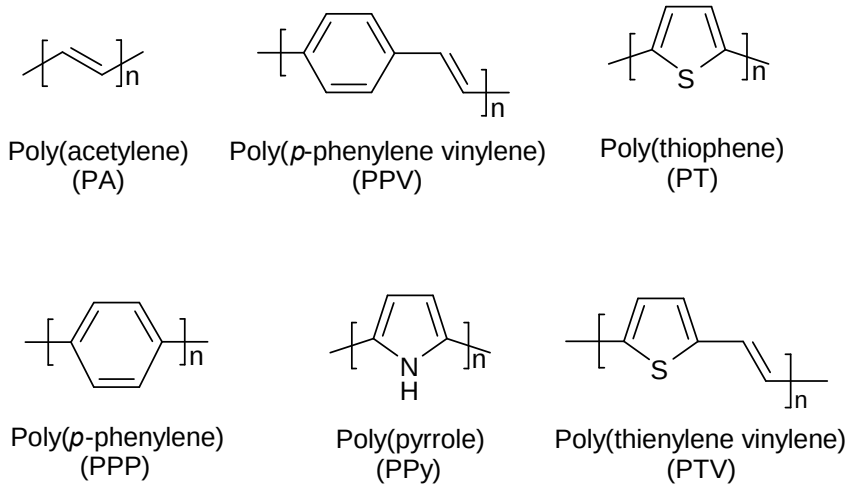

Figure 1-1: Molecular structure of a few conjugated polymers.

The conjugated polymer trans-polyacetylene (PA) will be taken as a model, as it has the simplest chemical structure of this group and because it was the starting point for research into conducting polymers. In PA each CH unit is linked by σ-bonds formed by three equivalent, triangular sp^2 hybrid orbitals, thus leaving a free fourth-orbital ($2p_z$). These remaining out-of-plane p_z orbitals on the carbon atoms overlap with neighboring p_z orbitals to give π-bonds. According to the molecular orbital theory the overlap of the p_z orbitals yields lower energy bonding (π) and higher energy anti-bonding (π*) molecular orbitals. This is exemplified in Figure 1-2 where the energy levels of PA with n ranging from 1 to infinity are shown as a function of the polymer length. Addition of every new acetylene unit causes hybridization of the energy levels yielding more and more levels until a point is reached at which there are bands rather than discrete levels[10]. The π-orbitals form the occupied valence band (VB) and the π*-orbitals generate the conduction band (CB).

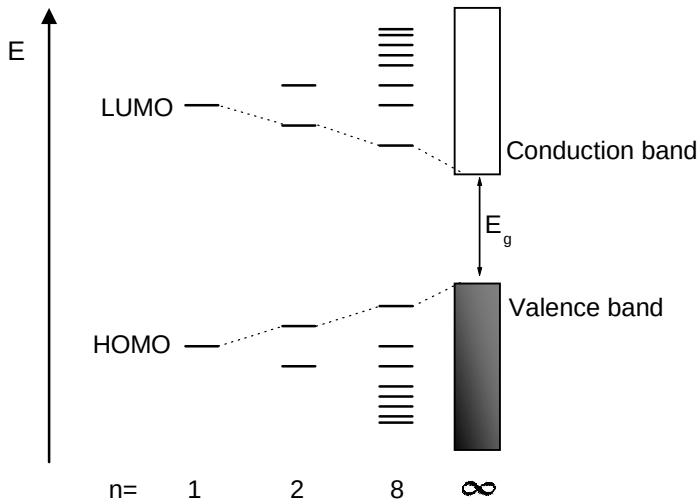

Figure 1-2: Band model for polyacetylene, where Eg is the band gap.

If the carbon-carbon bond lengths were equal PA would behave as a metal (Eg = 0 eV) since in this situation the double bonds are really delocalized along the polymer chain resulting in one π-electron per formula unit. (Figure 1-3; left) In this case no energy difference between the "bonding" valence band and the "anti-bonding" conduction band can occur due to the equivalency of both geometries. However, in real PA, the Peierls distortion[11] needs to be considered which gives rise to an energetically more favorable dimerization of the polymer backbone in longer single bonds and shorter double bonds. This "bond length alternation" makes both geometries not equivalent anymore. The result is a finite band gap (Eg) which is the energy difference between the highest occupied molecular orbital (HOMO) and the lowest unoccupied molecular orbital (LUMO).

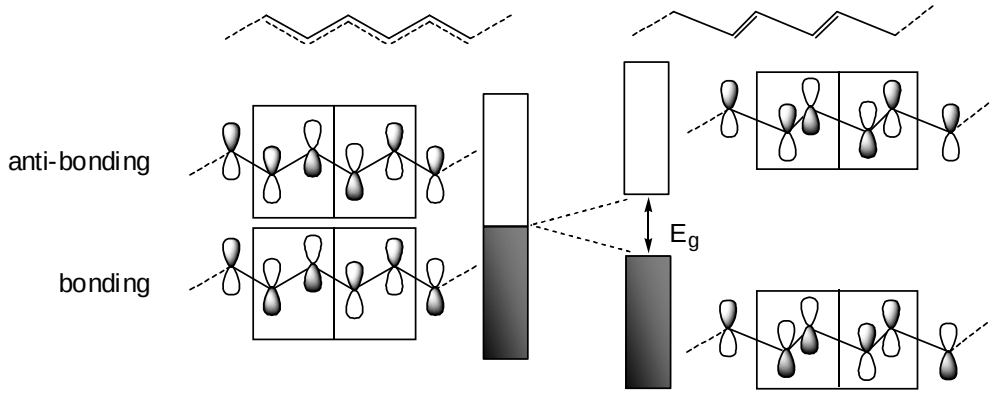

Figure 1-3: Band gap formation by localization of double bonds in PA[12].

This band gap determines whether we are dealing with an insulator (Eg > 4 eV), a semiconductor (Eg ≤ 4 eV) or a metal (Eg = 0 eV). Since the band gap of most conjugated polymers lies between 0.5 and 4 eV they belong to the class of semiconducting materials. Within this framework of the band model of conjugated polymers, a low band gap (LBG) polymer can be defined as a conjugated polymer with Eg < 2 eV. Since Eg depends upon the molecular structure of the repeat unit, synthetic chemists are provided with the opportunity and the challenge to control the energy gap through design at the molecular level as will

be shown later. Compared with the traditional inorganic semiconductors, conjugated polymers have a number of advantages. As organic polymeric materials, conjugated polymers can be processed from solution to give large area polymer films; they are also flexible and have low density which are distinct advantages compared to the brittle and heavy inorganic materials. For inorganic semiconducting materials as well as for conventional conjugated polymers, conductivity is only possible when there are partially empty valence bands or partially filled conduction bands which implies the introduction of charges onto the polymer chain. These charges can be introduced either by electron removal (oxidation or *p*-doping) or electron injection (reduction or *n*-doping). This can be realized by several methods like electrical stimulation (applying a bias), photodoping (photoinduced charge transfer) or chemical doping (addition of oxidizing or reducing agents)[13]. The majority of the known conjugated polymers today is built of electron releasing units, making them p-type semiconductors. A detailed study of the charge formation and behavior lies beyond this thesis but the interested reader can consult other sources[14-16].

1.2.2 Optical absorption properties of conjugated polymers

Optical properties are usually related to the interaction of a material with electromagnetic radiation in the frequency range from infrared (IR) to ultraviolet (UV)[17]. Since conjugated polymers are semiconductors with a band gap ranging from 0.5 eV to 4 eV most of them interact with visible light. When light with sufficient energy is absorbed by the material an electron is promoted (or excited) from the valence band into the conduction band creating an exciton (or electron-hole pair) as shown in Figure 1-4 (left).

The lowest energy (i.e. light with the highest wavelength) necessary to excite an electron has an energy equal to Eg thus exciting an electron from the HOMO into the LUMO. A decrease of Eg results in a red shift of the absorption spectrum. The exciton can eventually decay

to the ground state radiatively (i.e. photoluminescence) or non-radiatively. To determine Eg from a UV-Vis spectrum, the tangent on the low energetic side of the absorption spectrum is drawn (Figure 1-4, right). The intersection of this tangent and the abscissa gives a value for the band gap.

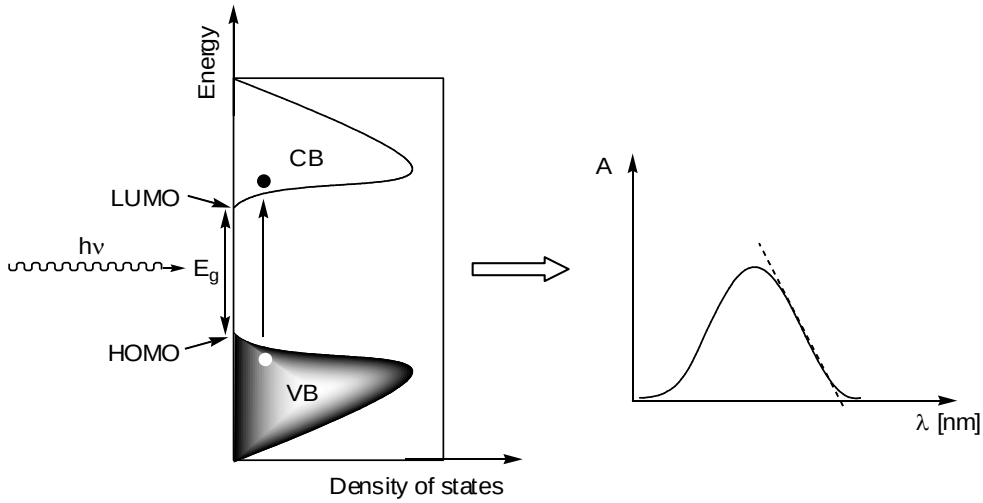

Figure 1-4: Density of states band structure (left); corresponding absorption spectrum (right).

Normally, in a UV-Vis spectrum, the absorbance is plotted as a function of the wavelength. To make the conversion from nanometer to electron-volt (eV), one can use the equation of Planck:

$$E = h\upsilon = \frac{hc}{\lambda}$$

In this equation, E is the energy (in J), h is the Planck constant ($6.626\ 10^{-34}$ Js), c is the speed of light ($3\ 10^{8}$ ms^{-1}), υ is the frequency (in s^{-1} or Hz) and λ is the wavelength (in m). Since 1 eV equals $1.602\ 10^{-19}$ J, a simple conversion equation can be derived:

$$E(eV) = \frac{1240.8}{\lambda\,(nm)}$$

It is clear now that the band gap of a conjugated polymer not only has a large influence on the electronic properties but also determines the optical properties such as absorbance (color), photoluminescence and electroluminescence (conversion of electrical energy into light). The ability to change these properties via chemical modification gives us a tool to make custom-made materials.

1.3 Band gap engineering

Since π-conjugated polymers allow virtually endless manipulation of their chemical structure, control of the band gap of these semiconductors is a research issue of ongoing interest. This so-called "band gap engineering" can give the polymer its desired electrical and optical properties. First of all, reduction of the band gap enhances the thermal population of the conduction band and thus increases the number of intrinsic charge carriers. Apart from immediate implications for electronic and optoelectronic devices, in the long term the decrease of Eg can lead to true "organic metals" showing intrinsic electrical conductivity without resorting to oxidative or reductive doping. The red shift of the absorption and emission spectra resulting from a decrease of Eg will make conjugated polymers excellent candidates for the absorption of light in plastic solar cells and potentially useful for the fabrication of LEDs operating in the near IR.

In the field of "band gap engineering" Roncali[18] did some excellent work on revealing the relationship between the structure and the band gap. According to him, the band gap of polyaromatic conjugated polymers is the sum of five contributions i.e. the energy related to the bond length alternation ($E^{\Delta r}$), the mean deviation from planarity (E^{θ}), the aromatic resonance energy (E^{res}), the inductive or mesomeric electronic effects of substituents (E^{sub}) and the intermolecular or interchain coupling in the solid state (E^{int}). The

different parameters determining the band gap of conjugated polymers are depicted in Figure 1-5.

$$Eg = E^{\Delta r} + E^{\theta} + E^{res} + E^{sub} + E^{int}$$

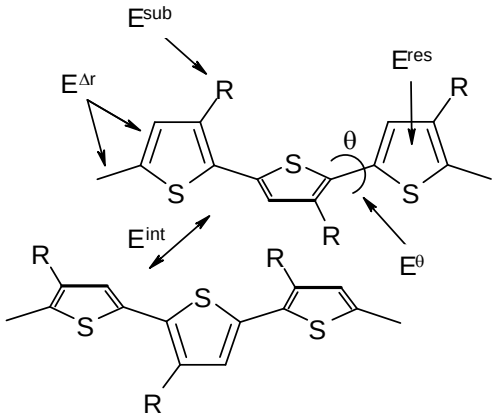

Figure 1-5: Different parameters determining the band gap of conjugated polymers.

Bond length alternation, $E^{\Delta r}$

As pointed out in Chapter 1.2.1, the degree of bond length alternation (Δr), which depends on Peierls instability, in the conjugated path represents a major contribution to the existence of a finite band gap. The larger Δr, the larger Eg. For PA Δr is related to the difference between a single and a double bond. Polyaromatic polymers differ from PA by their non-degenerate ground state i.e. the two limiting mesomeric forms, aromatic vs. quinoid, are not energetically equivalent. The "real" structure of polyaromatic polymers lies somewhere in between with more or less aromatic (quinoid) contribution. Therefore a slightly different definition of Δr was introduced by Brédas[19, 20]. He defined Δr for polyaromatics as the maximum difference between the length of a C-C bond inclined relative to the chain axis and a C-C bond parallel to the chain axis. From Figure 1-6 it is clear that aromatic poly(thiophene) (PT)

has a lower potential energy than quinoid PT. Thus, since the most stable form is normally adopted, PT preferentially occurs in a more aromatic structure.

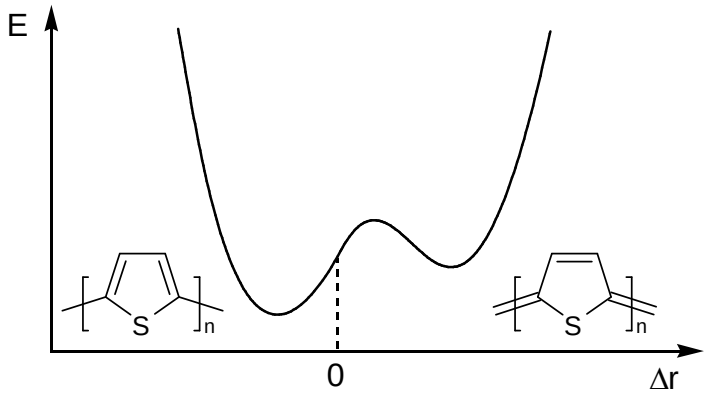

Figure 1-6: Potential energy diagram of PT.

Brédas calculated the evolution of the band gap of PT as a function of the geometry. First he considered the neutral polymer and than he altered the geometry from aromatic to quinoid. For each geometry, the degree of bond length alternation, Δr, was calculated. Starting from the aromatic geometry, the evolution of the Eg as a function of increasing quinoid contribution is depicted in Figure 1-7. His conclusion was that the band gap decreases as a function of increasing quinoid character of the backbone.

One of the reasons for the "high" band gap of PT (~2 eV) is the relatively small contribution of the energetically unfavorable quinoid structure to the ground state of the polymer resulting in a large single bond character of the thiophene-thiophene linkage and hence a large bond length alternation. Increasing the double bond character of the thiophene-thiophene linkage can be accomplished by making the quinoidal structure energetically more favorable as will be shown later.

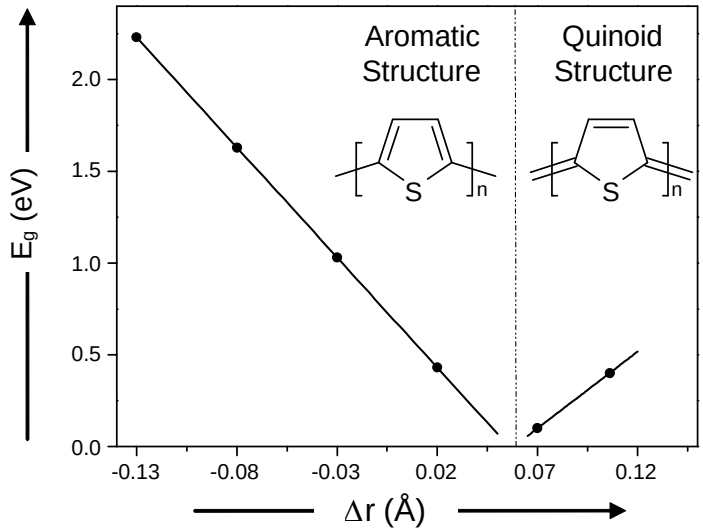

Figure 1-7: Evolution of the band gap of PT as a function of Δr. (Figure adapted from ref[20])

The mean deviation from planarity, E^{θ}

Although the band gap of conjugated polymers depends mainly on $E^{\Delta r}$, several other parameters play a crucial role. One of them is the occurrence of rotational disorder around the single bonds between the monomeric units. The orbital overlap (and hence Eg) varies approximately with the cosine of the twist angle (θ)[21], so that any departure from coplanarity will result in an increase of Eg (Figure 1-8).

Essentially, the deviation from coplanarity reduces the p_z-orbital overlap and hence reduces the double bond character i.e. conjugation between the monomeric units. As shown above, reduction of the double bond character implies an increase in bond length alternation.

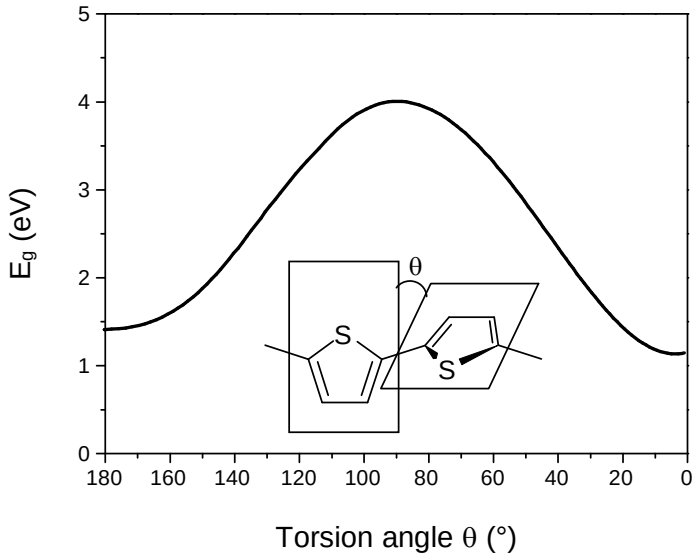

Figure 1-8: Torsion angle θ and evolution of Eg as a function of θ for PT.

Aromatic resonance energy, E^{res}

A third factor influencing the band gap is the aromatic resonance energy, E^{res}. The aromaticity of polyaromatics results in a competition between π-electron confinement within the ring and delocalization along the polymer backbone[22]. It is obvious that molecules with a large resonance energy i.e. highly aromatic will have a higher band gap since this high E^{res} prevents the delocalization. This can be noticed when comparing the resonance energy per electron (REPE) with the Eg[23]. A high REPE results in a high Eg. For REPE (benzene) = 0.065 and Eg (PPP) = 3 eV, REPE (pyrrole) = 0.039 and Eg (PPy) = 2.5 eV, REPE (thiophene) = 0.032 and Eg (PT) = 2 eV, etc. In terms of bond length alternation, it is clear that a molecule with high resonance energy has a low quinoid contribution and thus a large bond length alternation i.e. a small double bond character between the monomeric units.

Electronic effects of substitution, E^{sub}

The three parameters discussed up till now are intrinsic factors of the polymer backbone which minimize the band gap. The parameter discussed here, the electronic effects of substitution, is more a tool to fine-tune the HOMO and LUMO energy levels rather than a large minimization of Eg. The addition of an electron donating group implies a larger increase of the HOMO than of the LUMO i.e. lowering the oxidation potential of the polymer. When introducing an electron accepting group the LUMO decreases more than the HOMO and hence the reduction potential is lowered[24,25] (Figure 1-9). The change of the energy levels is proportional to the electron donating or acceptor strength of the substituents.

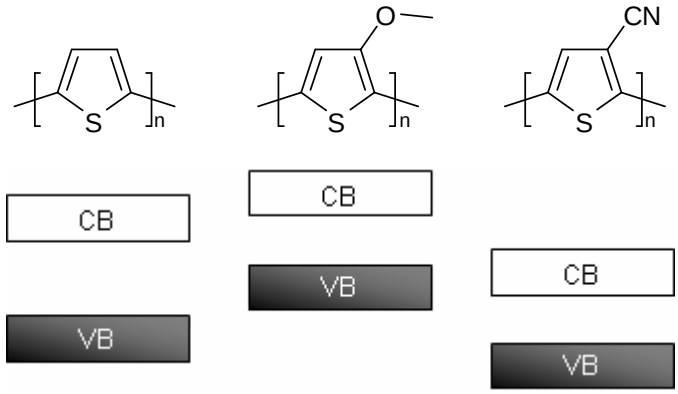

Figure 1-9: The effects of substitution on the energy levels.

Interchain coupling in the solid state (E^{int})

The above four factors determine the magnitude of the HOMO-LUMO gap of an isolated chain. However, the interactions between individual molecules which are responsible for their organization into a condensed phase can also represent an important contribution to the band gap. The ordering of molecules, which is strongly influenced by the nature and regiochemistry of the substituents, plays an important role in this context[26]. The $\pi-\pi$ interactions between the chains will force the

molecules into a more planar structure and as a consequence a decrease of Eg is seen due to a better delocalization of the electrons.

In conclusion, one can say that the increase of the double bond character between the monomeric units is of crucial importance in lowering the band gap. The introduction of substituents gives us an excellent tool to further fine-tune the energy levels. It is important to stress out that the above 5 factors are interconnected with each other. For instance the introduction of an alkyl side chain will affect E^{sub}, E^{θ} and E^{int}.

1.4 Overview of thiophene based low band gap polymers

The use of the above mentioned factors led to different approaches toward the development of low band gap (LBG) polymers. Since all polymers synthesized in this work are generally based on thiophene, this chapter will only deal about the thiophene based LBG polymers. Readers interested in other types of LBG materials can refer to some excellent reviews[12, 18, 27-29].

Basically two major approaches toward conjugated polymers can be distinguished. The first one is the direct synthesis toward the conjugated polymer via oxidative or reductive coupling. In this case the polymer consists out of a chain of aromatic molecules. The second approach, often referred to as precursor route, is an indirect way to obtain conjugated polymers. In this approach a non conjugated precursor polymer is converted into its conjugated form in such a way that the aromatic cores are connected via ethylene or ethyne linkages. Both approaches will be discussed in detail in chapters 2 and 3.

1.4.1 Poly(thiophene) and derivatives

Poly(thiophene) (**1**) and derivatives are not really considered as LBG polymers but they have triggered the research toward conjugated polymers with band gaps below 2 eV. Most of the LBG polymers are in fact based on thiophene so a short overview of this class of conjugated polymers is appropriate. In 1980 the first chemical preparation of PT was reported independently by two groups[30,31] and ever since a large number of articles concerning the synthesis and properties of PTs have been published. For the synthesis of PTs three main synthetic strategies have been employed, namely: electrochemical coupling, oxidative coupling and organometallic cross-coupling. These three routes will be discussed in detail in chapter 2.

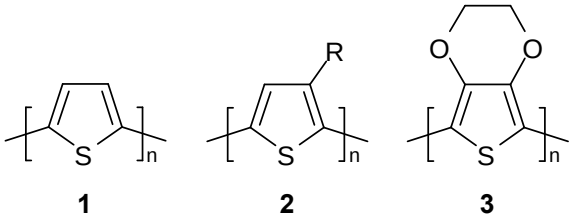

*Figure 1-10: PT (**1**), PAT (**2**) and PEDOT (**3**).*

PTs, like many other polyaromatic compounds, are insoluble in organic solvents due to their rigid backbone. This lack of solubility and processability is tackled by the introduction of flexible alkyl side chains[32, 33] at the 3- and/or 4-position creating poly(alkylthiophene)s (PATs) (**2**). Because of the introduction of substituents at the 3-position of PTs, a number of regioisomers are possible, namely head-to-tail (HT), head-to-head (HH) and random configurations[34] (Figure 1-11). Head-to-head coupling is sterically unfavorable for coplanarity and hence causes a significant loss of conjugation; however head-to-tail coupling does not limit conjugation.

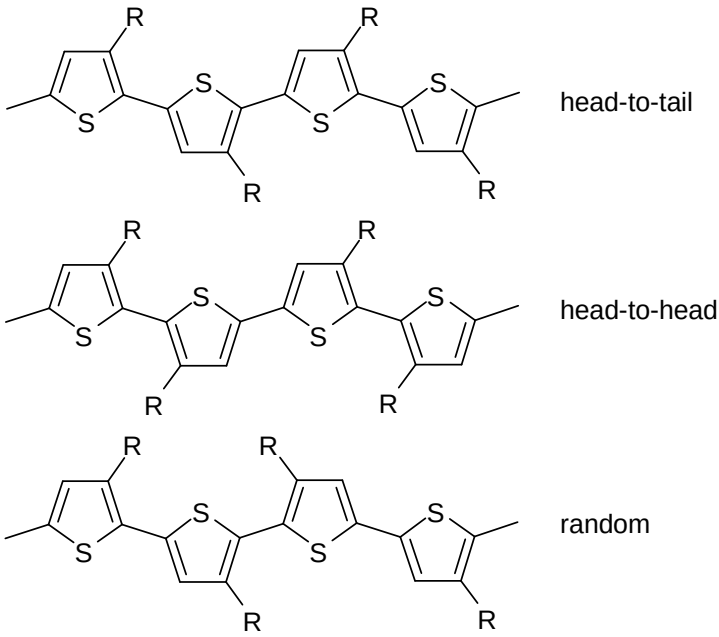

Figure 1-11: Different regioisomers in PAT.

Studies on regioregular HT-PATs, recently accessible via a number of elegant routes[35, 36], have shown that the Eg of these polymers ranges from 1.7 to 1.8 eV which is 0.3 eV lower than the Eg of PT. In this aspect, regioregular poly(3-hexylthiophene) (P3HT) (**4**), one of the most studied conjugated polymers nowadays, is a nice example on fine tuning the band gap with the introduction of a side chain. Normally one would expect that the introduction of long flexible side chains would induce rotational disorder and prevent interchain coupling in the solid state. In HT-P3HT however, the hexyl side chains induce a low energy planar conformation, leading to highly conjugated polymers[37]. Besides this, one of the most fascinating physical properties of regioregular HT-P3HT is the occurrence of supramolecular ordering[38] in the solid state as shown in Figure 1-12. The combination of both factors causes the lower band gap in HT-P3HT as compared to PT.

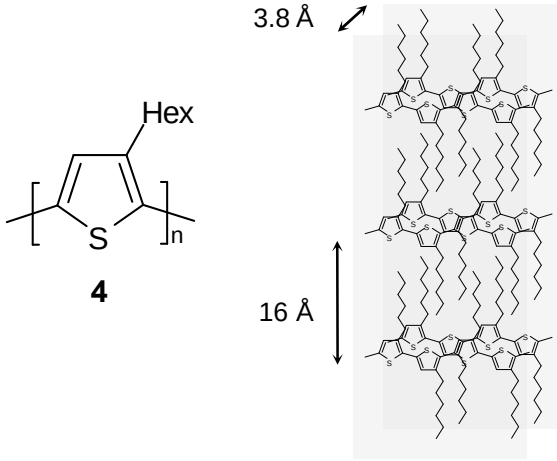

4

Figure 1-12: Self-assembled regioregular HT-P3HT superstructure.

During the second half of the 1980s, scientists at the Bayer AG research laboratories in Germany developed a new poly(thiophene) derivative[39], poly(3,4-ethylenedioxythiophene) **3** (PEDOT). It exhibits a band gap of 1.6-1.7 eV and is a nice example of how the introduction of electron rich substituents lowers the band gap[3,40]. In the field of plastic solar cells, the PEDOT:PSS[41] blend (**5**) (trade name BAYTRON® P) has to provide a selective contact between the cathode and the active layer.

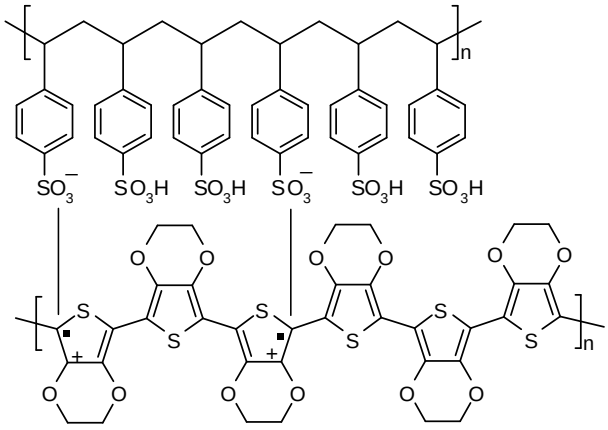

5

Figure 1-13: PEDOT:PSS blend (BAYTRON® P).

1.4.2 Poly(isothianaphtene) and derivatives

The first real LBG polymer ever reported was poly(isothianaphtene) (PITN) **6** in 1984 by Wudl[42]. PITN is an elegant example of lowering the band gap by increasing the double bond character of the thiophene-thiophene linkage. For PITN this is accomplished by making the quinoidal structure energetically more favorable. Both experimental measurements and theoretical calculations have revealed that PITN has a quinoid ground state structure[20,43,44]. The reason for this behavior is the gain in aromaticity in its fused 6-membered ring, which is larger than the loss of aromaticity in the thiophene ring upon going from the aromatic state to the quinoid state. The band gap of PITN is 1.1 eV which is roughly one full eV lower than that of PT.

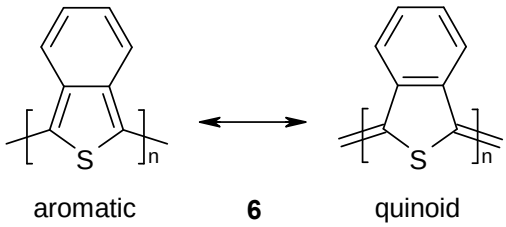

Figure 1-14: PITN in its aromatic and quinoid state.

Motivated by the desire to further reduce the band gap and at the same time increase the solubility, a wide variety of derivatives of PITN were synthesized in the years after the discovery. These include substituted PITN **7**[45,46], poly(thienopyrazine)s **8**[47,48] and fused poly(thienothiophene)s **9**[49]. This resulted indeed in soluble materials, but only of low molecular weight.

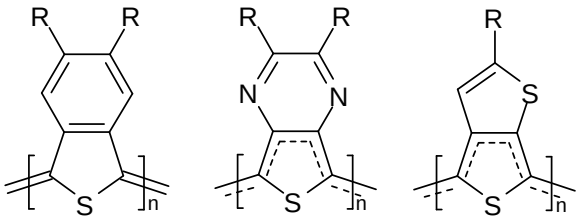

Figure 1-15: Overview of some PITN derivatives.

A somewhat different approach than that of PITN and derivatives was introduced by using terthienyls as precursors for polymerization. Poly(1,3-dithienylisothianaphtene) **10** is shown in Figure 1-16 as an example. A lot of work regarding these structures was performed in our lab[28]. In spite of showing low band gap properties one of the major disadvantages was a very difficult polymerization yielding only very low molecular weight polymers. This was explained by the rapid loss of reactivity of the radical cations involved in the polymerization.

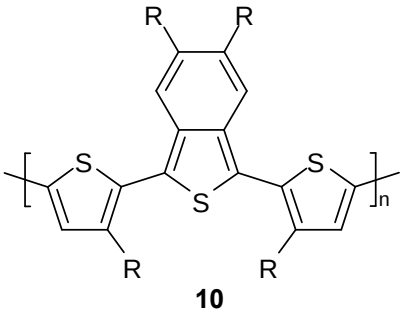

Figure 1-16: Poly(1,3-dithienylisothianaphtene) derivative.

1.4.3 Bridged poly(bithienyl)s

Another approach toward lower band gap materials concerns bridged bithienyls (Figure 1-17). In the simplest derivative (**11**) the bridge forces the molecule into a more planar conformation which enhances a better delocalization. The band gap of **11** is 1.8 eV[50]. An even further reduction of the band gap is shown when an electron-withdrawing group (**12**, **13**) is introduced at the carbon of the bridge. It

is believed that these groups introduce some anti-aromatic character. This increases the quinoid contribution and hence reduces the band gap (1.2 eV for **12**[51] and 0.9 eV for **13**[52]).

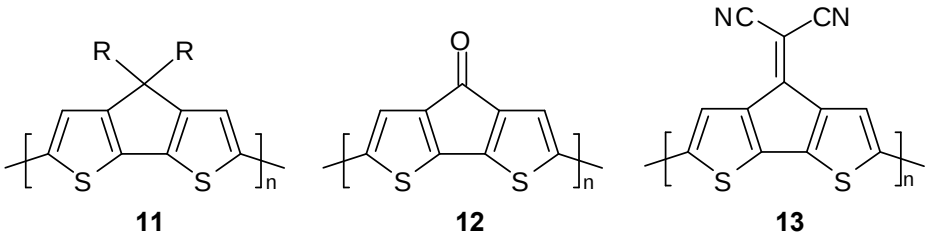

Figure 1-17: Some bridged poly(bithienyl)s.

1.4.4 Poly(dithienylethylene)s

Conjugated polymers obtained by the chemical or electropolymerization of dithienylethylene derivatives are in particular interesting since these polymers are excellent models for the corresponding poly(thienylene vinylene)s (see next section). Reported band gaps for these polymers were 1.8 eV for **14**[53], 1.7 eV for **15**[54] and even as low as 1.4 eV for polymer **16**[55]. These low band gaps are related to the presence of ethylene linkages of defined *trans*-configuration. They limit the statistical rotational disorder associated with the interring bonds and decrease the overall aromatic character of the π-conjugated backbone. The latter contributes to a lowering of the π-electron confinement in the aromatic thiophene rings[56].

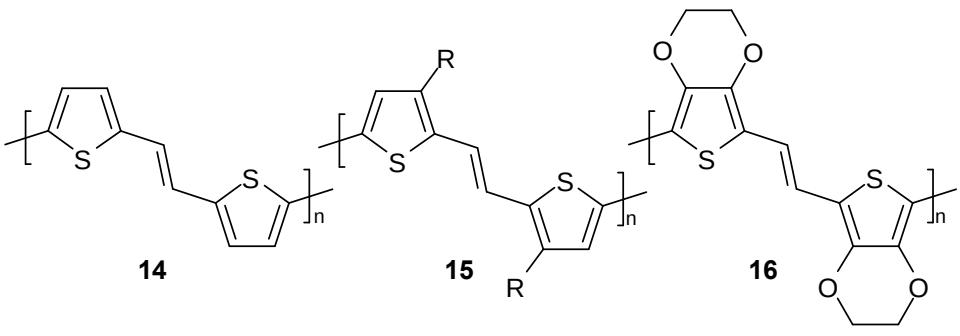

Figure 1-18: Overview of some poly(dithienylethylene) derivatives.

1.4.5 Poly(thienylene vinylene)s

In order to circumvent the problem of insolubility of most (unsubstituted) conjugated polymers, several precursor routes have been introduced over the past decades[57-59]. Two of these precursor routes were developed in our group, namely the sulphinyl[60] and the dithiocarbamate[61] precursor route. These precursor routes involve the formation of an intermediate non-conjugated, soluble and thus processable, precursor polymer which can be converted into the fully conjugated polymer after processing. The discovery of electroluminescence in poly(*p*-phenylene vinylene)s[62] triggered the development of these routes, which were later adapted to deal with the synthesis of poly(thienylene vinylene)s (PTV). As mentioned earlier for poly(dithienylethylene)s, PTVs have lower band gaps as compared to PTs because of two effects: a decrease in the overall aromatic character, allowing better π-electron delocalization due to less electron confinement and a limitation of the rotational disorder due to the presence of ethylene linkages of defined configuration. For PTV (**17**) a band gap of 1.7 eV[63] is reported and various structural modifications of PTV led to materials with band gaps as low as 1.2 eV for **19**[64]. A more detailed overview on the synthesis of PTV is given in chapter 3.

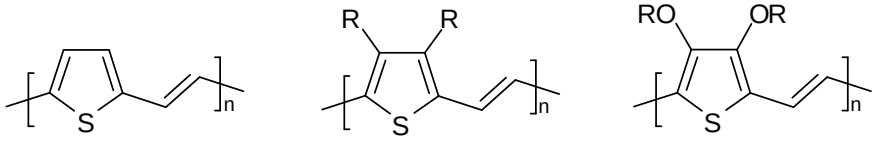

17 **18** **19**

Figure 1-19: Three examples of PTVs

1.4.6 Donor-acceptor systems

A last class of LBG materials discussed in this chapter are LBG polymers with donor-acceptor alternation along the polymer chain. It was shown with PITN **6** that reduction of the bond length alternation by

increasing the double-bond character between the repeating units of a conjugated polymer, results in a decreased band gap[20]. The driving force for such a process in PITN is the gain in aromaticity of the fused benzene ring. The interaction between a strong electron-donor (D) and a strong electron-acceptor (A) may also give rise to an increased double-bond character between these units, since they can accommodate the charges that are associated with such a mesomerism (D-A ⇔ $D^+=A^-$). Hence, a conjugated polymer with an alternating sequence of the appropriate donor- and acceptor-units in the main-chain may show a decreased band gap.

The donor-acceptor (D-A) repeating unit strategy was first introduced by Havinga and coworkers in 1992[65]. They described the synthesis of poly(squaraine)s (**20**) and poly(croconaine)s (**21**) made out of various donor molecules with strong electron accepting molecules like squaric acid (**22**) or croconic acid (**23**) as shown in Figure 1-20. The resulting polymers have band gaps down to 0.5 eV.

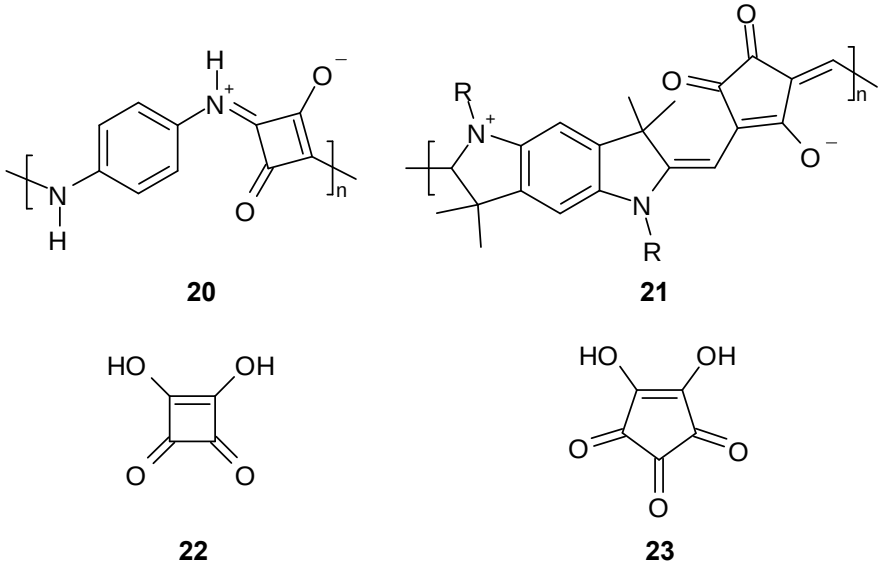

20 **21**

22 **23**

*Figure 1-20: Poly(squaraine) (**20**) and poly(croconaine) (**21**).*

In the following part, the two most important classes of low band gap donor-acceptor conjugated polymers based on thiophene will be discussed. As electron-donating moiety, thiophene often represents the best choice since it is an electron rich subunit that allows numerous chemical transformations.

Acceptor-units based on cyano- or nitro-substituents

The most obvious choice for the design of an electron-withdrawing subunit would be an aryl unit substituted with a cyano- or nitro-group, since the latter two are among the most widespread electron withdrawing groups in organic chemistry. Various literature reports exist in which low band gap polymers containing cyanovinylene spacers as the acceptor units and thiophene derivatives as the donor are made *via* electrochemical polymerization. Band gaps ranging from 1.1 eV (**27**) to 1.6 eV (**24**) were reported[66-71]. The monomers could be prepared by applying a *Knoevenagel* condensation between the corresponding acetonitrile function and an appropriate carboxaldehyde.

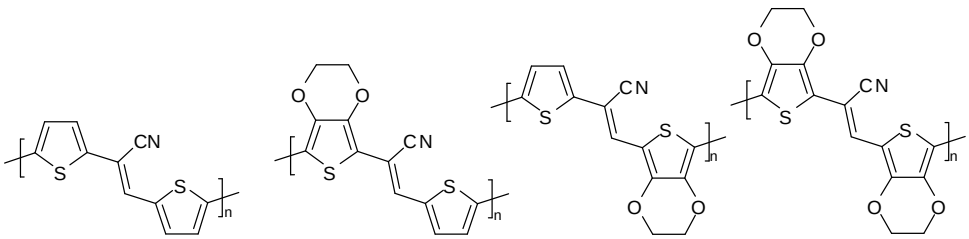

24 **25** **26** **27**

Figure 1-21: Some examples of D-A polymers containing cyanovinylene spacers.

Examples of conjugated polymers containing nitro-groups are shown in Figure 1-22. The band gaps for polymers **28** and **29** are 1.1 eV[72] and 1.5 eV[73] respectively.

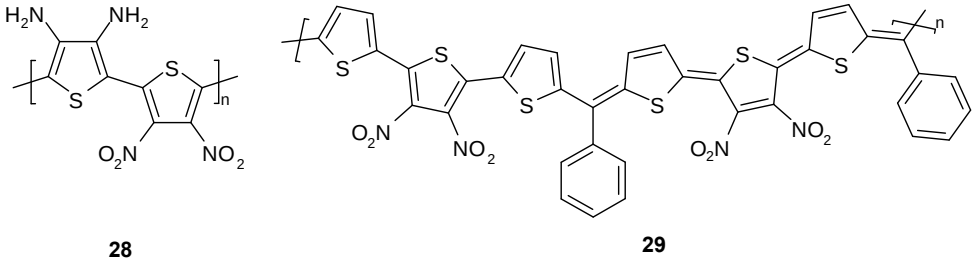

28 **29**

Figure 1-22: D-A conjugated polymers containing nitro-substituents.

Acceptor-units based on electron-deficient heterocycles

Another class of acceptor-units is based on an aryl unit bearing one or more electronegative atoms in the ring. Pyrazine and thiadiazole, fused onto phenyl (Figure 1-23) or thiophene (Figure 1-24) rings, contain two imine nitrogens which make them efficient electron withdrawing units. Electrochemically polymerized **30** and **31** show band gaps of 1.4 eV and 1.2 eV respectively[74, 75].

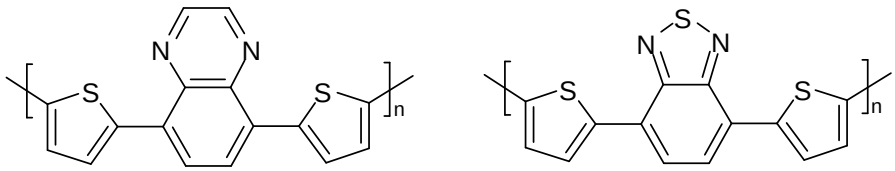

30 **31**

*Figure 1-23: Pyrazine (**30**) and thiadiazole (**31**) fused on a phenyl ring.*

The polymers (**32** and **33**) in which the electron acceptor moieties are attached to thiophene are also known to have lower band gaps[76]. Polymer **32** has a band gap of 1.1 eV, polymer **33** 0.9 eV, which made it the first donor-acceptor type polymer below 1 eV.

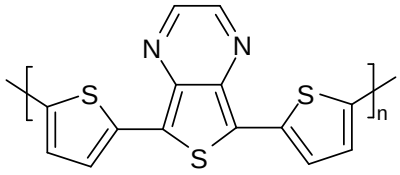

32

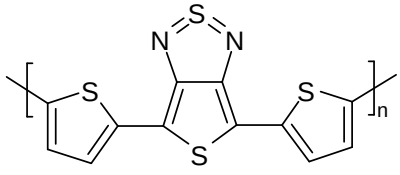

33

*Figure 1-24: Pyrazine (**32**) and thiadiazole (**33**) fused on a thiophene ring.*

In an attempt to further fine-tune the optical and electrochemical properties a lot of pyrazine- and thiadiazoloderivatives were synthesized. In Figure 1-25 a few examples are gathered. However, due to rotational disorder and sterical hindrance the band gaps of **34**[77] (1.6 eV), **36**[78] (1.7 eV) and **37**[79] (1.9 eV) were somewhat disappointing. **35** however showed a band gap of 1.3 eV[80]. Examples of thieno[3,4-*b*]pyrazine based polymers with a substituted thiophene unit as donor are polymers **38** and **39**, **38** is electrochemically synthesized and has a very low band gap of 0.36 eV[81]. The soluble **39** has a band gap of 1.56 eV[82]. Although this type of polymers are promising toward minimization of the band gap, their low solubility, difficult synthesis (low overall yield) and low molecular weight are still problems to be tackled and hinder further development toward device fabrication.

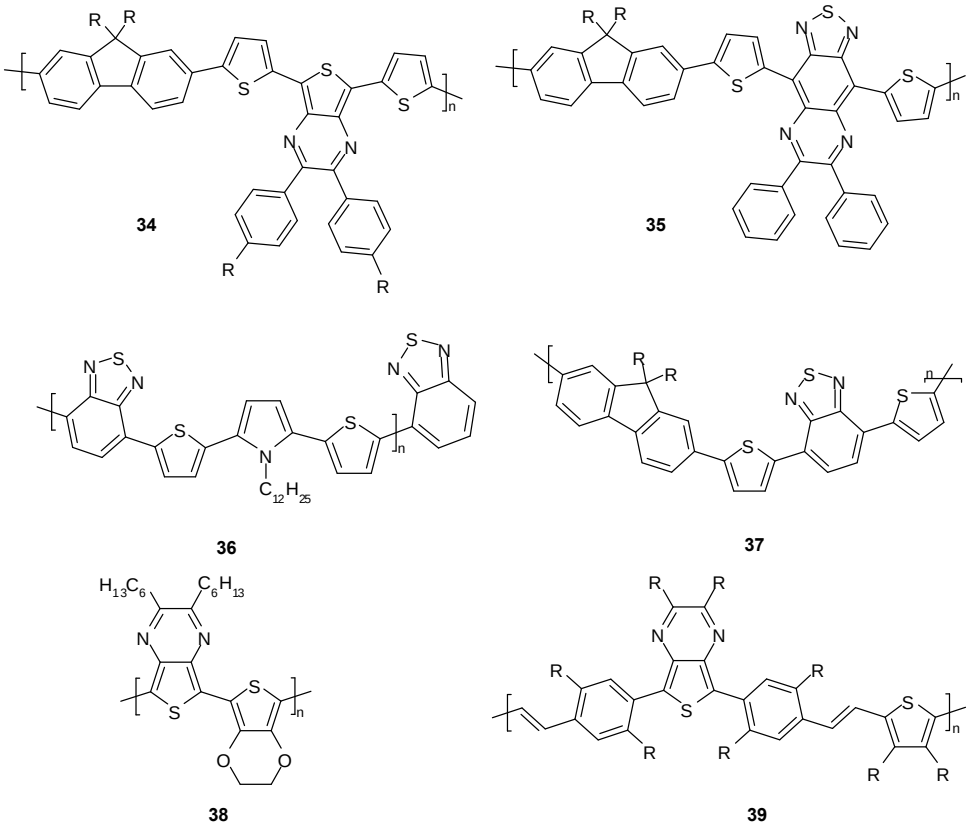

Figure 1-25: Some pyrazine- and thiadiazoloderivatives.

1.5 Plastic solar cells

1.5.1 Applications of conjugated polymers

Semiconducting polymers have now been used as active layers in most types of thin film electronic devices e.g. thin-film transistors (TFTs)[83-86], light emitting diodes (LEDs)[4,62,83,87], biosensors[88-90], smart windows[24,91], lasers[92,93] and photovoltaics (PVs)[5,6,9,94-99]. Many fundamental challenges remain to be studied before the widespread adoption of semiconducting organic materials in these applications is to be expected[8]. Although these devices operate quite differently, increases in their respective figures of merit have depended critically on the

synthesis of new materials and the improvement of processing methods using these materials.

Thin-film transistors (TFT) using semiconducting polymers are most likely to be used in low-performance applications such as displays[100] and potentially for low-performance radio-frequency identification tags[101]. These applications are considered "low performance" due to the low field-effect mobility of transistors in these devices relative to that of single crystalline silicon. The mobility defines the electrical resistance of a TFT and thereby the speed at which it can operate in a circuit. The mobility of semiconducting polymers is controlled both by molecular structure and by their microstructure in a thin film. It has been shown that semiconducting polymers can have a field-effect mobility that approaches that of amorphous silicon, which is used in most liquid crystal flat panel displays[102].

Polymer light emitting diodes are reserved for applications both in light-emitting displays[4] and in solid-state lighting[103,104]. Two of the most challenging performance requirements for these applications are coverage of the color spectrum and stable electrical performance. A reasonable value for the lifetime of a display is ~10,000 hours of use over five years; this target has nearly been achieved in prototype displays[105]. The synthesis and development of new, in particular blue, light-emitting polymers in parallel with the development of optimized device structures will help to address the requirements in performance for both of these applications.

Semiconducting polymers could perhaps have the greatest impact upon society through the development of polymer photovoltaic cells for power generation. The demand of energy has increased worldwide, mainly due to the development in areas like Asia and Africa[106]. Currently this demand in energy is satisfied mainly by fossil fuels and nuclear power. However, these energy sources are limited and their use has a serious environmental impact. Therefore research toward renewable energy sources has increased in last decades. Among others, photovoltaics offer great technological potential as a renewable,

alternative source for electrical energy. Since all polymers in this work were developed to serve in plastic solar cells, a more detailed explanation of this application will be given in this chapter.

In 1954, Chapin, Fuller, and Pearson developed the first photovoltaic cell based on a silicon p-n junction with an efficiency of 6 %[107]. Since then, solar cells have been made from many other semiconductors, using various device configurations and employing single-crystal, poly-crystalline, and amorphous thin-film structures[108]. Over the years the efficiency has reached 24 % for crystalline Si solar cells in the laboratory[109]. Today Si-based solar cells are by far the most dominating type of PVs used and account for 99 % of all PVs[110]. However, to improve processability, lower manufacturing costs, and create flexibility, solar cells based on conjugated polymeric materials are extensively investigated during the last years. Before discussing the development of plastic PVs, the basic principles of the photovoltaic effect are outlined.

1.5.2 The photovoltaic principle in plastic solar cells

Almost all plastic solar cells have a planar-layered structure, where the organic light-absorbing layer is sandwiched between two different electrodes. One of the electrodes must be transparent, often indium-tin-oxide (ITO). The other electrode is very often aluminum. In general, in a plastic photovoltaic cell three processes occur in the conversion of solar energy into electrical energy[99].

- Absorption of light
- Charge transfer and separation of the opposite charges
- Charge transport and collection at the electrodes

When light is absorbed an electron is promoted from the highest occupied molecular orbital (HOMO) to the lowest unoccupied molecular orbital (LUMO) forming an exciton (1) (Figure 1-26). In a PV device this

process must be followed by the dissociation of the exciton upon which the charges are created (2).

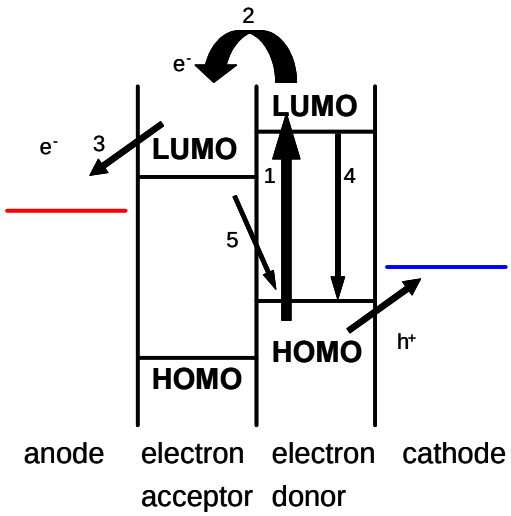

Figure 1-26: Schematic drawing of the working principle of a plastic solar cell.

This is one of the key steps in the conversion of solar light into electrical energy in photovoltaic devices. In most plastic solar cells, charges are created by photoinduced electron transfer. In this process an electron is transferred from an electron donor, a p-type semiconductor, to an electron acceptor, an n-type semiconductor. For efficient charge generation, it is important that the charge-separated state is the thermodynamically and kinetically most favorite pathway after photo-excitation. It only occurs when it is energetically favorable for the electron in the excited state of the donor to be transferred to the much more electronegative acceptor. Therefore, it is important that the energy of the absorbed photon is used for generation of the charge-separated state and is not lost via competitive processes (4) like fluorescence, non-radiative decay, internal conversion or intersystem crossing. In addition, it is of importance that the charge-separated state is stabilized, so that the photogenerated charges can migrate to one of the electrodes (3). Therefore, the back electron transfer (5) should be slowed down as much as possible. The electron must than reach the

anode (Al) while the hole must reach the cathode (ITO). In order to achieve charge separation, an electrical field is needed, which is provided by the asymmetrical workfunctions of the electrodes. This asymmetry is the reason why the electron-flow is more favored from the low-workfunction electrode to the high-workfunction electrode. The light harvesting process along with the positioning of energy levels is depicted in Figure 1-26.

Much terminology surrounds photovoltaic devices. Below are some of the important terms defined and discussed in light of plastic solar cells. This section by no means gives a full description of all details; the interested reader can find a very comprehensive work in ref[99]. It is more intended to give the (chemical) reader a basic understanding of (the physics of) plastic photovoltaic devices. A graph of current (I) *versus* voltage (V) is a common way to illustrate the properties of solar cells. In the dark, the I-V curve passes through the origin – with no potential, no current flows. But when the device is exposed to light, the I-V curve shifts downward, as illustrated in Figure 1-27. The following terms are often used to characterize solar cells; some items are also shown in Figure 1-27.

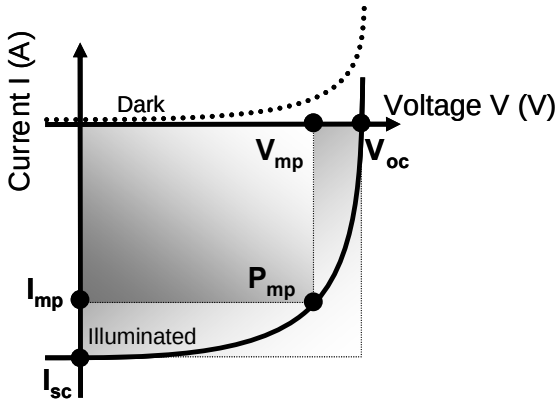

Figure 1-27: Typical I-V curve for a solar cell in the dark (dotted line) and under illumination (solid line). Some important photovoltaic parameters are indicated.

Air Mass (AM) – A measure of how much atmosphere sunlight must travel through to reach the earth's surface. This is denoted as "AM(x)", where x is the inverse of the cosine of the zenith angle of the sun. A typical value for solar cell measurements is AM 1.5, which means that the sun is at an angle of about 48°. Air mass describes the spectrum of radiation, but not its intensity. For solar cell purposes, the intensity is commonly fixed at 100 W/cm^2.

Open-Circuit Voltage (V_{oc}) – The maximum possible voltage across a photovoltaic cell; the voltage across the cell in sunlight when no current is flowing.

Short-Circuit Current (I_{sc}) – This is the current that flows through an illuminated solar cell when there is no external resistance (i.e., when the electrodes are simply connected or short-circuited). The short-circuit current is the maximum current that a device is able to produce. Under an external load, the current will always be less than I_{sc}.

Maximum Power Point (P_{mp}) – The point (I_{mp}, V_{mp}) on the I–V curve where the maximum power is produced. Power (P) is the product of current and voltage ($P = I \cdot V$) and is illustrated in the figure as the area of the rectangle formed between a point on the I–V curve and the axes. The maximum power point is the point on the I–V curve where the area of the resulting rectangle is largest.

Fill Factor (FF) – The ratio of a photovoltaic cell's actual maximum power output to its theoretical power output if both current and voltage were at their maxima, I_{sc} and V_{oc}, respectively. This is a key quantity used to measure cell

performance. It is a measure of the "squareness" of the I–V curve. The formula for FF in terms of the above quantities is:

$$FF = \frac{I_{mp} \cdot V_{mp}}{I_{sc} \cdot V_{oc}}$$

Power Conversion Efficiency (PCE or η_e) – The ratio of power output to power input. In other words, PCE measures the amount of power produced by a solar cell relative to the power available in the incident solar radiation (P_{in}). P_{in} is the sum over all wavelengths and is generally fixed at 100 W/cm^2 when solar simulators are used. This is the most general way to define the efficiency. The formula for PCE, in terms of quantities defined above, is:

$$\eta_e = \frac{I_{mp} \cdot V_{mp}}{P_{in}} = \frac{I_{sc} \cdot V_{oc} \cdot FF}{P_{in}}$$

In the remainder of this section a short historical overview is given of the most successful approaches toward plastic solar cells to date. (Note: unless otherwise stated all efficiencies are PCE given under AM 1.5 conditions.)

Single layer devices

The first generation of organic photovoltaic cells was based on single organic layers sandwiched between two metal electrodes of different work functions[111, 112]. The difference in work function provides an electric field that drives separated charge carriers toward the respective contacts. This electric field is seldom sufficient to break up the photogenerated exciton. Instead the exciton diffuses within the organic layer until it reaches a contact, where it may be broken up to supply separate charges, or recombine. Since exciton diffusion lengths are short, typically 1-10 nm for organic materials[113], only those excitons

generated in a small region within <10 nm from the contacts contribute to the photocurrent. The exciton diffusion limits the charge carrier generation in such a device. Single layer solar cells of this type made with PPV delivered power conversion efficiencies of less than 0.1 % under white light illumination[114].

Bilayer heterojunction devices

The next breakthrough was achieved in 1986 by introducing the bilayer heterojunction concept[115]. In the first device a copper phthalocyanine and a tetracarboxylic derivative were placed between the electrodes and yielded a power conversion efficiency of 0.95 %. Following this discovery, conjugated polymers were also investigated in such devices and in 1993, Sariciftci *et al.*, triggered by their discovery of the ultra fast photoinduced charge transfer from conjugated polymers onto fullerenes[116], first applied this two-layer technique to a conjugated polymer solar cell by evaporating C_{60} on top of a spin-cast poly(2-methoxy-5-(-2'-ethyl-hexyloxy)-1,4-phenylene vinylene) (MEH-PPV)[117]. In this cell, the MEH-PPV was used to absorb visible light and transport holes to the ITO electrode following exciton dissociation at the interface. The C_{60}, with an electron affinity about 0.7 eV larger than the conjugated polymer was used to accept electrons and transport them to the aluminum electrode. The first devices based on these materials yielded efficiencies of 0.1 %[113]. However after optimization, efficiencies of 1.9 % were reached[118].

Bulk heterojunctions devices

From the previous devices it was clear that the exciton dissociation is most effective at the interface of the p- and n-type material in heterojunction cells, thus the exciton should be formed within its diffusion length of the interface. Since typical diffusion lengths are in the range of 10 nm[113], this limits the effective light-harvesting

layer. However, for most organic semiconductors the film thickness should be more than 100 nm in order to absorb enough of the light. The paradox is that thicker film layers increase light absorption but only a small fraction of the excitons will reach the interface and dissociate. A revolutionary development in plastic photovoltaics came in the mid-1990s with the introduction of a dispersed heterojunction, where an electron accepting and an electron donating material are blended together and in this way a large increase of the interface region was obtained. Yu first reported on solar cells made out of a mixture of MEH-PPV and C_{60} with a reported monochromatic conversion efficiency of 2.9 %[119]. By changing the acceptor material into [6,6]-phenyl C_{61} butyric acid methyl ester (PCBM), optimization of the device fabrication and changing the donor into another PPV derivative, namely poly-[2-(3,7-dimethyloctyloxy)-5-methyloxy]-*p*-phenylene vinylene (MDMO-PPV) power efficiencies of 3 % under AM1.5 illumination were reached[120].

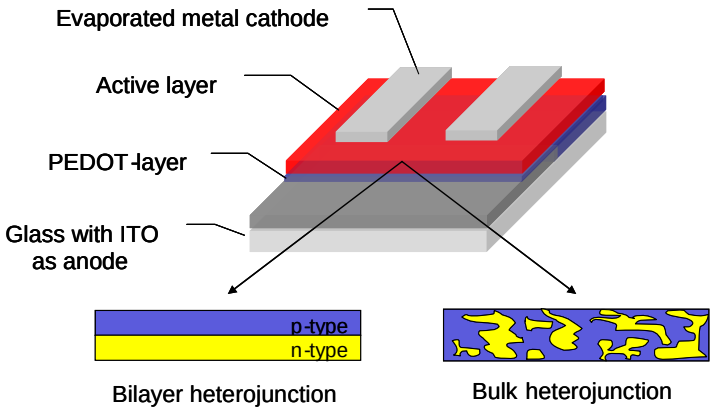

Figure 1-28: Diagram of the layered structure of a plastic solar cell. The difference between a bilayer heterojunction and a bulk heterojunction is depicted as well.

At the same time the first reports of polymer/polymer bulk heterojunction PV were published with poly(2,5,2',5'-tetrahexyloxy-7,8'-dicyanodi-*p*-phenylenevinylene) (CN-PPV) as acceptor and MEH-PPV as the donor polymer[121,122]. Afterwards several other polymer:polymer

combinations were examined, but performances remained rather low, mainly because of the lack of suitable acceptor polymers[123-126]. This points out that research toward suitable acceptor polymers is still necessary in order to once make a real all-polymer solar cell.

It is clear that control of the morphology in dispersed heterojunction devices is a critical point[127,128]. The degree of phase separation and domain size depend on solvent choice, speed of evaporation, solubility, miscibility of the donor and acceptor, etc. The most promising results in optimizing the morphology, again in combination with fullerene derivatives have been obtained with P3HT (Eg = 1.8 eV). Apart from having a lower band gap than MDMO-PPV (Eg = 2.2 eV), this material has the ability to form well-structured layers inducing ordering and hence a better morphology of the active layer after an additional annealing step[129]. Efficiencies of 5 % for such P3HT:PCBM-bulk heterojunction solar cells were recently reached[130].

1.5.3 Band gap tuning of polymers for solar cells

Another critical issue is the rather narrow absorption of the active layer in the bulk heterojunction. Since most of the available conjugated polymers were originally developed for visible-LEDs, they exhibit band gaps > 2 eV. Hence, there is a clear mismatch between the absorption spectrum of these materials and the terrestrial solar spectrum, which extends into the near infrared (Figure 1-29). As already shown for P3HT, new low band gap materials with absorption extending to the 700-900 nm (Eg = 1.7 – 1.3 eV) region are needed for efficient photon harvesting.

In 2001 the first report of a low band gap polymer used in a photovoltaic device was published by Shaheen *et al.*[131]. He incorporated poly(1,3-dithienylisothianaphtene) derivatives (**10**), synthesized by Vangeneugden[28], into a bulk heterojunction solar cell. A PCE of 0.4 % was reached. This report triggered other groups to focus on low band

gap polymers for solar cells[78-80, 132-139], and currently, Konarka holds the record with a low band gap solar cell of 3.2 %[140].

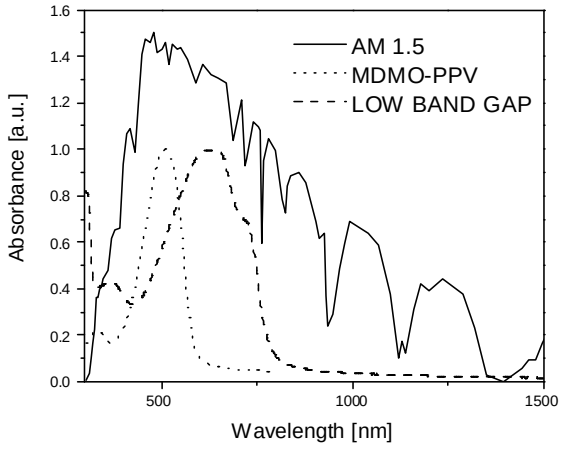

Figure 1-29: Standard AM1.5 terrestrial solar spectrum (solid) compared to the absorption spectrum of MDMO-PPV (dot) and a low band gap polymer (dash).

However one must be careful in just lowering the band gap. A good low band gap polymer has two challenges to overcome. One is the unavoidable reduction of the open-circuit voltage (V_{oc}) compared with high band gap polymers, because the V_{oc} is related to the energy difference between the lowest unoccupied molecular orbital (LUMO) of the electron acceptor and the highest occupied molecular orbital (HOMO) of the electron donor. The other challenge is to have a large enough driving force for electron transfer from the polymer to the electron acceptor. This means that the LUMO of the electron donor must be closer in energy to vacuum than the LUMO of the electron acceptor in order to have enough driving force for exciton dissociation at the interface of the electron donor and acceptor. When decreasing the band gap of a polymer, both the LUMO level and the HOMO level are affected. The LUMO position of the polymers might be shifted away from the vacuum level so much that the use of new electron acceptors with lower LUMO levels than the commonly used PCBM are needed for preparing an

efficient solar cell. In a recent publication, Scharber[141] describes some design rules for electron donor materials. Based on his model the ideal material parameters for a conjugated polymer-PCBM device were determined. He claims that the efficiency of a solar cell can be predicted solely as a function of the band gap and the LUMO level of the donor. So besides a reduction of the band gap, new donor materials must be designed to optimize the LUMO as this parameter dominantly drives the solar cell efficiency.

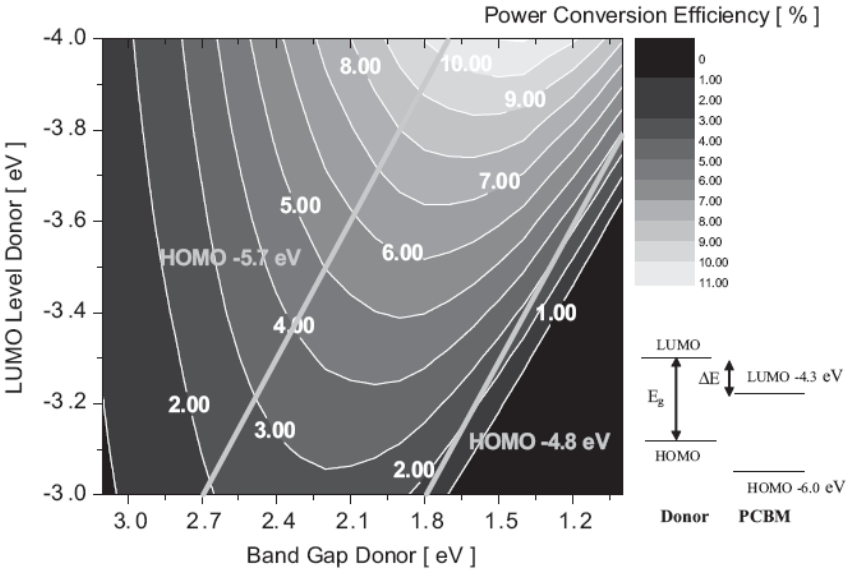

Figure 1-30: Contour plot showing the calculated energy-conversion efficiency (contour lines and colors) versus the band gap and the LUMO level of the donor polymer according to the model described by ref[141]. Straight lines starting at 2.7 eV and 1.8 eV indicate HOMO levels of –5.7 eV and –4.8 eV, respectively. A schematic energy diagram of a donor PCBM system with the band gap energy (Eg) and the energy difference (ΔE) is also shown. (Figure adapted from ref[141]).

Figure 1-30 shows a contour plot where the x- and y-axes are the band gap and the LUMO level of the donor, respectively, and the contour lines indicate constant power-conversion efficiencies. The straight lines in Figure 1-30 define lines of constant donor HOMO levels

of –5.7 and –4.8 eV. In this aspect, it is clear that a very important task lies in the hands of synthetic chemists. Through a better understanding of band gap engineering, the HOMO and LUMO levels of the materials can be tailored and the mythical 10 % efficiency border can be reached.

1.6 Aim and outline

The aim of the research described in this dissertation is to discover well defined and reliable synthetic pathways toward new low band gap materials. The reason for the need of these low band gap polymers is their application in plastic solar cells in which these materials are responsible for the capturing of light. Basically two major approaches toward conjugated polymers can be distinguished. The first one is the direct synthesis toward the conjugated polymer via oxidative or reductive coupling. The second approach, often referred to as precursor route, is an indirect way to obtain conjugated polymers. In this approach a non conjugated precursor polymer is converted into its conjugated form.

In **chapter 2**, a family of 6 polymers based on *bis*-(1-cyano-2-thienyl vinylene)phenylene is synthesized *via* the first approach. The structure consists of a central dialkoxyphenylene core (donor) *p*-disubstituted by two thiophene derivatives (donor) through a cyanovinylene linker (acceptor). The polymers are prepared by chemical oxidation of the monomers using $FeCl_3$. By changing the thiophene moiety we are able to tune the polymers electronic and solubility properties. Moreover, our approach to keep the central core constant leads to a toolbox to create a whole range of monomers, and thus polymers, with different heteroaromatic rings linked to the central core. Further, a more polar polymer with a dioligo(oxyethylene)phenylene central core is discussed as well as a polymer bearing a push-pull molecule. All polymers are tested in solar cells.

A second way to come to processable polymers is the precursor approach, described in **chapter 3**. This involves the formation of an intermediate non-conjugated, soluble and thus processable, precursor polymer which can be converted into the fully conjugated polymer after processing. The use of such a precursor approach implies the formation of a double bond between the aromatic parts. Based on earlier successful results, of all known precursor routes, the dithiocarbamate route has been picked as the method of choice. In the first part of this chapter, two particular dithiocarbamate precursor polymers and the corresponding conjugated polymers, poly(3,4-diphenyl-2,5-thienylene vinylene) and poly(3,4-bis(4-butylphenyl)-2,5-thienylene vinylene), are successfully synthesized. These polymers are also tested in solar cells. In the second part, the thiophene unit is replaced by a thiazolo[5,4-*d*]thiazole unit. It is reported that this replacement is effective to reduce the sterical interactions due to the absence of hydrogen atoms.

For future reference, a comprehensive experimental procedure of the purification of $FeCl_3$ is given in the **appendix** and the dissertation is completed with two **summaries**: one in English, followed by one in Dutch, a list of **publications** and the **acknowledgements**.

1.7 References

1. Rånby B., in: W. R. Salaneck, I. Lundstrom and B. Rånby (Eds.), "Conjugated Polymers and Related Materials: The Interconnection of Chemical and Electronic Structure" Oxford University Press, Oxford, **1993,** 15-26.
2. Shirakawa H., Louis E. J., Macdiarmid A. G.*, et al.*, "Synthesis of Electrically Conducting Organic Polymers - Halogen Derivatives of Polyacetylene, (Ch)X" *J. Chem. Soc.-Chem. Commun.* (16), **1977**, 578.
3. Groenendaal B. L., Jonas F., Freitag D.*, et al.*, "Poly(3,4-ethylenedioxythiophene) and its derivatives: Past, present, and future" *Adv. Mater.* 12, (7), **2000**, 481.
4. Geffroy B., Le Roy P. and Prat C., "Organic light-emitting diode (OLED) technology: materials, devices and display technologies" *Polym. Int.* 55, (6), **2006**, 572.
5. Hoppe H. and Sariciftci N. S., "Organic solar cells: An overview" *J. Mater. Res.* 19, (7), **2004**, 1924.
6. Spanggaard H. and Krebs F. C., "A brief history of the development of organic and polymeric photovoltaics" *Sol. Energy Mater. Sol. Cells* 83, (2-3), **2004**, 125.
7. de Gans B. J., Duineveld P. C. and Schubert U. S., "Inkjet printing of polymers: State of the art and future developments" *Adv. Mater.* 16, (3), **2004**, 203.
8. Sheats J. R., "Manufacturing and commercialization issues in organic electronics" *J. Mater. Res.* 19, (7), **2004**, 1974.
9. Brabec C. J., "Organic photovoltaics: technology and market" *Sol. Energy Mater. Sol. Cells* 83, (2-3), **2004**, 273.
10. Salzner U., Lagowski J. B., Pickup P. G.*, et al.*, "Comparison of geometries and electronic structures of polyacetylene, polyborole, polycyclopentadiene, polypyrrole, polyfuran, polysilole, polyphosphole,

polythiophene, polyselenophene and polytellurophene" *Synth. Met.* 96, (3), **1998**, 177.

11. Peierls R.E., "Quantum Theory of Solids", Oxford University Press, London, **1955**.
12. van Mullekom H. A. M., Vekemans J. A. J. M., Havinga E. E.*, et al.*, "Developments in the chemistry and band gap engineering of donor-acceptor substituted conjugated polymers" *Mater. Sci. Eng. R-Rep.* 32, (1), **2001**, 1.
13. Heeger A. J., "Semiconducting and metallic polymers: the fourth generation of polymeric materials" *Synth. Met.* 125, (1), **2001**, 23.
14. Chandrasekhar P., "Conducting polymers, fundamentals and applications", Kluwer Academic Publishers, Boston, **1999**.
15. Karl N., "Charge carrier transport in organic semiconductors" *Synth. Met.* 133, **2003**, 649.
16. Skotheim T.A., Elsenbaumer R. L. and Reynolds J. R., "Handbook of Conducting Polymers, 2nd ed." Marcel Dekker Inc., New York, **1998**.
17. Rohatgi M., "Fundamentals of Photochemistry", Wiley Eastern Ltd., New Delhi, **1978**.
18. Roncali J., "Synthetic principles for bandgap control in linear pi-conjugated systems" *Chem. Rev.* 97, (1), **1997**, 173.
19. Bredas J. L., "Relationship between Band-Gap and Bond Length Alternation in Organic Conjugated Polymers" *J. Chem. Phys.* 82, (8), **1985**, 3808.
20. Bredas J. L., "Theoretical Design of Polymeric Conductors" *Synth. Met.* 17, (1-3), **1987**, 115.
21. Bredas J. L., Street G. B., Themans B.*, et al.*, "Organic Polymers Based on Aromatic Rings (Polyparaphenylene, Polypyrrole, Polythiophene) - Evolution of the Electronic-Properties as a Function of the Torsion Angle between Adjacent Rings" *J. Chem. Phys.* 83, (3), **1985**, 1323.

22. Hernandez V., Castiglioni C., Delzoppo M.*, et al.*, "Confinement Potential and Pi-Electron Delocalization in Polyconjugated Organic Materials" *Phys. Rev. B* 50, (14), **1994**, 9815.

23. Conwell E.M., in: H. S. Nalwa (Eds.), "Handbook of Organic Conductive Molecules and Polymers" Vol. 4, John Wiley & Sons, Chichester, **1997**, 2.

24. Gustafsson-Carlberg J. C., Inganas O., Andersson M. R.*, et al.*, "Tuning the Bandgap for Polymeric Smart Windows and Displays" *Electrochim. Acta* 40, (13-14), **1995**, 2233.

25. Cutler C. A., Burrell A. K., Officer D. L.*, et al.*, "Effect of electron withdrawing or donating substituents on the photovoltaic performance of polythiophenes" *Synth. Met.* 128, (1), **2002**, 35.

26. Samuelsen E. J. and Mardalen J. in: H. S. Nalwa (Eds.), "Handbook of Organic Conductive Molecules and Polymers" Vol. 3, John Wiley & Sons, Chichester, **1997**, 87.

27. Ajayaghosh A., "Donor-acceptor type low band gap polymers: polysquaraines and related systems" *Chem. Soc. Rev.* 32, (4), **2003**, 181.

28. Van Geneugden D. "Poly(1,3-dithienylisothianaphtene) derivatives; synthesis, characterisation and possible applications of a new class of low bandgap materials", *Ph. D. dissertation*, **1999,** Limburgs Universitair Centrum, Diepenbeek.

29. Roncali J., "Conjugated Poly(Thiophenes) - Synthesis, Functionalization, and Applications" *Chem. Rev.* 92, (4), **1992**, 711.

30. Lin J. W. P. and Dudek L. P., "Synthesis and Properties of Poly(2,5-Thienylene)" *J. Polym. Sci. Pol. Chem.* 18, (9), **1980**, 2869.

31. Yamamoto T., Sanechika K. and Yamamoto A., "Preparation of Thermostable and Electric-Conducting Poly(2,5-Thienylene)" *J. Polym. Sci. Pol. Lett.* 18, (1), **1980**, 9.

32. Elsenbaumer R. L., Jen K. Y. and Oboodi R., "Processible and Environmentally Stable Conducting Polymers" *Synth. Met.* 15, (2-3), **1986**, 169.

33. McCullough R. D., "The chemistry of conducting polythiophenes" *Adv. Mater.* 10, (2), **1998**, 93.

34. Leclerc M., Martinez Diaz F. and Wegner G., "Structural analysis of poly(3-alkylthiophene)s" *Makromol. Chem.* 190, **1989**, 3105.

35. Chen T. A. and Rieke R. D., "Polyalkylthiophenes with the Smallest Bandgap and the Highest Intrinsic Conductivity" *Synth. Met.* 60, (2), **1993**, 175.

36. McCullough R. D. and Lowe R. D., "Enhanced Electrical-Conductivity in Regioselectively Synthesized Poly(3-Alkylthiophenes)" *J. Chem. Soc.-Chem. Commun.* (1), **1992**, 70.

37. Chen T. A., Wu X. M. and Rieke R. D., "Regiocontrolled Synthesis of Poly(3-Alkylthiophenes) Mediated by Rieke Zinc - Their Characterization and Solid-State Properties" *J. Am. Chem. Soc.* 117, (1), **1995**, 233.

38. McCullough R. D., Lowe R. D., Jayaraman M.*, et al.*, "Design, Synthesis, and Control of Conducting Polymer Architectures - Structurally Homogeneous Poly(3-Alkylthiophenes)" *J. Org. Chem.* 58, (4), **1993**, 904.

39. Jonas F., Heywang G., Schmidtberg W.*, et al.*, "Polythiophenes, process for their preparation and their use" EP0339340, **1989**.

40. Roncali J., Blanchard P. and Frere P., "3,4-Ethylenedioxythiophene (EDOT) as a versatile building block for advanced functional p-conjugated systems" *J. Mater. Chem.* 15, (16), **2005**, 1589.

41. Jonas F. and Krafft W., "New polythiophene dispersions, their preparation and their use" EP0440957, **1991**.

42. Wudl F., Kobayashi M. and Heeger A. J., "Poly(Isothianaphthene)" *J. Org. Chem.* 49, (18), **1984**, 3382.

43. Hoogmartens I., Adriaensens P., Vanderzande D.*, et al.*, "Low-Bandgap Conjugated Polymers - a Joint Experimental and Theoretical-Study of the Structure of Polyisothianaphthene" *Macromolecules* 25, (26), **1992**, 7347.

44. Hoogmartens I., Adriaensens P., Carleer R.*, et al.*, "An Investigation into the Electronic-Structure of Poly(Isothianaphthene)" *Synth. Met.* 51, (1-3), **1992**, 219.

45. King G. and Higgins S. J., "Synthesis and Characterization of Novel Substituted Benzo C Thiophenes and Polybenzo C Thiophenes - Tuning the Potentials for N-Doping and P-Doping in Transparent Conducting Polymers" *J. Mater. Chem.* 5, (3), **1995**, 447.

46. Ikenoue Y., Wudl F. and Heeger A. J., "A Novel Substituted Poly(Isothianaphthene)" *Synth. Met.* 40, (1), **1991**, 1.

47. Pomerantz M., Chalonergill B., Harding L. O.*, et al.*, "Poly(2,3-Dihexylthieno 3,4-B Pyrazine) - a New Processable Low Band-Gap Polyheterocycle" *J. Chem. Soc.-Chem. Commun.* (22), **1992**, 1672.

48. Kastner J., Kuzmany H., Vegh D.*, et al.*, "Raman-Spectra of Poly(2,3-R,R-Thieno 3,4-B Pyrazine) - a New Low-Band-Gap Polymer" *Macromolecules* 28, (8), **1995**, 2922.

49. Pomerantz M. and Gu X. M., "Poly(2-decylthieno 3,4-b thiophene). A new soluble low-bandgap conducting polymer" *Synth. Met.* 84, (1-3), **1997**, 243.

50. Zotti G., Schiavon G., Berlin A.*, et al.*, "Novel, Highly Conducting, and Soluble Polymers from Anodic Coupling of Alkyl-Substituted Cyclopentadithiophene Monomers" *Macromolecules* 27, (7), **1994**, 1938.

51. Lambert T. L. and Ferraris J. P., "Narrow-Band Gap Polymers - Polycyclopenta 2,1-B-3,4-B' Dithiophen-4-One" *J. Chem. Soc.-Chem. Commun.* (11), **1991**, 752.

52. Ferraris J. P. and Lambert T. L., "Narrow Bandgap Polymers - Poly-4-Dicyanomethylene-4h-Cyclopenta 2,1-B-3,4-B' Dithiophene (Pcdm)" *J. Chem. Soc.-Chem. Commun.* (18), **1991**, 1268.

53. Martinez M., Reynolds J. R., Basak S.*, et al.*, "Electrochemical Synthesis and Optical Analysis of Poly (2,2'-Dithienyl)-5,5'-Diylvinylene" *J. Polym. Sci. Pt. B-Polym. Phys.* 26, (4), **1988**, 911.

54. Catellani M., Luzzati S., Musco A.*, et al.*, "Synthesis and Characterization of Alkyl-Substituted Poly E-1,2-(2,2'-Dithienyl)Ethylene S" *Synth. Met.* 62, (3), **1994**, 223.

55. Sotzing G. A. and Reynolds J. R., "Poly[Trans-Bis(3,4-Ethylenedioxythiophene)Vinylene] - a Low-Band-Gap Polymer with Rapid Redox Switching Capabilities between Conducting Transmissive and Insulating Absorptive States" *J. Chem. Soc. Chem. Commun.* (6), **1995**, 703.

56. Blanchard P., Brisset H., Illien B.*, et al.*, "Bridged dithienylethylenes as precursors of small bandgap electrogenerated conjugated polymers" *J. Org. Chem.* 62, (8), **1997**, 2401.

57. Gilch H.G. and Wheelwright W.L., "Polymerisation of □-halogenated *p*-xylenes with base" *J. Polymer Science* (4), **1966**, 1337.

58. Wessling R. A., "The Polymerization of Xylylene Bisdialkyl Sulfonium Salts" *J. Polymer Science* (72), **1985**, 55.

59. Son S., Dodabalapur A., Lovinger A.J.*, et al.*, "Luminesence enhancement by the introduction of disorder into poly(p-phenylene vinylene)" *Science* 269, (5222), **1995**, 376.

60. Vanderzande D. J., Issaris A. C., VanderBorght M. J.*, et al.*, "A general approach to precursors for poly(arylene vinylene) derivatives: Mechanism, scope and modifications" *Macromol. Symp.* 125, **1998**, 189.

61. Henckens A., Lutsen L., Vanderzande D.*, et al.*, "Synthesis of PTV via the Dithiocarbamate route, a new precursor route towards conjugated polymers" *Proc. SPIE Int. Soc. Opt. Eng.* 5464, **2004**, 52.

62. Burroughes J. H., Bradley D. D. C., Brown A. R.*, et al.*, "Light-Emitting-Diodes Based on Conjugated Polymers" *Nature* 347, (6293), **1990**, 539.

63. Eckhardt H., Shacklette L. W., Jen K. Y.*, et al.*, "The Electronic and Electrochemical Properties of Poly(Phenylene Vinylenes) and Poly(Thienylene Vinylenes) - an Experimental and Theoretical-Study" *J. Chem. Phys.* 91, (2), **1989**, 1303.

64. Cheng H. and Elsenbaumer R. L., "New Precursors and Polymerization Route for the Preparation of High-Molecular-Mass Poly(3,4-Dialkoxy-2,5-Thienylenevinylene)S - Low-Band-Gap Conductive Polymers" *J. Chem. Soc.-Chem. Commun.* (14), **1995**, 1451.

65. Havinga E. E., Tenhoeve W. and Wynberg H., "Alternate Donor-Acceptor Small-Band-Gap Semiconducting Polymers - Polysquaraines and Polycroconaines" *Synth. Met.* 55, (1), **1993**, 299.

66. Ho H. A., Brisset H., Frere P.*, et al.*, "Electrogenerated Small Bandgap Pi-Conjugated Polymers Derived from Substituted Dithienylethylenes" *J. Chem. Soc.-Chem. Commun.* (22), **1995**, 2309.

67. Wagner P., Aubert P-H., Lutsen L.*, et al.*, "Conjugated polymers based on new thienylene - PPV derivatives for solar cell applications" *Electrochem. Commun.* 4, (11), **2002**, 912.

68. Sotzing G. A., Thomas C. A., Reynolds J. R.*, et al.*, "Low band gap cyanovinylene polymers based on ethylenedioxythiophene" *Macromolecules* 31, (11), **1998**, 3750.

69. Seshadri V. and Sotzing G. A., "Polymerization of two unsymmetrical isomeric monomers based on thieno[3,4-*b*]thiophene containing cyanovinylene spacers" *Chem. Mat.* 16, (26), **2004**, 5644.

70. Thomas C. A., Zong K. W., Abboud K. A.*, et al.*, "Donor-mediated band gap reduction in a homologous series of conjugated polymers" *J. Am. Chem. Soc.* 126, (50), **2004**, 16440.

71. Galand E. M., Kim Y. G., Mwaura J. K.*, et al.*, "Optimization of narrow band-gap propylenedioxythiophene : cyanovinylene copolymers for optoelectronic applications" *Macromolecules* 39, (26), **2006**, 9132.

72. Zhang Q. T. and Tour J. M., "Alternating donor/acceptor repeat units in polythiophenes. Intramolecular charge transfer for reducing band gaps in fully substituted conjugated polymers" *J. Am. Chem. Soc.* 120, (22), **1998**, 5355.

73. Zhang Q. H., Li Y. and Yang M. J., "A novel low band gap polymer PDTNTBQ" *Synth. Met.* 146, (1), **2004**, 69.

74. Kitamura C., Tanaka S. and Yamashita Y., "Design of narrow-bandgap polymers. Syntheses and properties of monomers and polymers containing aromatic-donor and o-quinoid-acceptor units" *Chem. Mat.* 8, (2), **1996**, 570.

75. Karikomi M., Kitamura C., Tanaka S.*, et al.*, "New Narrow-Bandgap Polymer Composed of Benzobis(1,2,5-Thiadiazole) and Thiophenes" *J. Am. Chem. Soc.* 117, (25), **1995**, 6791.

76. Tanaka S. and Yamashita Y., "Syntheses of Narrow-Band Gap Heterocyclic Copolymers of Aromatic-Donor and Quinonoid-Acceptor Units" *Synth. Met.* 69, (1-3), **1995**, 599.

77. Zhang F. L., Mammo W., Andersson L. M.*, et al.*, "Low-bandgap alternating fluorene copolymer/methanofullerene heterojunctions in efficient near-infrared polymer solar cells" *Adv. Mater.* 18, (16), **2006**, 2169.

78. Dhanabalan A., van Duren J. K. J., van Hal P. A.*, et al.*, "Synthesis and characterization of a low bandgap conjugated polymer for bulk heterojunction photovoltaic cells" *Adv. Funct. Mater.* 11, (4), **2001**, 255.

79. Svensson M., Zhang F. L., Veenstra S. C.*, et al.*, "High-performance polymer solar cells of an alternating polyfluorene copolymer and a fullerene derivative" *Adv. Mater.* 15, (12), **2003**, 988.

80. Perzon E., Wang X. J., Admassie S.*, et al.*, "An alternating low band-gap polyfluorene for optoelectronic devices" *Polymer* 47, (12), **2006**, 4261.

81. Akoudad S. and Roncali J., "Electrogenerated poly(thiophenes) with extremely narrow bandgap and high stability under n-doping cycling" *Chem. Commun.* (19), **1998**, 2081.

82. Shahid M., Ashraf R. S., Klemm E.*, et al.*, "Synthesis and properties of novel low-band-gap thienopyrazine-based poly(heteroarylenevinylene)s" *Macromolecules* 39, (23), **2006**, 7844.

83. Burroughes J. H., Jones C. A. and Friend R. H., "New Semiconductor-Device Physics in Polymer Diodes and Transistors" *Nature* 335, (6186), **1988**, 137.

84. Chua L. L., Zaumseil J., Chang J. F.*, et al.*, "General observation of n-type field-effect behaviour in organic semiconductors" *Nature* 434, (7030), **2005**, 194.

85. Horowitz G., "Organic field-effect transistors" *Adv. Mater.* 10, (5), **1998**, 365.

86. Newman C. R., Frisbie C. D., da Silva D. A.*, et al.*, "Introduction to organic thin film transistors and design of n-channel organic semiconductors" *Chem. Mat.* 16, (23), **2004**, 4436.

87. Bradley D. D. C., "Conjugated Polymer Electroluminescence" *Synth. Met.* 54, (1-3), **1993**, 401.

88. Davis J., Vaughan D. H. and Cardosi M. F., "Elements of biosensor construction" *Enzyme Microb. Technol.* 17, (12), **1995**, 1030.

89. Gerard M., Chaubey A. and Malhotra B. D., "Application of conducting polymers to biosensors" *Biosens. Bioelectron.* 17, (5), **2002**, 345.

90. Heeger P. S. and Heeger A. J., "Making sense of polymer-based biosensors" *Proc. Natl. Acad. Sci. U. S. A.* 96, (22), **1999**, 12219.

91. Argun A. A., Aubert P. H., Thompson B. C.*, et al.*, "Multicolored electrochromism polymers: Structures and devices" *Chem. Mat.* 16, (23), **2004**, 4401.

92. McGehee M. D. and Heeger A. J., "Semiconducting (conjugated) polymers as materials for solid-state lasers" *Adv. Mater.* 12, (22), **2000**, 1655.

93. Hide F., DiazGarcia M. A., Schwartz B. J.*, et al.*, "Semiconducting polymers: A new class of solid-state laser materials" *Science* 273, (5283), **1996**, 1833.

94. Brabec C. J., Sariciftci N. S. and Hummelen J. C., "Plastic solar cells" *Adv. Funct. Mater.* 11, (1), **2001**, 15.

95. Nelson J., "Organic photovoltaic films" *Materials Today* 5, (5), **2002**, 20.

96. Meissner D., "Plastic solar cells" *Photon* 2, **1999**, 34.

97. Dennler G. and Sariciftci N. S., "Flexible conjugated polymer-based plastic solar cells: From basics to applications" *Proc. IEEE* 93, (8), **2005**, 1429.

98. Coakley K. M. and McGehee M. D., "Conjugated polymer photovoltaic cells" *Chem. Mat.* 16, (23), **2004**, 4533.

99. Brabec C. J., Dyakonov V., Parisi J*, et al.*, *Organic Photovoltaics, concepts and realization,* Springer-Verlag, Berlin, **2003**.

100. Chabinyc M. L. and Salleo A., "Materials requirements and fabrication of active matrix arrays of organic thin-film transistors for displays" *Chem. Mat.* 16, (23), **2004**, 4509.

101. Clemens W., Fix I., Ficker J*., et al.*, "From polymer transistors toward printed electronics" *J. Mater. Res.* 19, (7), **2004**, 1963.

102. Ong B. S., Wu Y. L., Liu P*., et al.*, "High-performance semiconducting polythiophenes for organic thin-film transistors" *J. Am. Chem. Soc.* 126, (11), **2004**, 3378.

103. Schubert E. F. and Kim J. K., "Solid-state light sources getting smart" *Science* 308, (5726), **2005**, 1274.

104. Gong X., Ma W. L., Ostrowski J. C*., et al.*, "White electrophosphorescence from semiconducting polymer blends" *Adv. Mater.* 16, (7), **2004**, 615.

105. Liu M. S., Niu Y. H., Luo J. D*., et al.*, "Material and interface engineering for highly efficient polymer light emitting diodes" *Polym. Rev.* 46, (1), **2006**, 7.

106. International Energy Agency "*Key World Energy Statistics",* **2005**.

107. Chapin D.M., Fuller C.S. and Pearson G.L., "A New Silicon p-n Junction Photocell for Converting Solar Radiation into Electrical Power" *J. Appl. Phys.* 25, **1954**, 676.

108. Miles R. W., Hynes K. M. and Forbes I., "Photovoltaic solar cells: An overview of state-of-the-art cell development and environmental issues" *Prog Cryst Growth Ch* 51, (1-3), **2005**, 1.

109. Green M. A., Emery K., King D. L.*, et al.*, "Solar cell efficiency tables (version 28)" *Prog. Photovoltaics* 14, (5), **2006**, 455.

110. Goetzberger A., Hebling C. and Schock H. W., "Photovoltaic materials, history, status and outlook" *Mater. Sci. Eng. R-Rep.* 40, (1), **2003**, 1.

111. Weinberger B. R., Akhtar M. and Gau S. C., "Polyacetylene Photo-Voltaic Devices" *Synth. Met.* 4, (3), **1982**, 187.

112. Glenis S., Tourillon G. and Garnier F., "Influence of the Doping on the Photovoltaic Properties of Thin-Films of Poly-3-Methylthiophene" *Thin Solid Films* 139, (3), **1986**, 221.

113. Halls J. J. M., Pichler K., Friend R. H.*, et al.*, "Exciton diffusion and dissociation in a poly(p-phenylenevinylene)/C-60 heterojunction photovoltaic cell" *Appl. Phys. Lett.* 68, (22), **1996**, 3120.

114. Karg S., Riess W., Meier M.*, et al.*, "Characterization of Light-Emitting-Diodes and Solar-Cells Based on Poly-Phenylene-Vinylene" *Synth. Met.* 57, (1), **1993**, 4186.

115. Tang C. W., "2-Layer Organic Photovoltaic Cell" *Appl. Phys. Lett.* 48, (2), **1986**, 183.

116. Sariciftci N. S., Smilowitz L., Heeger A. J.*, et al.*, "Photoinduced Electron-Transfer from a Conducting Polymer to Buckminsterfullerene" *Science* 258, (5087), **1992**, 1474.

117. Sariciftci N. S., Braun D., Zhang C.*, et al.*, "Semiconducting Polymer-Buckminsterfullerene Heterojunctions - Diodes, Photodiodes, and Photovoltaic Cells" *Appl. Phys. Lett.* 62, (6), **1993**, 585.

118. Geens W., Aernouts T., Poortmans J.*, et al.*, "Organic co-evaporated films of a PPV-pentamer and C-60: model systems for donor/acceptor polymer blends" *Thin Solid Films* 403, **2002**, 438.

119. Yu G., Gao J., Hummelen J. C.*, et al.*, "Polymer Photovoltaic Cells - Enhanced Efficiencies Via a Network of Internal Donor-Acceptor Heterojunctions" *Science* 270, (5243), **1995**, 1789.

120. Munters T., Martens T., Goris L.*, et al.*, "A comparison between state-of-the-art 'gilch' and 'sulphinyl' synthesised MDMO-PPV/PCBM bulk hetero-junction solar cells" *Thin Solid Films* 403, **2002**, 247.

121. Yu G. and Heeger A. J., "Charge Separation and Photovoltaic Conversion in Polymer Composites with Internal Donor-Acceptor Heterojunctions" *J. Appl. Phys.* 78, (7), **1995**, 4510.

122. Halls J. J. M., Walsh C. A., Greenham N. C.*, et al.*, "Efficient Photodiodes from Interpenetrating Polymer Networks" *Nature* 376, (6540), **1995**, 498.

123. Zhang F. L., Jonforsen M., Johansson D. M.*, et al.*, "Photodiodes and solar cells based on the n-type polymer poly(pyridopyrazine vinylene) as electron acceptor" *Synth. Met.* 138, (3), **2003**, 555.

124. Breeze A. J., Schlesinger Z., Carter S. A.*, et al.*, "Improving power efficiencies in polymer - polymer blend photovoltaics" *Sol. Energy Mater. Sol. Cells* 83, (2-3), **2004**, 263.

125. Snaith H. J., Arias A. C., Morteani A. C.*, et al.*, "Charge generation kinetics and transport mechanisms in blended polyfluorene photovoltaic devices" *Nano Lett.* 2, (12), **2002**, 1353.

126. Halls J. J. M., Cornil J., dos Santos D. A.*, et al.*, "Charge- and energy transfer processes at polymer/polymer interfaces: A joint experimental and theoretical study" *Phys. Rev. B* 60, (8), **1999**, 5721.

127. Hoppe H. and Sariciftci N. S., "Morphology of polymer/fullerene bulk heterojunction solar cells" *J. Mater. Chem.* 16, (1), **2006**, 45.

128. Hoppe H., Niggemann M., Winder C.*, et al.*, "Nanoscale morphology of conjugated polymer/fullerene-based bulk-heterojunction solar cells" *Adv. Funct. Mater.* 14, (10), **2004**, 1005.

129. Padinger F., Rittberger R. S. and Sariciftci N. S., "Effects of postproduction treatment on plastic solar cells" *Adv. Funct. Mater.* 13, (1), **2003**, 85.

130. Reyes-Reyes M., Kim K. and Carroll D. L., "High-efficiency photovoltaic devices based on annealed poly(3-hexylthiophene) and 1-(3-methoxycarbonyl)-propyl-1-phenyl-(6,6)C-61 blends" *Appl. Phys. Lett.* 87, (8), **2005**, 083506.

131. Shaheen S. E., Vangeneugden D., Kiebooms R.*, et al.*, "Low band-gap polymeric photovoltaic devices" *Synth. Met.* 121, (1-3), **2001**, 1583.

132. Colladet K., Nicolas M., Goris L.*, et al.*, "Low-band gap polymers for photovoltaic applications" *Thin Solid Films* 451-52, **2004**, 7.

133. Egbe D. A. M., Nguyen L., Carbonnier B.*, et al.*, "Thiophene-containing poly(arylene-ethynylene)-alt-poly(arylenevinylene)s: Synthesis, characterisation and optical properties" *Polymer* 46, (23), **2005**, 9585.

134. Brabec C. J., Winder C., Sariciftci N. S.*, et al.*, "A low-bandgap semiconducting polymer for photovoltaic devices and infrared emitting diodes" *Adv. Funct. Mater.* 12, (10), **2002**, 709.

135. Winder C., Matt G., Hummelen J. C.*, et al.*, "Sensitization of low bandgap polymer bulk heterojunction solar cells" *Thin Solid Films* 403, **2002**, 373.

136. Winder C. and Sariciftci N. S., "Low bandgap polymers for photon harvesting in bulk heterojunction solar cells" *J. Mater. Chem.* 14, (7), **2004**, 1077.

137. Perzon E., Wang X. J., Zhang F. L.*, et al.*, "Design, synthesis and properties of low band gap polyfluorenes for photovoltaic devices" *Synth. Met.* 154, (1-3), **2005**, 53.

138. Zhang F. L., Perzon E., Wang X. J.*, et al.*, "Polymer solar cells based on a low-bandgap fluorene copolymer and a fullerene derivative with photocurrent extended to 850 nm" *Adv. Funct. Mater.* 15, (5), **2005**, 745.

139. Nguyen L. H., Gunes S., Neugebauer H.*, et al.*, "Precursor route poly(thienylene vinylene) for organic solar cells: Photophysics and photovoltaic performance" *Sol. Energy Mater. Sol. Cells* 90, (17), **2006**, 2815.

140. Muhlbacher D., Scharber M., Morana M.*, et al.*, "High photovoltaic performance of a low-bandgap polymer" *Adv. Mater.* 18, (21), **2006**, 2884.

141. Scharber M. C., Mühlbacher D., Koppe M. *, et al.*, "Design Rules for Donors in Bulk-Heterojunction Solar Cells - Towards 10 % Energy-Conversion Efficiency" *Adv. Mat.* 18, (6), **2006**, 789.

Chapter Two

Low Band Gap Polymers based on the Donor – Acceptor Approach[1, 2]

Abstract: *This chapter focuses on the design of low band gap polymers via the donor-acceptor approach. First an overview of the known polymerization routes toward poly(thiophene) analogues is given. Subsequent, a family of six polymers based on bis-(1-cyano-2-thienyl vinylene)phenylene is synthesized using the chemical oxidation method with* $FeCl_3$*. The polymers deviate in side chains and thiophene derivatives. All polymers show low band gap behavior and are tested in bulk heterojunction plastic solar cells.*

2.1 Introduction

2.1.1 Structures

As been pointed out in chapter 1, one of the most promising strategies to tailor the energy levels of conjugated polymers is the donor-acceptor route[3]. The central concept forming the basis of this route is that the interaction between alternating electron rich donors and electron deficient acceptors will result in a compressed band gap. Furthermore, by changing the substituents of the polymer, the band gap can be fine-tuned. Various literature reports exist in which this route is used to electrosynthesize low band gap polymers containing cyanovinylene spacers as the acceptor units and thiophene derivatives

as the donor. Band gaps ranging from 1.1 to 1.6 eV were reported[4-7]. However, for photovoltaic devices soluble low band gap polymers are needed since the conjugated polymer must be blended with a complementary acceptor to achieve a bulk heterojunction. In this chapter we present a family of conjugated polymers based on *bis*-(1-cyano-2-thienyl vinylene)phenylene[8-13]. The structure consists of a central dialkoxyphenylene core (donor) *p*-disubstituted by two thiophene derivatives (donor) through a cyanovinylene linker (acceptor) as shown in Figure 2-1. By changing the thiophene moiety we were able to tune the polymers electronic and solubility properties. Moreover, our approach to keep the central core constant leads to a toolbox to create a whole range of monomers, and thus polymers, with different heteroaromatic rings linked to this central core. A more polar polymer **P5** with a dioligo(oxyethylene)phenylene central core will be discussed in section 2.6. In part 2.7, a push-pull molecule **P6** is introduced as a side chain in order to study the molecular orientation concept for plastic solar cells[14,15-17]. Essentially, the polymerization toward these materials consists of the creation of a thiophene-thiophene linkage and in the next part some methods to polymerize thiophene-derivatives are discussed.

2.1.2 Synthesis of poly(thiophene) derivatives

Poly(thiophene) (PT) and derivatives have been prepared by three main methods[18-22], namely, electrochemical polymerization, organometallic cross-coupling and oxidative coupling methods.

2.1.2.1 Electrochemical polymerization

Since the first reports, the synthesis of PTs by electrochemical oxidation has been widely used[23]. Although the mechanism is not fully understood, it is proposed that the polymerization proceeds *via* the coupling of two radical cations, formed by the oxidation of the monomer as outlined in Figure 2-2. Aromatization of the bithiophene intermediate is the driving force for the transformation of the dihydro-dimer.

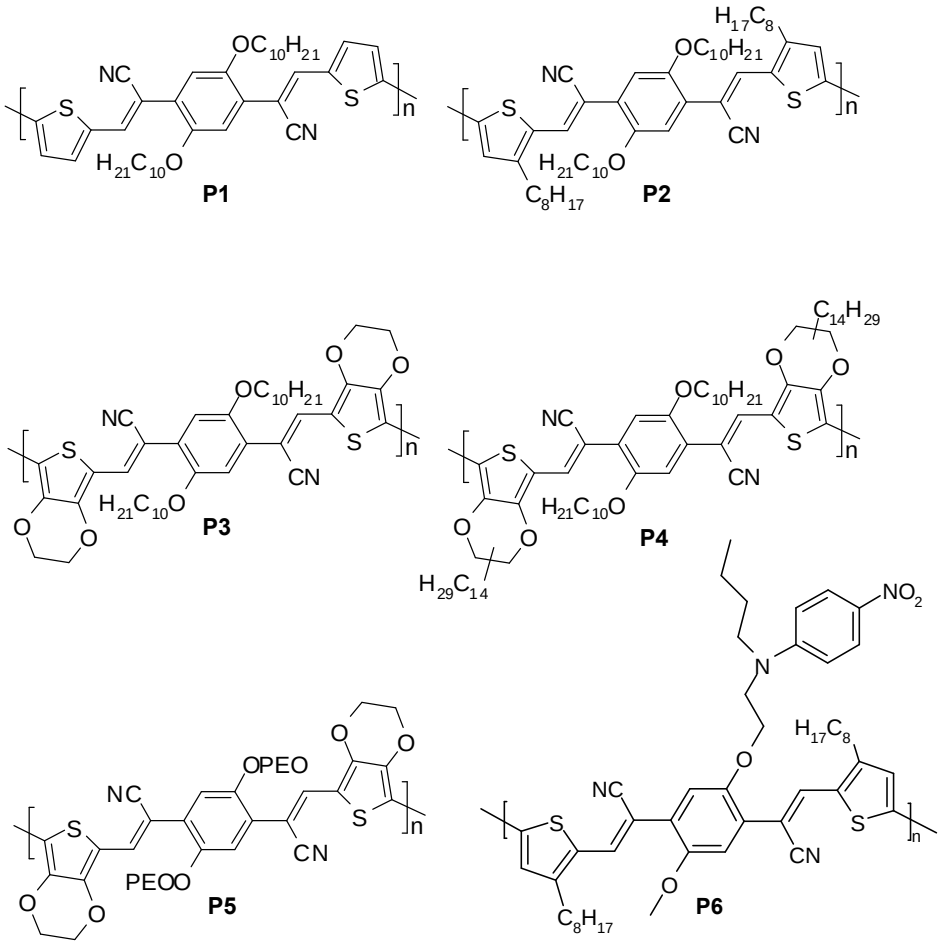

Figure 2-1: Overview of the materials prepared in this study.

The dimer, having a lower oxidation potential than the monomer, is readily oxidized and undergoes further coupling with the monomeric radical cation. The polymer is deposited in its oxidized conducting form onto the electrode, allowing the polymerization to proceed. The electrochemical polymerization of substituted thiophenes has also been used to synthesize a variety of functional polymers[4-7,24-28]. This method is straightforward and has the advantages that during the polymerization homogeneous, stable films are formed and, since no catalyst is required, this method leads to materials with high purity. The

main drawbacks are the formation of 2,4-couplings between thiophene units and the very wide molecular weight distributions.

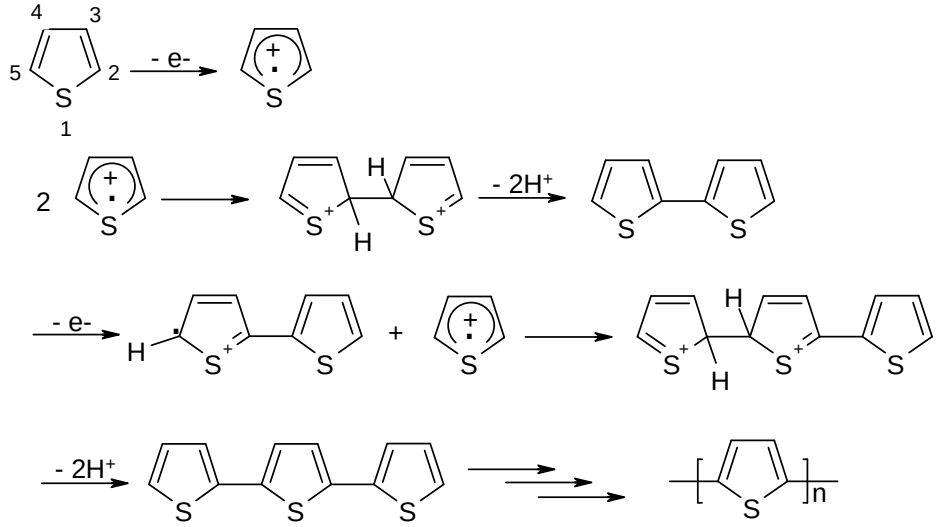

Figure 2-2: Electrochemical polymerization of thiophene[23].

2.1.2.2 Organometallic cross-coupling methods[29]

***Kumada* cross-coupling**

The cross-coupling of organomagnesium compounds with arylhalides was first discovered by Kumada *et al*. in 1972[30]. In 1980 the first PTs were prepared *via* this route[31,32]. The reaction is normally carried out with a *Grignard* compound and the corresponding aryl halide in the presence of either a Ni catalyst, e.g. $NiCl_2$(dppp) (dppp = 1,3-bis(diphenyl-phosphino)-propane), or, less frequently, a Pd catalyst employing dry diethylether or THF as the solvent[33]. An elegant example of the *Kumada* cross-coupling polymerization is described by McCullough[34,35] for the synthesis of regioregular poly(3-alkylthiophene)s or P3ATs (Figure 2-3). This synthetic method regiospecifically generates 2-bromo-5-(bromomagnesio)-3-alkylthiophene, which is polymerized with catalytic amounts of Ni(dppp)Cl_2 to give P3ATs with 98-99 % HT couplings. In this approach, HT-P3ATs were prepared in yields of 44-69

% (chloroform-soluble solids only) in a one-pot, multistep procedure. Molecular weights for HT-P3ATs are typically in the range of M_n = 20k to 40k (PD = 1.4).

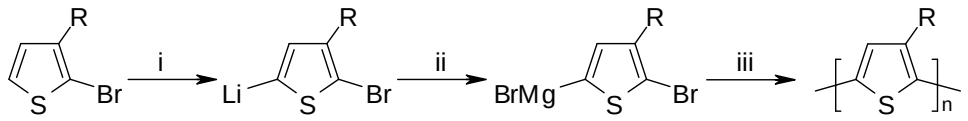

*Figure 2-3: Regioregular poly(alkylthiophene)s via Kumada cross-coupling (McCullough route): (i) LDA; (ii) $MgBr_2$*Et_2O; (iii) Ni(dppp)Cl_2.*

Recently, the same group has reported a simplified procedure, the *Grignard* Metathesis (GRIM) method, for the synthesis of P3AT[36-38] and poly(3-alkoxythiophene)s[39,40]. Treatment of 2,5-dibromo-3-alkylthiophene with a *Grignard* reagent yields two regioisomers. After the addition of a catalytic amount of Ni(dppp)Cl_2 only one of the isomers is consumed, forming P3AT with 98-99 % HT couplings[38]. However, a major disadvantage of the *Kumada* cross coupling is the limited functional group compatibility of *Grignard* reagents.

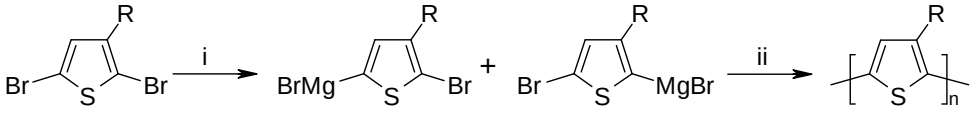

Figure 2-4: Regioregular poly(alkylthiophene)s via the Grignard Metathesis method: (i) RMgBr, THF; (ii) Ni(dppp)Cl_2.

Negishi **cross-coupling**

A second important route is the *Negishi* cross-coupling between an organozinc intermediate and an arylhalide. Rieke first described the synthesis of HT-P3AT *via* this coupling method[41-43]. In the *Rieke* method, 2,5-dibromo-3-alkylthiophene is added to a solution of highly reactive "*Rieke* zinc" (Zn*)[44]. This metal reacts quantitatively to form a mixture of the isomers 2-bromo-3-alkyl-5-(bromozincio)thiophene (**a**) and 2-(bromozincio)-3-alkyl-5-bromothiophene (**b**). The ratio between these two isomers is dependent upon the reaction temperature and, to a much

lesser extent, the sterical influence of the alkyl substituent. The addition of a Ni cross-coupling catalyst, Ni(dppe)Cl_2 (dppp = 1,3-bis(diphenyl-phosphino)-ethane), leads to the formation of a regioregular HT-P3AT (Figure 2-5). The yields for these reactions are reported to be ~75 %. Molecular weights for polymers prepared by this method are M_n = 24k to 34k (with a PD = 1.4). One advantage of the *Rieke* method over the *McCullough* method is that highly reactive *Rieke* zinc affords a functional-group-tolerant synthesis[45].

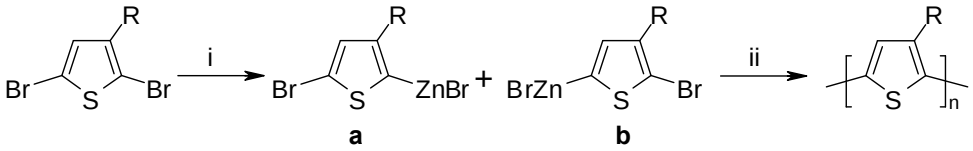

Figure 2-5: Regioregular poly(alkylthiophene)s via Negishi cross-coupling (Rieke route): (i) Zn/THF; (ii) Ni(dppp)Cl_2*

Suzuki **cross-coupling**

The name *Suzuki* cross-coupling[46] or *Suzuki–Miyaura* cross-coupling refers to the cross-coupling of organoboron compounds and aryl halides. The reaction is generally catalyzed by Pd(PPh_3)$_4$ or Pd(OAc)$_2$. The broad availability of organoboron compounds and a high functional group tolerance make the Suzuki cross-coupling particularly attractive. Drawbacks however, are low molecular weight polymers and low yields[47-51]. As an example the synthesis of regioregular poly(3-octylthiophene) is presented in Figure 2-6[52].

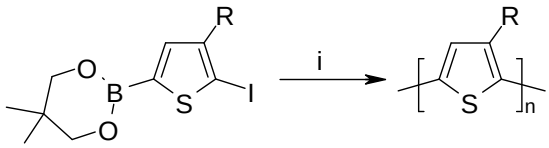

Figure 2-6: Regioselective synthesis of poly(3-octylthiophene) via Suzuki cross-coupling: (i) Pd(OAc)$_2$, K_2CO_3.

Stille cross-coupling

The cross-coupling reaction of arylstannanes and arylhalides was extensively studied by Stille and was named after him[53]. The main advantage of the *Stille* cross-coupling is its compatibility with a wide variety of functional groups. However, this coupling requires a higher temperature (about 100 °C) to facilitate the transmetalation step from the weakly nucleophilic stannane to the intermediate aryl palladium halide. A typically used catalyst is $Pd(PPh_3)_4$ or $Pd(PPh_3)_2Cl_2$. An example of the *Stille* cross-coupling[54] is shown in Figure 2-7, however only low molecular weight polymers are obtained[55].

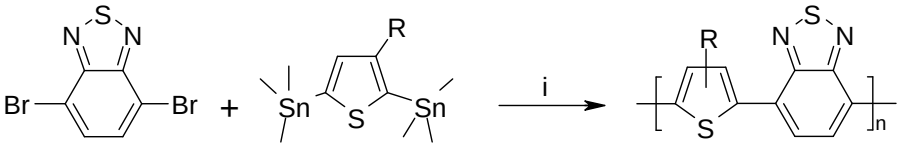

Figure 2-7: Example of the Stille cross-coupling: (i) $Pd(PPh_3)_2Cl_2$, DMF.

Despite these advances, the above synthetic procedures have some drawbacks. In comparison with the oxidative and electrochemical coupling methods extra modifications on the level of the monomer are necessary. The *McCullough* method requires highly purified starting materials, most important of which is the monomer, 2-bromo-3-alkylthiophene. In addition, this method requires cryogenic temperatures. Another disadvantage is the limited functional group compatibility of the *Grignard* reagents[34]. The *Rieke* method starts with the easy-to-purify 2,5-dibromo-3-alkylthiophene (since the compound is the highest boiling fraction in the crude mixture in its preparation), however, it requires the non-trivial preparation of *Rieke* zinc *via* alkali metal reduction of zinc halides, employs cryogenic temperatures, and necessitates long reaction times[42]. Both *Suzuki*[52] and *Stille* coupling methods also suffer from many of the above drawbacks. In addition, there have been no reports of using the above methods for the large-scale synthesis of HT-P3ATs and mostly the molecular weights of, other

than P3AT, derivatives are rather low. However, these high molecular weight polymers are necessary for better processability and higher mobilities[56, 57].

2.1.2.3 Oxidative coupling methods

Conducting PTs are formed upon the oxidation of thiophene with arsenic(V)pentafluoride (AsF_5)[58]. However, due to the poisonous properties of AsF_5 this method has not been widely adopted. A more convenient method was developed by Sugimoto in 1986[59]. He used iron(III)trichloride ($FeCl_3$) as the oxidizing agent and chloroform as the solvent under anhydrous conditions to synthesize P3AT. Subsequent reduction with ammonia provided the neutral polymer in good yields. Niemi has reported on the mechanism of the $FeCl_3$ synthesis of P3ATs[60]. According to him, the $FeCl_3$ initiates an oxidation of the alkylthiophene to produce a radical center predominantly at the 5-position of thiophene which than reacts with a neutral thiophene, upon propagation the polymer is formed (Figure 2-8). However Barbarella *et al.*[61] and Andersson *et al.*[62] proposed a slightly different mechanism in which two radical cations react, similar to the mechanism for the electrochemical polymerization (Figure 2-2). Despite the large number of papers concerning the polymerization of thiophene derivatives with $FeCl_3$, the reaction mechanism is still unclear and subject to controversial interpretations.

Materials prepared by the $FeCl_3$ method produce P3ATs with molecular weight ranging from M_n = 30k to 300k and with polydispersities ranging from 1.3 to 5[63,64]. The oxidative coupling of thiophenes provides materials with higher molecular weights than the routes described above and it does not appear to generate 2,4-couplings in P3ATs. The main disadvantage of this method is the low regiospecificity (discussed in detail in chapter 1) which leads to about 20 % regiochemical defects for P3AT that are polymerized in this way[63]. The need to remove large quantities of iron salts after polymerization is another drawback[65]. The Fe impurity level affects device performance of

PT in field effect transistors[65] and in LEDs[66]. However, rigorous purification can reduce the Fe-impurities to only 0.008 %[67]. This coupling reaction is simple and has now been widely employed for the synthesis of all kinds of poly(thiophene)s from thiophene with alkyl[63,64,68], alkoxy[69,70], functionalized alkyl[71-77] and other thiophene derivatives[10,78-81].

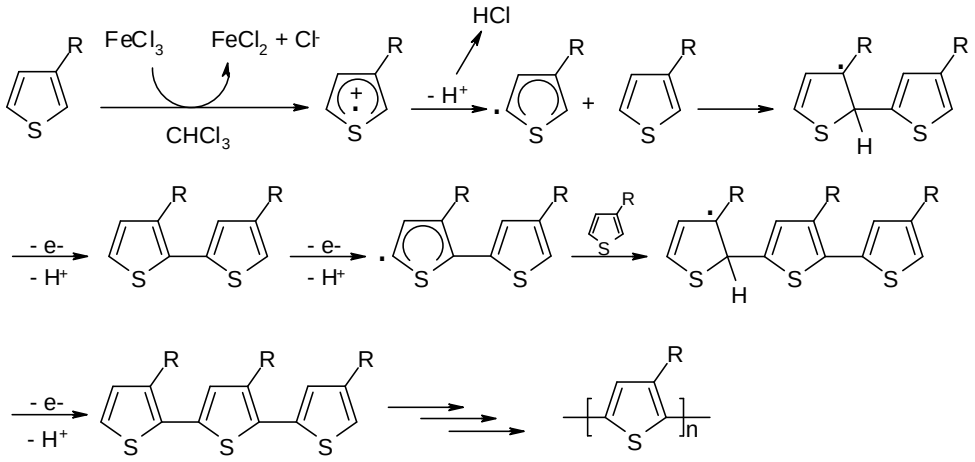

Figure 2-8: Proposed mechanism of the oxidative polymerization toward P3AT with $FeCl_3$ by Niemi[60].

2.2 Monomer synthesis

The starting compound for the central core, 1,4-bis[3',7'-dimethyloctyl)oxy]benzene (**2**) is synthesized using a *Williamson* etherification with *p*-hydroquinone and 1-chloro-3,7-dimethyloctane (**1**). This chloride is prepared from the corresponding alcohol in high yield. In the second step compound (**2**), according to an adapted literature procedure[82] using concentrated HCl and *p*-formaldehyde in acetic anhydride, yields 1,4-bischloromethyl-2,5-bis[3',7'-dimethyloctyl)oxy]-benzene (**3**). The aromatic acetonitrile (**4**) was prepared from **3** *via* nucleophilic substitution with sodium cyanide in DMF. The overall yield of the four steps is 40 %.

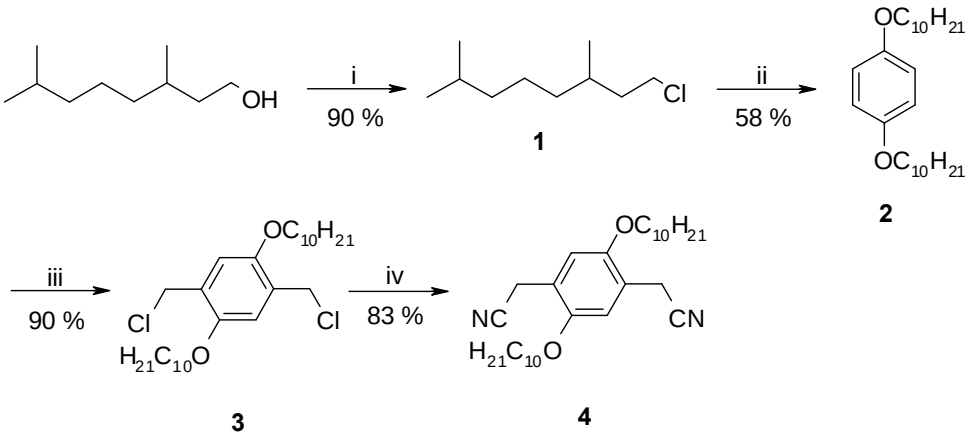

Figure 2-9: Synthesis of the central core: (i) $SOCl_2$, Py, 100 °C, (ii) hydroquinone, KOH, NaI, EtOH, reflux, (iii) p-CH_2O, Ac_2O, HCl, 90 °C, (iv) NaCN, DMF, reflux.

The thiophene carboxaldehydes (**5a-d**) were either commercial available (**5a**) or prepared *via* a *Vilsmeier* formylation with $POCl_3$ and DMF from the respective thiophene derivatives. For 3-octyl-2-thienylaldehyde (**5b**) a ratio of 9/1 (as determined by ^{1}H-NMR) of 2- to 5-formyl isomers was found which is a ratio similar to literature data[83].

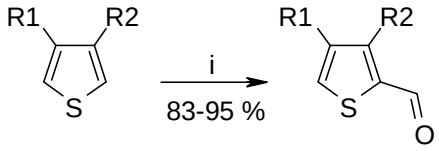

5a-d

a: R1 = R2 = H
b: R1 = H, R2 = *n*-octyl
c: R1, R2 = O-CH_2-CH_2-O
d: R1, R2 = O-CH_2-CH(*n*-tetradecyl)-O

Figure 2-10: Synthesis of the thiophene carboxaldehydes: (i) $POCl_3$, DMF, 55 °C.

The aryl unit with a cyanogroup is among the most widespread electron withdrawing groups in organic chemistry and can be easily obtained by applying a *Knoevenagel* condensation[4,84] of a thiophene carboxaldehyde (**5a-d**) with an aromatic acetonitrile moiety (**4**) in

refluxing methanol containing sodium *t*-butoxide. Yields of this *Knoevenagel* condensation are in the range of 46-72 %.

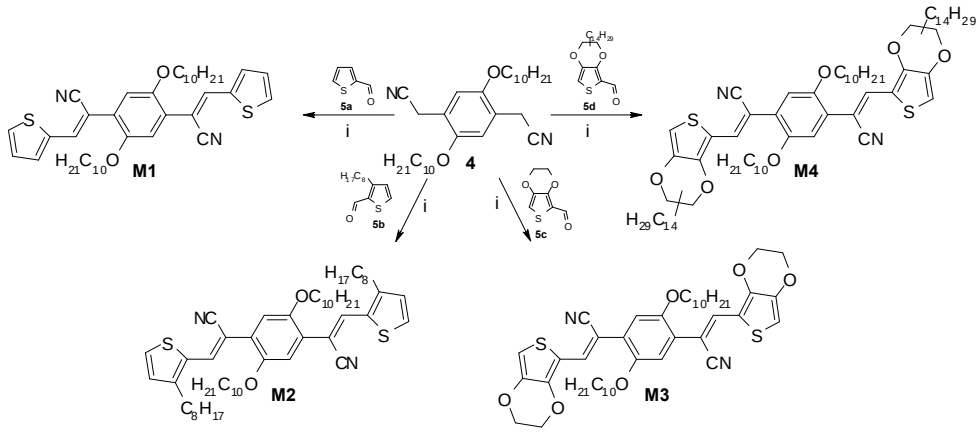

Figure 2-11: Knoevenagel condensation: (i) Na-tBuO, MeOH, reflux.

By this synthesis method four monomers were prepared which structure consists of a central dialkoxyphenylene core *p*-disubstituted by two thiophene derivatives through a cyanovinylene linker. The long alkoxychains on the central core enhance the solubility of the final polymer. By keeping both the central core and the acceptor strength constant, the influence of thiophenes with different donor characteristics was studied. Furthermore the influence of extra solubilizing chains on the thiophene part was studied.

Structural characterization of M3

As an example the NMR spectra of monomer **M3** will be analyzed in detail. For the proton and carbon chemical shift assignment, we made use of one dimensional techniques like ^{1}H-NMR (Figure 2-13) and ^{13}C-NMR (Figure 2-17) in combination with 2D-NMR techniques like direct coupling HETCOR (J = 140 Hz) (heteronuclear chemical shift correlation) (Figure 2-14 and Figure 2-15) and long range HETCOR (J = 8 Hz) (Figure 2-16). A direct coupling HETCOR indicates which proton is attached to the corresponding carbon atom. So a clear distinction between all proton resonances can be made. For the determination and

assignment of the quaternary carbon resonances a long range HETCOR experiment was set up. In such experiment a correlation is made between a carbon atom shift and a proton shift 2 and/or 3 bonds further. For reasons of clarity the atomic numbering of the protons and carbons were made separately (Figure 2-12).

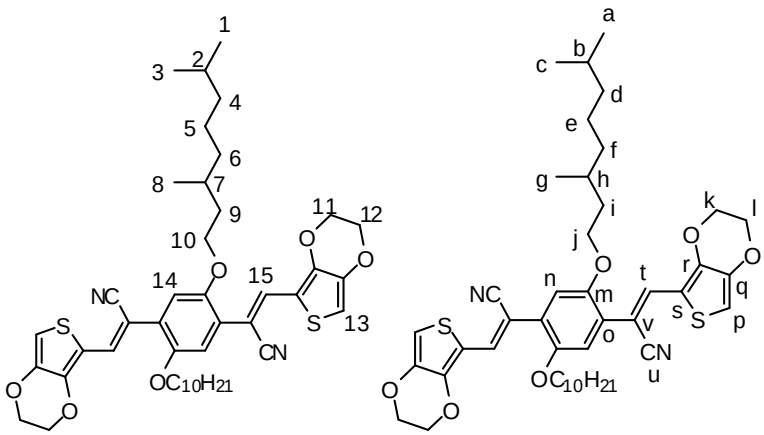

*Figure 2-12: Atomic numbering of **M3**; ^{1}H (left) and ^{13}C (right)*

^{1}H NMR chemical shift assignment

In the ^{1}H-NMR spectrum of **M3** a clear distinction can be made between the aliphatic, the etheric and the aromatic/olefinic protons. Since the C_{10} side chain is identical to the side chain in MDMO-PPV, the assignment was already accomplished[82] and identical chemical shift values were observed (inset of Figure 2-13). By means of integration, the assignment of the etheric protons H_{10}-H_{12} could be made. Two aromatic signals, H_{13} and H_{14} can be assigned by comparing their chemical shift values with those of the starting compounds and as expected, the remaining vinylic proton H_{15} is assigned to the most downfield signal. An overview of the ^{1}H chemical shift values is given in Table 2-1.

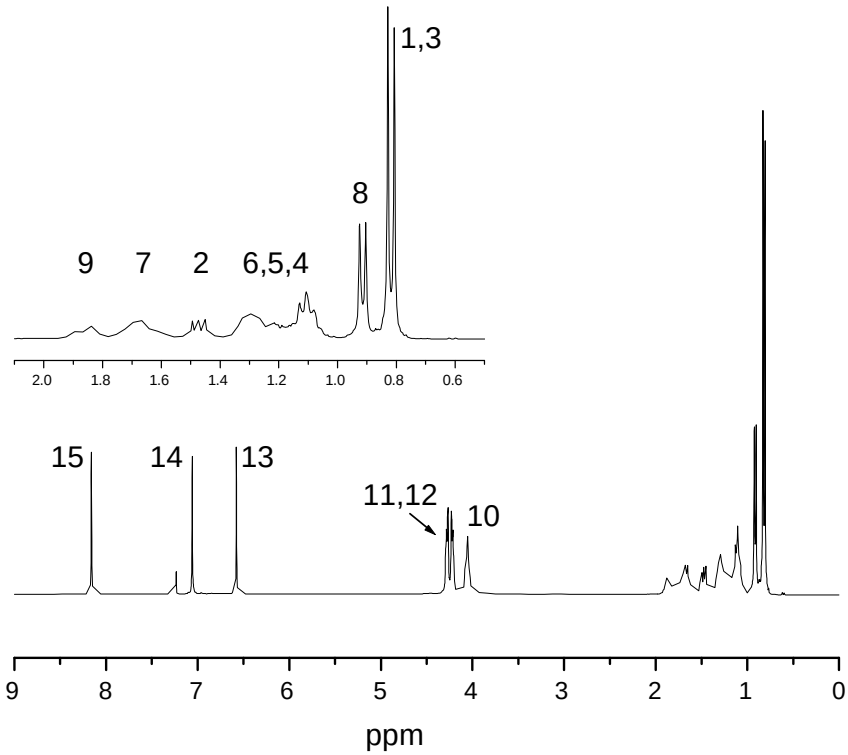

*Figure 2-13: ^{1}H-NMR of **M3** in $CDCl_3$.*

*Table 2-1:^{1}H NMR chemical shift values of **M3**.*

Proton	δ (ppm)	Proton	δ (ppm)	Proton	δ (ppm)
1-3	0.82	8	0.92	13	6.59
2	1.47	9	1.86	14	7.07
4-5-6	1.30-1.10	10	4.06	15	8.16
7	1.67	11-12	4.28-4.23		

^{13}C NMR chemical shift assignment

After assigning the proton chemical shifts, the assignment of the corresponding carbon signals is straightforward by means of direct HETCOR. In Figure 2-14 the aliphatic part of the direct coupling HETCOR spectrum is shown. From this spectrum, carbons C_a-C_i can be assigned.

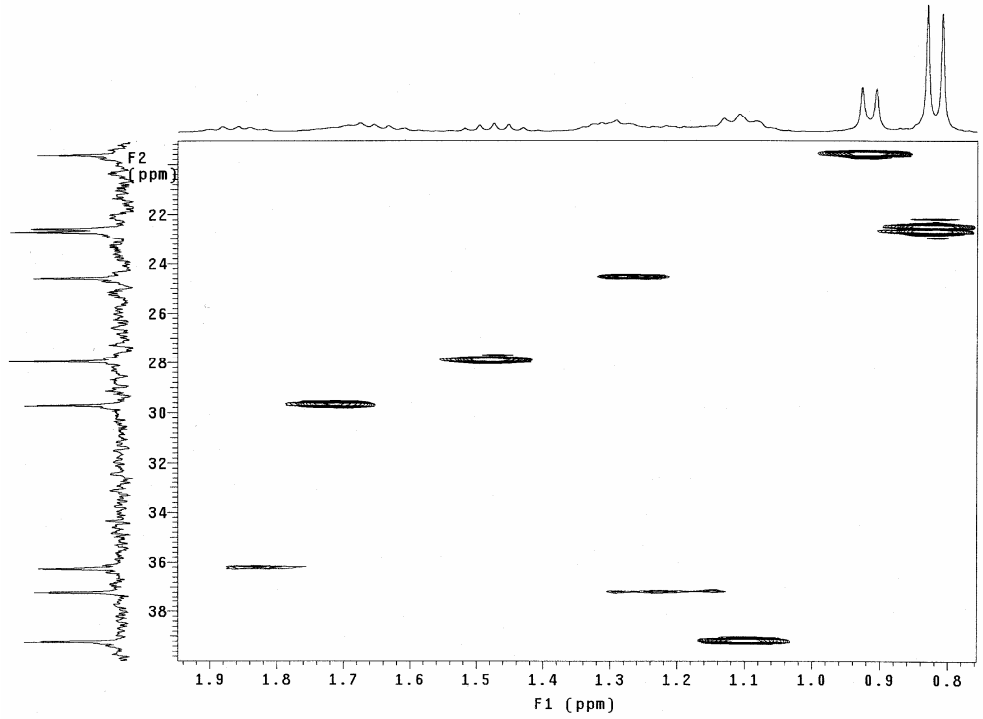

*Figure 2-14: Aliphatic part of the direct HETCOR spectrum of **M3**.*

From the etheric and aromatic part of the direct coupling HETCOR spectrum (Figure 2-15) carbons C_j-C_l can be assigned. By this method, also the aromatic and olefinic carbons C_n, C_p and C_t are determined. This still leaves 7 quaternary aromatic carbon signals unassigned.

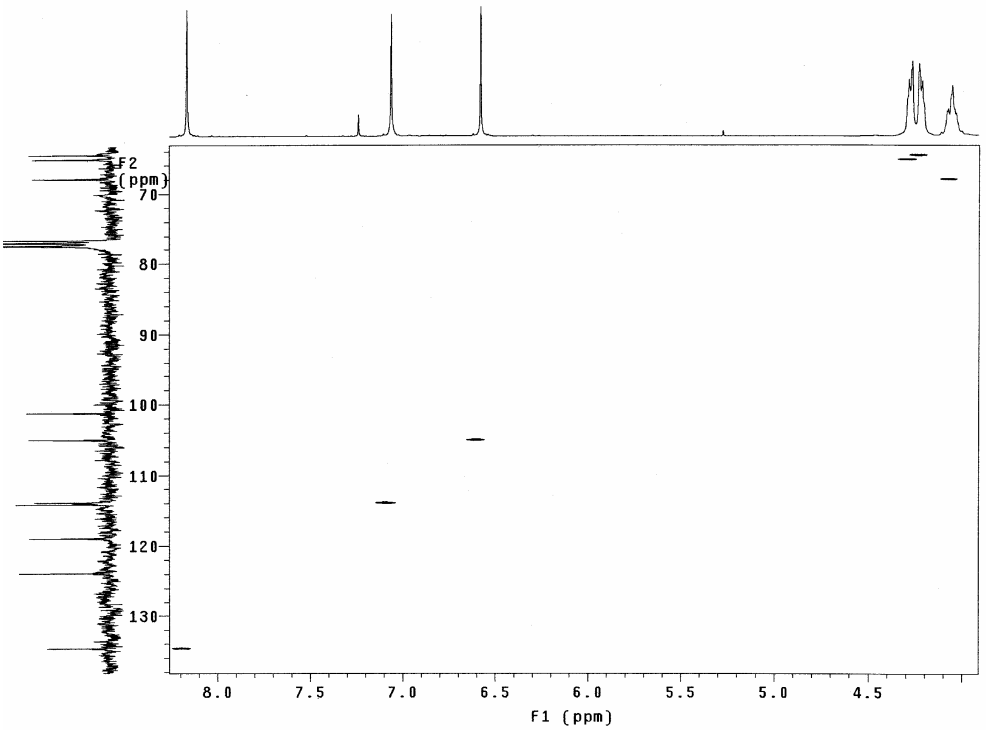

*Figure 2-15: Aromatic and alkoxy part of the direct HETCOR spectrum of **M3**.*

In long range HETCOR experiments of phenylic systems mainly (vicinal) $^{3}J_{C\text{-}H}$ couplings are visualized. This means $^{3}J_{C\text{-}H}$ couplings between H_{13} and the carbons C_r and C_s, between H_{14} and C_m, C_o and C_v and between H_{15} and C_o, C_r and C_u. According to the correlations observed in Figure 2-16, the resonance at 123.8 ppm correlates with H_{14} and H_{15} and thus can be assigned to C_o. Further H_{14} correlates with a resonance at 101.2 ppm and a resonance at 150.5 ppm. It is clear that the signal at 150.5 ppm can be assigned to C_m since it is more downfield (next to O atom) than C_v (next to C atom) which, as a consequence, can be assigned to the signal at 101.2 ppm. The resonance at 114.2 ppm correlates with H_{13} and H_{15} which means that this signal should be allocated to C_r. However, it is unlikely that an aromatic carbon atom next to an oxygen atom gives a signal that far upfield. A more plausible explanation is found if a $^{2}J_{C\text{-}H}$ coupling is considered between H_{15} and C_s and to assign the signal at 144.2 ppm to C_r. The last correlation

between the signal at 118.9 ppm and H_{15} originates from C_u. All assignments but one are made, which automatically means that C_q can be allocated to the signal at 141.3 ppm. An overview of the ^{13}H chemical shift values is given in Table 2-2 and Figure 2-17.

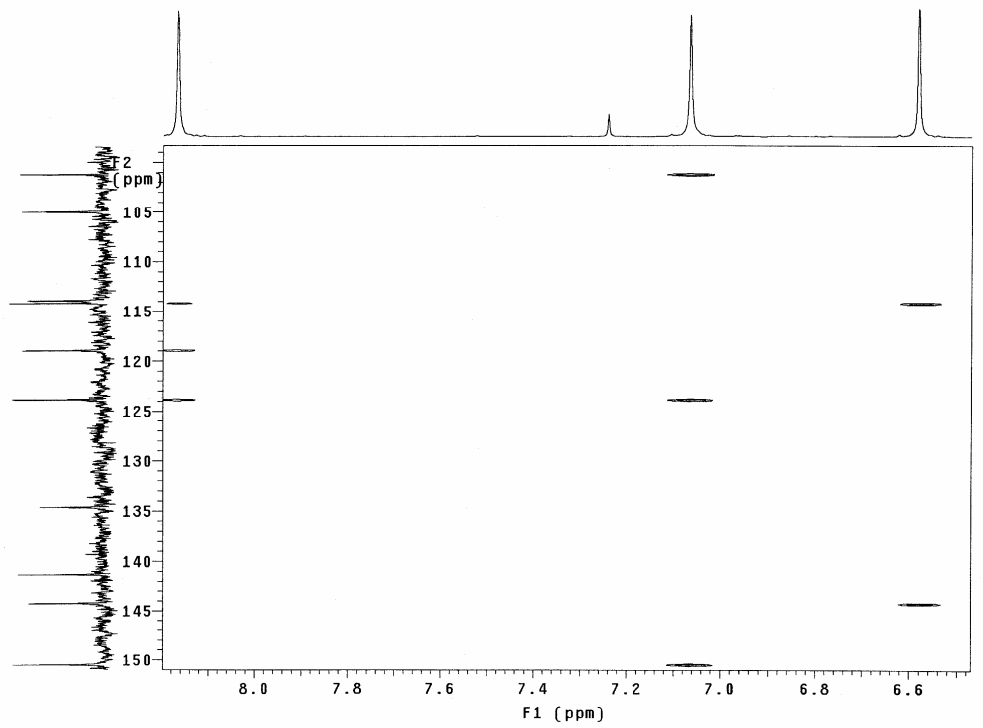

*Figure 2-16: Aromatic part of the long range HETCOR spectrum of **M3**.*

*Table 2-2: ^{13}C NMR chemical shift values of **M3**.*

Carbon	δ (ppm)	Carbon	δ (ppm)	Carbon	δ (ppm)
a-c	22.6-22.7	i	36.2	q	144.2
b	27.9	j	67.87	r	141.3
d	39.21	k-l	64.5-65.1	s	114.2
e	24.6	m	150.5	t	134.6
f	37.2	n	113.9	u	118.9
g	19.6	o	123.8	v	101.2
h	29.7	p	105.0		

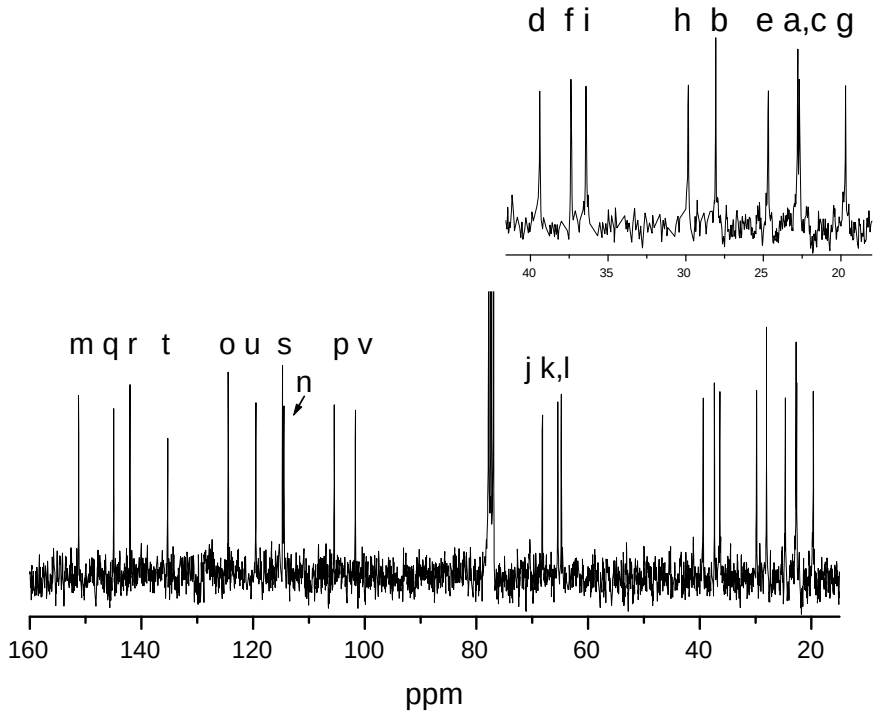

*Figure 2-17: ^{13}C-NMR of **M3** in $CDCl_3$.*

2.3 Polymerization

The chemical oxidative polymerization with $FeCl_3$ is a convenient way to polymerize these monomers. It is the most straightforward method since no further modifications of the monomers are required. The main disadvantage of this method is the low regiospecificity which leads to about 20 % regiochemical defects for P3AT polymerized in this way[63]. These defects involve head-to-head (HH) and head-to-tail (TT) couplings besides the wanted head-to-tail (HT) couplings as shown in chapter one. However, since all synthesized monomers are symmetrically substituted, the resulting polymers will always be completely regioregular, both in substitution and in composition of the aromatic units. Our aim was to find the best possible polymerization

conditions leading to the maximum amount of soluble neutral polymers with the highest molecular weights. This is relevant for the processability and mechanical properties of films made of these conjugated polymeric materials. To meet this goal, several parameters were investigated.

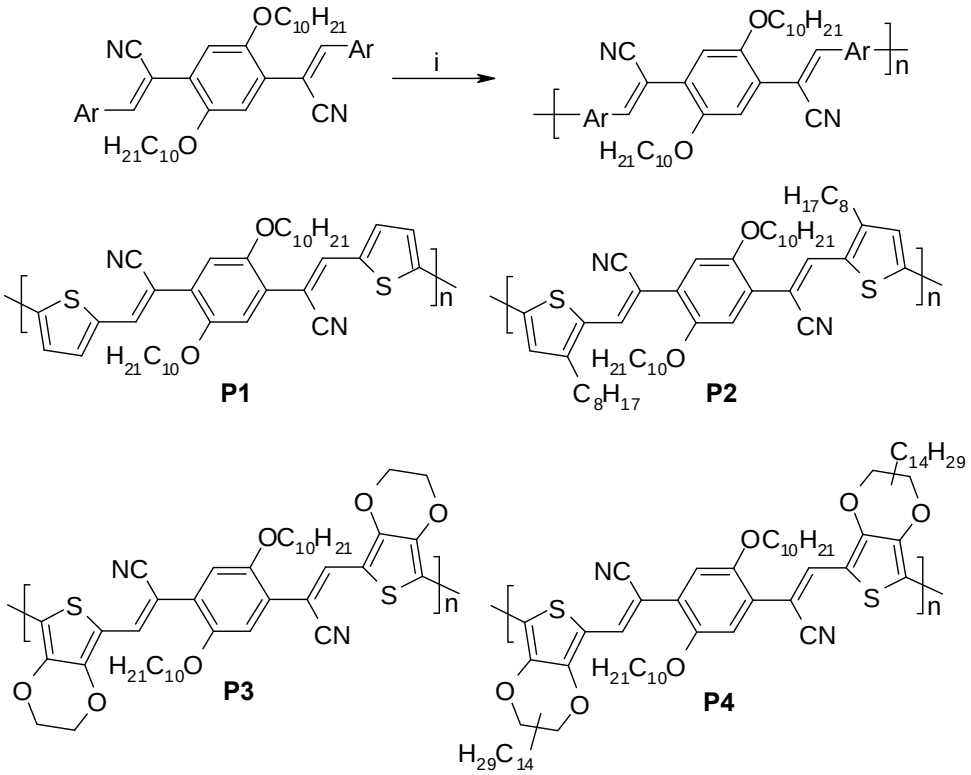

Figure 2-18: Oxidative polymerization: (i) $FeCl_3$, $CHCl_3$, RT.

2.3.1 Influence of time

The polymers were prepared by chemical oxidation of the monomers using $FeCl_3$ according to a procedure similar to that of Sugimoto *et al.*[59] (Figure 2-18). Polymerization of the monomers has been performed using three different reaction conditions (Table 2-3), deviating in the reaction times employed. The reaction proceeds with the formation of an initial dark-blue color and a subsequent black

precipitate. After the polymerization, the polymers contain residual iron(III)salts which can be reduced in concentration with rigorous purification. A first precipitation in MeOH and a second in MeOH/Hydrazine not only removes residual $FeCl_3$, the latter also dedopes the polymers. Further traces of iron(III)salts are removed by Soxhlet extraction with methanol. During this step the polymer is also purified from unreacted monomer. Further extraction with acetone removes oligomeric and low molecular weight fractions from the polymer and the soluble fraction is eventually collected by extraction with chloroform.

*Table 2-3: Polymerization results for monomers **M1 - M4**.*

	Time [h]	M_w[a]	M_n[a]	PD[a]	Y1[b] [%]	Y2[c] [%]
P1	24	136000	53000	2.5	52	26
	48	32000	5500	5.8	24	35
	72	18000	5600	3.1	22	57
P2	24	35000	15000	2.3	82	91
	48	43000	7000	6.2	28	80
	72	7900	2500	3.2	30	85
P3	24	189000	65000	2.9	56	20
	48	33000	7700	4.3	31	43
	72	33000	10000	3.3	37	41
P4	24	40000	14000	3.0	76	82
	48	21000	7000	3.0	14	90
	72	24000	3500	6.7	18	93

[a] *Determined by means of SEC in THF against polystyrene standards.*

[b] *Overall yield.*

[c] *Soluble polymer yield with respect to the overall yield.*

Polymerization results are shown in Table 2-3 where the characteristics of the different polymers from the different polymerizations are summarized. The weight-average molecular weights (M_w), the number-average molecular weights (M_n) and molecular weight distribution (PD) of the polymers have been determined by analytical SEC in THF against polystyrene standards. The reported overall yields (Y1) were determined after extraction with acetone and the soluble polymer yield (Y2) indicates the soluble fraction of the polymer in chloroform.

It is clear that, for all polymers, longer reaction times cause lower molecular weights and lower overall yields (Y1). This is probably due to the presence of HCl in the reaction medium, although most of the HCl, formed during the reaction, is removed by the argon flux. The small amount that is left, in combination with very long reaction times induces degradation of the polymer chains, yielding highly dispersed, low molecular weight polymers. Our attempt to increase the solubility of the polymers by introduction of long alkyl side chains (**P2** and **P4**) was successful as indicated by the high soluble polymer yield (Y2) comprised between 80 and 93 %. Another surprising observation for these alkyl substituted polymers (**P2** and **P4**) is that the molecular weights are much lower than for the non-alkylated polymers (**P1** and **P3**). Possibly, the sterical hindrance induced by the alkyl side chains on the thiophene units makes the monomers less reactive and causes the lower molecular weights.

2.3.2 Reproducibility

One of the problems regarding this polymerization is that, under the same conditions, the method often gives variable results in yield, molecular weight and polydispersity. However, to improve the reproducibility of the polymerizations, anhydrous $FeCl_3$ was freshly prepared from commercial $FeCl_3$. A detailed procedure for the purification of $FeCl_3$ is given in the appendix. During the polymerization,

fast stirring and a strong argon flow ensures that the HCl, formed during the reaction, is removed from the reaction vessel. This is an important issue since the evolved HCl consumes $FeCl_3$, probably by complexation ($FeCl_4^-$) and this results in lower yields and polymers with lower molecular weights[60]. As an example the results of experiments in duplex of **P3** are compared in Table 2-4. In method 1 commercial $FeCl_3$ was used without further purification and no Ar flow was used. In method 2 purified $FeCl_3$ was used as well as an Ar flow. All other parameters were kept the same. It is clear that by using optimized reaction conditions a substantial better reproducibility can be achieved. Furthermore higher M_w and overall yields were obtained.

*Table 2-4: Reproducibility of the oxidative polymerization of **P3***

	Method 1[a]		**Method 2[b]**	
	Batch 1	**Batch 2**	**Batch 1**	**Batch 2**
Yield	20	37	50	56
M_w	80000	39500	175000	189000
PD	6.8	2.1	2.5	2.9

[a] *Commercial $FeCl_3$ and no Ar flow*

[b] *Purified $FeCl_3$ and Ar flow*

2.4 Characterization

The following characterization of electronic properties has been carried out on the samples prepared with a polymerization time of 24 h, since they have the highest molecular weights and the lowest polydispersities.

2.4.1 Optical absorption

The electronic absorption data of the various polymers are listed in Table 2-5. All spectroscopic properties were measured both as thin film on quartz (Figure 2-19a) and in chloroform solution (Figure 2-19b).

*Table 2-5: Optical data of the polymers **P1 - P4** measured both in $CHCl_3$ solution and as thin film.*

	$CHCl_3$ solution		**Film**		
	λ_{max} [nm]	**λ_{onset} [nm]**	**λ_{max} [nm]**	**λ_{onset} [nm]**	**Eg [eV][a]**
P1	500	650	520	700	1.77
P2	490	600	540	720	1.72
P3	580	710	630	780	1.59
P4	560	680	570	720	1.72

[a]*Calculated from the intersection of the tangent on the low energetic edge of the absorption spectrum with the abscissa.*

Figure 2-19a shows that the absorption maximum (λ_{max}) of **P2** exhibits a 20 nm red shift as compared to **P1**. This shift is also observed for the band gap. The low energetic edge of the absorption spectrum of **P1** is at 700 nm which corresponds to a band gap (Eg) of 1.77 eV, while for **P2** the absorption onset is at 720 nm corresponding to a Eg = 1.72 eV. This behavior is a result of the electron-releasing effect of the octyl chains. Apparently, the electronic substituent effect created by the introduction of the alkyl side chains is larger than the possible effect of reduced electronic interchain interactions as well as the increased disorder in the conjugated system due to sterical hindrance imparted by the octyl side chains. The effect of sterical hindrance can be seen in **P3** when compared to **P4**. Here there is a blue shift of 60 nm. This is due to the larger interchain distances imposed by the substituents attached at a sp^3 carbon which leads to a bigger decrease of π-stacking interactions in the solid-state. The low energy shoulder, seen for **P1** (630 nm) and

P3 (720 nm) and the absence hereof for **P2** and **P4** is a further evidence of strong π-stacking interactions for the former two polymers and more disorder for the latter two. When comparing **P3** with **P1**, **P3** shows a bathochromic shift of 100 nm compared to **P1** and the band gap of **P3** is 0.2 eV lower than the band gap of **P1**. Here, as it is also observed by comparing the optical data of poly(thiophene) (λ_{max} = 480 nm, Eg = 1.9 eV) with poly(3,4-ethylenedioxythiophene) (λ_{max} = 610 nm, Eg = 1.6 eV), the strong electron releasing ethylenedioxy groups in **P3** causes this shift.

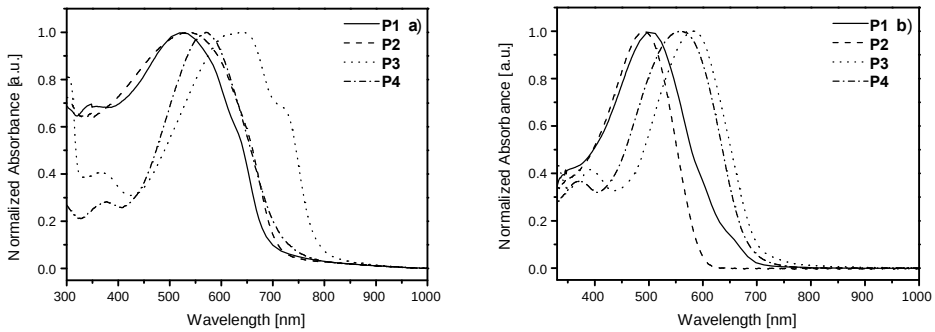

*Figure 2-19: Normalized UV-Vis absorption spectra of **P1 - P4** as thin film (**a**) and in $CHCl_3$ solution (**b**).*

Due to the absence of π-stacking in solution (Figure 2-19b; Table 2-5), overall, the λ_{max} and λ_{onset} values are lower than in the solid state although all trends mentioned above are also observed in solution. For **P4**, when measured in solution the optical spectrum remains practically identical to the the spectrum measured in film, with however a small (ca. 10 nm) hypsochromic shift of the absorption maximum. This again confirms that for **P4** almost no additional π-stacking interaction is observed when going from solution to a thin film.

Overall, as we expected, all four polymers show low band gaps and by increasing the electron-releasing effect the band gap of the polymers decreases from **P1>P2>P3**. For **P4**, the introduction of alkyl substituents gives rise to a higher band gap compared to **P3**. The

reason for this behavior is related to the sterical hindrance imparted by the tetradecyl substituents that affect the planarity of the molecule.

It is noteworthy that no significant degradation of the conjugated system is observed in the temperature dependent UV-Vis spectrum during the heating process until 225 – 250 °C[85, 86]. Notwithstanding, thermal stability up to 225 – 250 °C is sufficiently high for potential device applications.

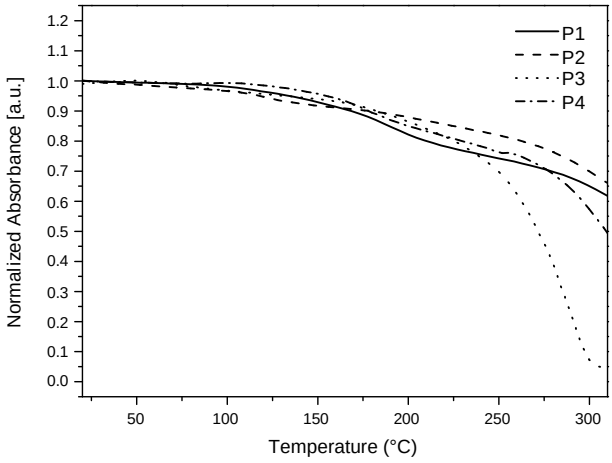

*Figure 2-20: UV-Vis absorbance profiles at λ_{max} as a function of temperature for **P1**-**P4**.*

2.4.2 Electrochemistry

Cyclic voltammetry (CV) using 0,1 M $TBAPF_6$ as a supporting electrolyte in anhydrous acetonitrile (ACN) was employed to study the electrochemical behavior of the polymers and to estimate their highest occupied molecular orbital (HOMO) and lowest unoccupied molecular orbital (LUMO) energy levels. The cyclic voltammograms display quasi reversible oxidation and reduction processes (Figure 2-21) for all the polymers.

Therefore, electrochemically determined band gaps derived from the difference between onset potentials for oxidation and reduction of polymers can be deduced using following equation:

$$E_g = E_{onset}^{ox} - E_{onset}^{red}$$

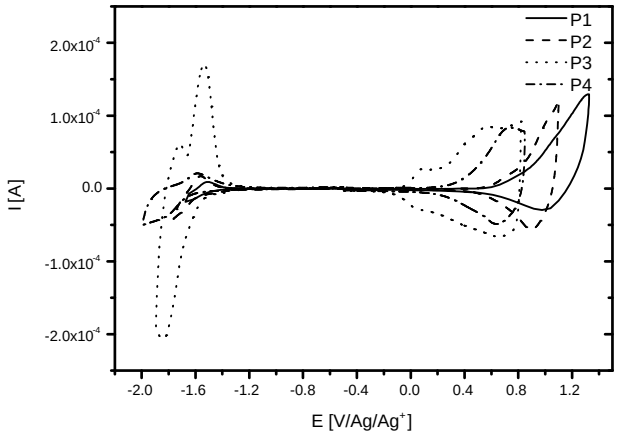

*Figure 2-21: Cyclic voltammograms of the oxidation and reduction behavior of thin films of **P1 - P4**.*

The CV data of the various polymers is gathered in Table 2-6. With an ethylenedioxy group incorporated (**P3**), a decrease in band gap of ca. 0.7 eV was found going from **P1** to **P3**. Due to the introduction of the ethylenedioxy group attached on the thiophene ring, the oxidation onset of **P3** decreases, *i.e.* the HOMO level increases, where there is only a minimal effect on the reduction onset, *i.e.* the LUMO level remains comparatively unchanged. As a result, an electron donating group like an ethylenedioxy group lowers the band gap energy significantly.

The effect of alkyl chain substitution on the oxidation and reduction process of the polymers can also be compared by using the values of **P1** and **P2** reported in Table 2-6. The onset oxidation and reduction potentials do not change when an octyl side chain is attached onto the thiophene ring, *i.e.* the HOMO and LUMO energy levels remain

unchanged. The redox potentials of **P3** and **P4** can also be compared. **P4** has an additional alkyl substitution on the ethylenedioxy group of **P3**. This increases the oxidation potentials as compared with their non-substituted analogue **P3**, *i.e.* HOMO level decreases, as a result of the decreased coplanarity of the molecules imparted by the alkyl chains. Also in this case, the alkyl substitution has no influence on the reduction potential. This results in an increase of the electrochemical band gap. Important to note is that it is impossible to understand the influence of the cyanovinylene linkage when this series of polymers is used. However, it is suggested that the reduction is mainly dominated by the presence of the cyanovinylene bound since the LUMO energy levels of the four polymers do not significantly change. The variations of the band gap are mainly determined by the HOMO of the polymer.

*Table 2-6: Electrochemical data of the polymers **P1 - P4**.*

	E^{ox}_{onset} [V]	E^{red}_{onset} [V]	HOMO [eV]	LUMO [eV]	Eg [eV]
P1	+ 0.62	-1.46	-5.50	-3.42	2.08
P2	+ 0.57	-1.55	-5.48	-3.36	2.12
P3	- 0.04	-1.60	-4.83	-3.27	1.56
P4	+ 0.40	-1.63	-5.34	-3.31	2.03

The oxidation process can also be observed visually. A color change of the films from blue to light yellow was observed upon oxidation. Subsequently, in the reverse process, upon dedoping the color of the film returned to blue. This observation further confirms the reversibility of the p-doping process.

From these results, it is clear that changing of the substituents on the thiophene unit allows the modulation of the HOMO/ionization potential. This should be useful to enhance the absorption of photons in the active layer of a plastic solar cell and to facilitate efficient charge collection at the electrodes.

Figure 2-22 exhibits the resulting energy band diagram in relation to the relative energy levels of the most frequently employed acceptor in organic solar cells, PCBM, and the workfunctions of indium tin oxide (ITO) and aluminum (Al), which are usually applied as electrodes in polymer solar cells. The HOMO of the polymers **P3** and **P4** is distinctively higher in energy than that of PCBM. However, not the HOMO energy levels but the relative positions of the donor LUMO and the acceptor LUMO are important for the intended charge transfer. The difference between the LUMOs of **P1** - **P4** and PCBM is in the range of 0.6 eV, which is sufficiently high to enable an unrestricted and directed charge transfer.

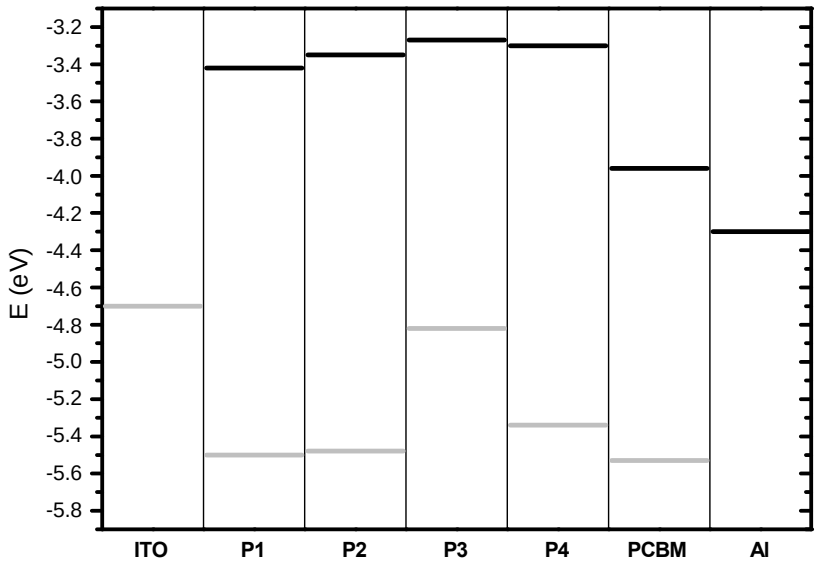

*Figure 2-22: Energy band diagram with HOMO/LUMO levels of **P1 - P4** and PCBM in relation to the work function of the common electrode materials ITO and Al.*

2.4.3 Charge-Transfer processes

Charge-Transfer processes were studied in close collaboration with Aranzazu Aguirre and Griet Janssen from the group of Etienne

Goovaerts at the physics department of the University Antwerp[87] and Le Huong Nguyen and Helmut Neugebauer from the group of Serdar Sariciftci at the Linz Institute for Organic Solar Cells (LIOS) in Austria[88].

Photoluminescence (PL) of the polymers (**P2** or **P3**) and their blend with PCBM was measured to check if there is an interaction of the two components in the excited state. PL quenching is often indicative of a charge transfer for many donor-acceptor blends[89]. The occurrence of charge transfer is confirmed by the quenching of the PL-emission (by a factor of ~5) when going from the pristine **P2** to the **P2**/PCBM film (Figure 2-23a) and, correspondingly, with the drastic decrease of the decay time (Figure 2-23b). It should be mentioned that the PL efficiency, even in the pure **P2** polymer film, is much lower than usually observed in MDMO-PPV. This points to a competition with an efficient non-radiative decay process. Further, one notices the large Stokes shift between the absorption maximum of the **P2** film (Figure 2-19) and the PL emission (Figure 2-23a). (~200 nm compared to a Stokes shift of ~100 nm for MDMO-PPV). This relatively large Stokes shift indicates an important configurational relaxation in the excited state.

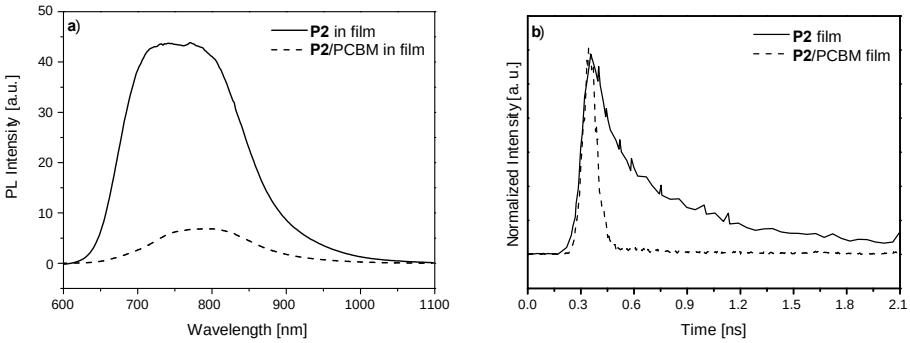

*Figure 2-23: **a)** Photoluminescence spectra of thin spin coated films of **P2** and of the blend **P2**/PCBM. **b)** Time decay (normalized) of the PL emission of **P2** and **P2**/PCBM films. The decay of the **P2**/PCBM blend is resolution limited by the response of the streak camera detector.*

Figure 2-24 shows PL (solid lines) of pristine **P3**. As can be noticed, **P2** shows stronger PL compared to **P3**. Also for this polymer, when adding PCBM as an acceptor at a ratio 1:2 wt, the PL of the pristine polymer is quenched by a factor of 5, implying that there is an interaction between the two components in the excited state.

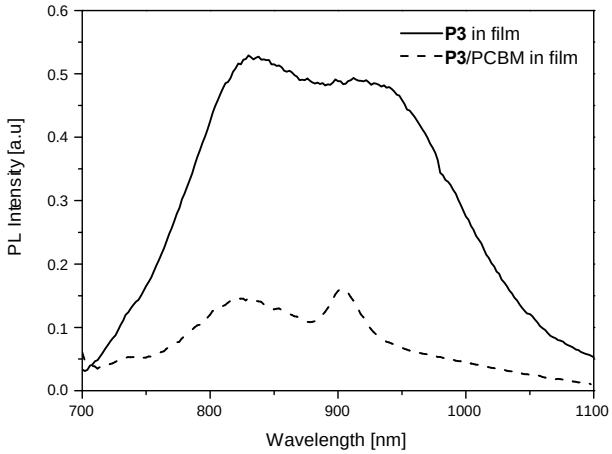

*Figure 2-24: Photoluminescence spectra of thin spin coated films of **P3** (solid line) and of the blend **P3**/PCBM (dashed line).*

Photoinduced absorption (PIA) spectra of pristine **P2** and a blend of **P2**:PCBM (1:2 wt) films are shown in Figure 2-25 (left). Two PIA features of pristine **P2** are observed at 1.10 and 1.5 eV with an additional shoulder at 1.64 eV (solid line). The photoexcitation pattern of **P2** is more complicated compared to that of **P3** (Figure 2-25 right). This could be the results of the disorder effect introduced by the long alkyl side chain (C_8H_{17}) in **P2**. The PIA of the composite of **P2** with PCBM (1:2 wt) (dashed line, Figure 2-25 left) shows analogous absorption features at 1.2 and 1.7 eV. Additionally, observation of a weak absorption is obtained at < 0.7 eV which is assigned to low-energy absorption. The broad absorption centered at 1.2 eV is designated to the contribution of the overlapping between the shifted peak at 1.1 eV and the PCBM

radical anion band (expected at 1.2 eV). Hence, there is indication of photoinduced charge generation in this composite system.

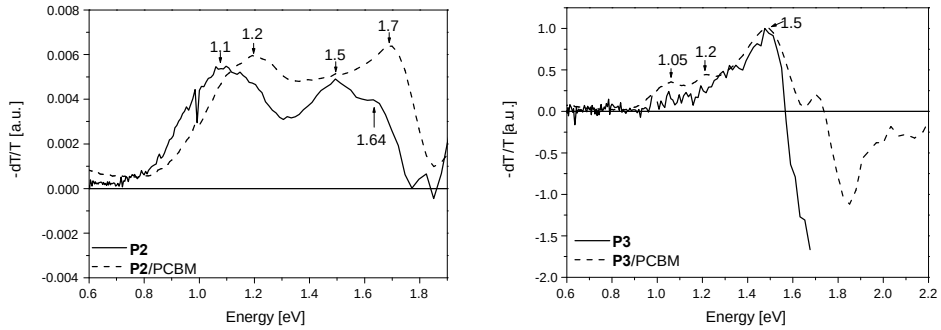

*Figure 2-25: PIA spectra of pristine polymer (solid line) and the polymer/PCBM blend at 1:2 wt. (dashed line) recorded at 80 K following chopped cw excitation at 514 nm, 218 Hz: left for **P2**; right for **P3.***

The PIA spectra of a pristine **P3** film and a blend of **P3**:PCBM (1:2 wt) are shown in Figure 2-25 (right). The PIA spectrum of the pristine **P1** exhibits a pronounced single absorption peak at 1.5 eV (solid line), which is attributed to a $T_n \leftarrow T_1$ transition of the T_1 triplet excited state. In the mixture with PCBM three new peaks are observed at < 0.8, 1.05 and 1.2 eV (dashed line). We propose the weak PIA bands around <0.8 and 1.05 eV are attributed to low-energy and high-energy polaronic absorptions. A PIA band around 1.2 eV is assigned to the known absorption of the methanofullerene radical anion which was often observed at 1.15 to 1.2 eV[90, 91]. The obtained PIA results supported by PL quenching are an evidence for charge transfer in the composite upon photoexcitation.

Further proof for photoinduced charge transfer is given by Light-induced Electron Paramagnetic Resonance (LI-EPR) measurements, showing the creation of two radicals upon illumination of the blends (Figure 2-26). LI-EPR measurements were performed by Aranzazu Aguirre and Griet Janssen from the group of Etienne Goovaerts at the physics department of the University Antwerp. **P2** was used as a model

system for these measurements. The two light induced EPR features, shown in Figure 2-26, are comparable to those commonly found in the EPR analysis of the charge transfer process in donor/acceptor blends like the standard MDMO-PPV/PCBM blend[92]. The signal at 3.3582 T corresponding to a g-value of g = 2.0000 is assigned to the negative PCBM−radical. The signal at lower field values (around 3.354 T) is assigned to the positive polaron (P^+) on **P2**, at g-values slightly larger than 2, close to that of the polaron in MDMO-PPV. Instead of the normally expected first derivative signal, an absorption-like shape of the P^+ radical was observed which is an indication of saturation effects and has been observed before for other blends[92]. It is also important to notice that radicals are formed previous to illumination, probably due to the presence of impurities in the polymer, despite rigorous purification.

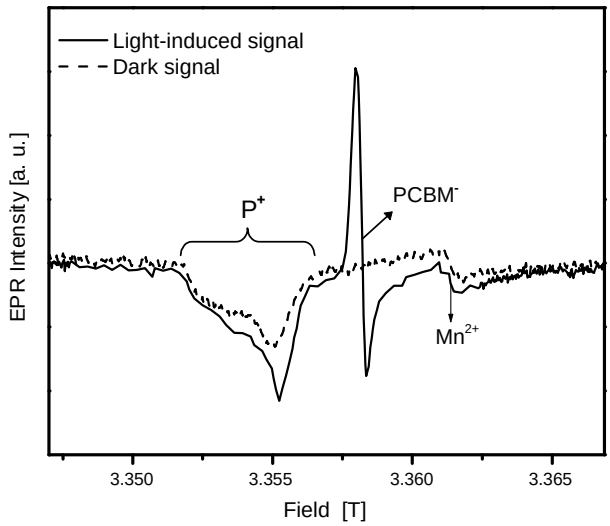

*Figure 2-26: EPR spectra of the **P2**/PCBM blend (T = 100 K). The dashed and solid line show the spectrum without and under illumination (λ_{exc} = 488 nm), respectively. The signal at low field values is assigned to the positive polaron (P^+) and the one at high field values to the $PCBM^-$ radical.*

2.5 Photovoltaic devices

Photovoltaic studies on solar cell devices were performed by Le Huong Nguyen and Helmut Neugebauer from the group of Serdar Sariciftci at the Linz Institute for Organic Solar Cells (LIOS) in Austria[88].

Typical I-V characteristics of ITO/PEDOT:PSS/**P2**:PCBM/LiF/Al (named **P2** device) and ITO/PEDOT:PSS/**P3**:PCBM/LiF/Al (named **P3** device) devices are shown, both in dark (dashed line) and under AM 1.5 illumination (solid line), in Figure 2-27a and Figure 2-27b respectively. The **P2** device performance shows open circuit voltages (V_{OC}) of 650 mV, short circuit currents (I_{SC}) of 0.5 mA/cm^2, fill factors (FF) of 0.42 and a conversion efficiency (η) of about 0.14 % while the **P3** device exhibits lower V_{OC} (400 mV), lower FF (0.22) but significantly higher I_{SC} (1.64 mA.cm^{-2}) leading to the same value of η = 0.14 %. Optimization of the device parameters by thermal annealing shows a slight increase in the final photovoltaic performance for the **P3** device with the following characteristics: V_{OC} = 350 mV, I_{SC} = 1.87 mA.cm^{-2}, FF = 0.29 (grey line in Figure 6b) which results in η = 0.19 % while annealing did not show improved effects on the **P2** device.

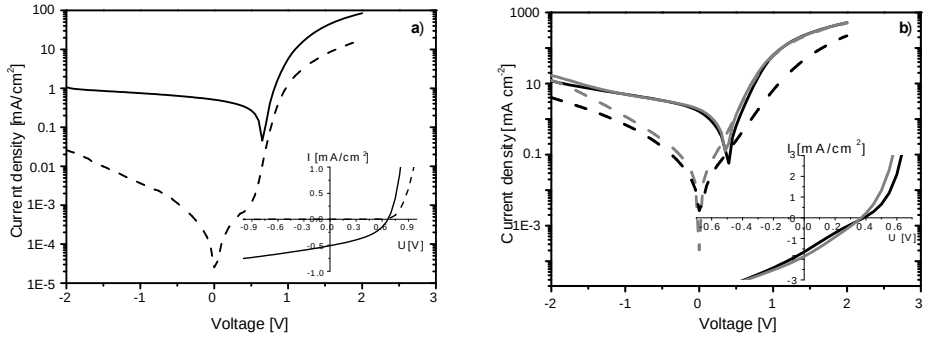

*Figure 2-27: Semilogarithmic and linear (inset) representations of I-V characteristics of **a)** ITO/PEDOT:PSS/**P2**:PCBM/LiF/Al and **b)** ITO/PEDOT:PSS/**P3**:PCBM/LiF/Al cells before (black line) and after (grey line) annealing. The solid line represents data obtained under illumination, while the dashed line is measured in the dark.*

Figure 2-28 shows the incident photon-to-current efficiency (IPCE) spectra (black lines) of the **P2** (Figure 2-28a) and the **P3** device (Figure 2-28b) with the normalized absorption of the corresponding pristine polymer films (dashed lines). With this technique the number of electrons produced from the cell under short-circuit conditions is related to the number of incident photons.

The photocurrent spectrum of the **P2** device shows an onset at about 710 nm (1.75 eV), close to the optical band gap and exhibits a maximum of 3 % at 600 nm (Figure 2-28a) while the IPCE spectrum for **P3** device extends its onset to higher wavelength at about 780 nm (1.54 eV) with a maximum absorption of more than 12% at 550 nm. **P3** possesses a quite low band gap (Eg = 1.59 eV) resulting in an increase in absorption of light. As a consequence the I_{SC} increases but at the same time V_{OC} is lowered. The lower band gap of the polymer resulting from a decrease in the oxidation potential (*i.e.* increasing the HOMO level) may therefore reduce the V_{OC} since the V_{OC} of polymer/fullerene-based solar cells depends on the energy difference between the HOMO of the donor and the LUMO of the acceptor[93]. The octyl substitution in **P2** decreases the HOMO level as compared to **P3**. This leads to an increase in V_{OC} for the **P2** device.

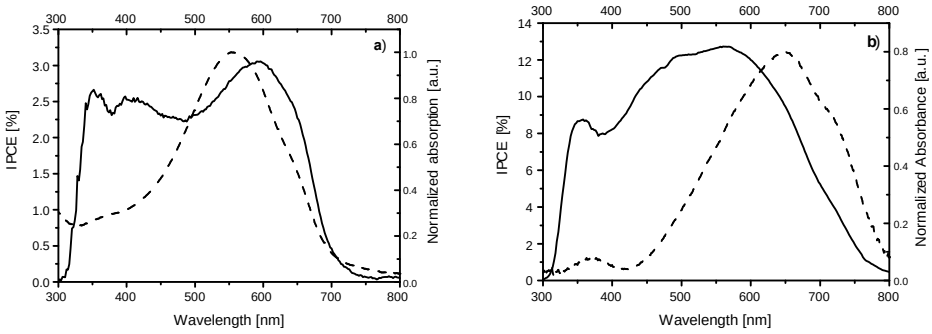

*Figure 2-28: Photocurrent spectrum of photovoltaic devices **a)** ITO/PEDOT:PSS/**P2**:PCBM/LiF/Al; **b)** ITO/PEDOT:PSS/**P3**:PCBM/LiF/Al (solid line) and the normalized optical absorptions for the corresponding pristine polymers (dashed line).*

To gain more insight into the effects of alkyl side chains on photoinduced charge transfer and photovoltaic performance, the morphology of the active layers was investigated using atomic force microscopy (AFM). Figure 2-29 shows the nanomorphology of the active layers of the **P2** and **P3** devices.

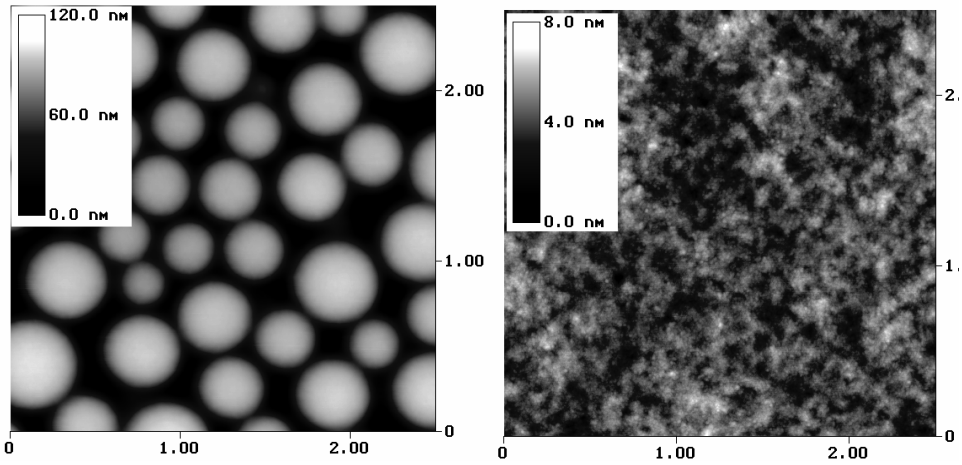

*Figure 2-29: AFM nanomorphology of the active layer of photovoltaic devices ITO/PEDOT:PSS/**P2**:PCBM/LiF/Al (left) and ITO/PEDOT:PSS/**P3**:PCBM/LiF/Al (right).*

Going from **P3** to **P2** with the introduction of the long alkyl side chains the surface roughness is increased which points directly to an increased nanoscale phase-separation within the film blend. Both polymer structures have long alkoxychains on the central core to provide solubility of the polymers. A **P3** device film shows a flat surface, no significant phase separation while dramatically larger phase separation was observed in the case of **P2** which may point to an alkyl side chain effect. Consequently the interfacial area in the active layer **P2** blend is reduced (compared to **P3**) leading to insufficient charge generation and separation in the **P2** blend. As a result I_{SC} of **P2** device is reduced significantly. It is important to note that the morphology can be influenced by other parameters as different solvents, etc. However in this case, the strong phase separation obtained for **P2** appears rather as

an issue of the alkyl side chain effect than as a solubility problem because the introduction of extra solubilizing chains for **P2** on the thiophene unit additionally increases the solubility.

The results for solar cell performance are disappointing in spite of both the lower band gap of the polymer and the efficient charge transfer in the blends with PCBM. Also, the electrochemical potentials are compatible with the requirements for this type of solar cells[94], with reasonable V_{OC} values although lower than in optimal devices. The low I_{SC} values observed for these devices eventually point to a low mobility of the charge carriers. Indeed, the hole mobility in the pure polymer films measured in a field effect transistor was found to be below 10^{-6} cm^2/Vs for all polymers.

2.6 Low band gap polymer with more polar side chains

2.6.1 Introduction

In an attempt to study the influence of the side chain on the central core, polymer **P5** is synthesized. **P5** has a similar structure as **P3** accept for the side chains on the benzene unit. In **P3** an alkoxy side chain was introduced while in **P5** a more polar oligoethylene side chain is used. The influence on the polymerization, solubility and electronic properties are examined and compared with the values of **P3**.

2.6.2 Synthesis

The synthesis strategy is similar to the synthesis of the previous polymers with only some small adaptations (Figure 2-30). The starting compound 1,4–bischloromethyl-2,5-bis{2-[2-(2-methoxy-ethoxy)-ethoxy]-ethoxy}benzene **6** is synthesized according to a literature procedure[95]. The aromatic acetonitrile (**7**) is then prepared from **6** *via* nucleophilic substitution with sodium cyanide in DMF. Subsequent

Knoevenagel condensation[4,84] of 3,4-ethylenedioxy-2-thienylaldehyde **(5c)** with **6** in refluxing methanol containing sodium *t*-butoxide gives the monomer **M5** in 88 % yield.

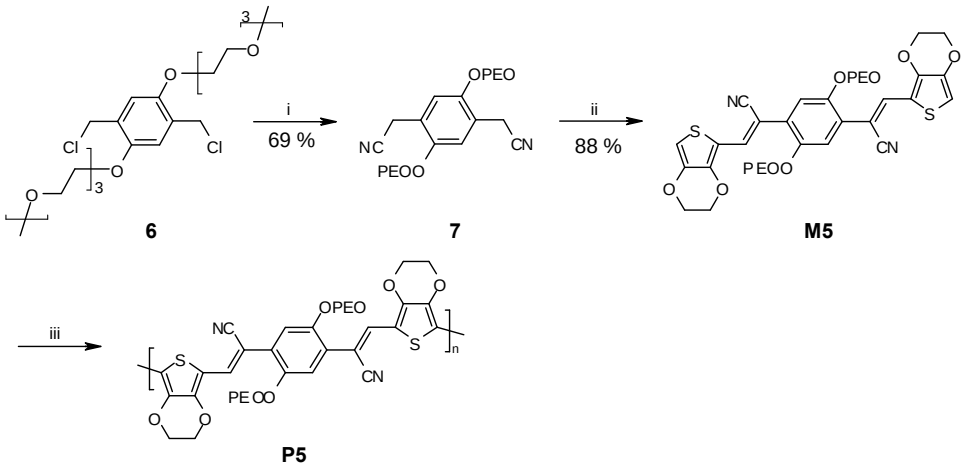

*Figure 2-30: Synthetic route toward the synthesis of monomer **M5** and polymer **P5**. (i) NaCN, DMF, reflux; (ii) **5c**, Na-tBuO, MeOH, reflux; (iii) $FeCl_3$, $CHCl_3$.*

The polymer iss prepared by chemical oxidation of the monomers using $FeCl_3$. The results of the polymerizations are shown in Table 2-7. The reported overall yields (Y1) were determined after extraction with acetone and the soluble polymer yield (Y2) indicates the soluble fraction of the polymer in chloroform. Since previous data revealed that shorter reaction times increase the molecular weights an experiment with a reaction time of only 3 h was carried out. However, with a short reaction time, only oligomers were obtained. The results of the polymerization for 24 h were somewhat better, but still way below the molecular weight obtained for **P3.** However one must be careful when interpreting these data. In view of the differences in solubility, molecular weights of both polymers were measured in different solvents. Hence, a straightforward comparison is impossible. Notwithstanding, these observed molecular weights suggest that the introduction of the more flexible oligo(oxyethylene) side chains makes the monomer significantly less reactive. This may be the result of a difference in sterical hindrance or

solvation/aggregation effects. The same trend was observed when adding long alkyl side chains in polymers **P2** and **P4**. It is also impossible to say whether the higher soluble polymer yield (Y2) is related to the more flexible oligo(oxyethylene) side chains or rather to the lower molecular weight.

*Table 2-7: Polymerization results for monomer **M5**.*

	Time [h]	M_w[a]	M_n[a]	PD[a]	Y1[b] [%]	Y2[c] [%]
P5	3	7900	6900	1.2	34	72
	24	28000	18900	1.4	70	70

[a]*Determined by means of SEC in DMF against polystyrene standards.*

[b]*Overall yield.*

[c]*Soluble polymer yield with respect to the overall yield.*

2.6.3 Characterization

2.6.3.1 Optical absorption

All spectroscopic properties were measured both as thin film on quartz substrates and in chloroform solution (Figure 2-31). UV-Vis absorption spectroscopy shows that the absorption maximum of **P5** in a thin film (λ_{max} = 570 nm) exhibits a 60 nm blue shift as compared to **P3** (λ_{max} = 630 nm, Figure 2-19). In solution this difference is only 10 nm (λ_{max} = 570 nm for **P5** and λ_{max} = 580 nm for **P3**). Another surprising fact is that λ_{max} of **P5** in a thin film is the same as in solution. The reason for this behavior is related to the difference in conformation of the conjugated backbone imparted by the oligo(oxyethylene) side chains, *i.e.* the planarity of the conjugated backbone is modified. The high energy shoulder, seen for **P3** in film (λ_{max} = 720 nm) and the absence thereof for **P5** provides further evidence of strong π-stacking interactions for the former polymer and more disorder for the latter. Apparently the flexible oligo(oxyethylene) side chains prevent **P5** from

closely packing in a thin film. The band gap for **P5** as derived from UV-Vis spectroscopy is 1.6 eV.

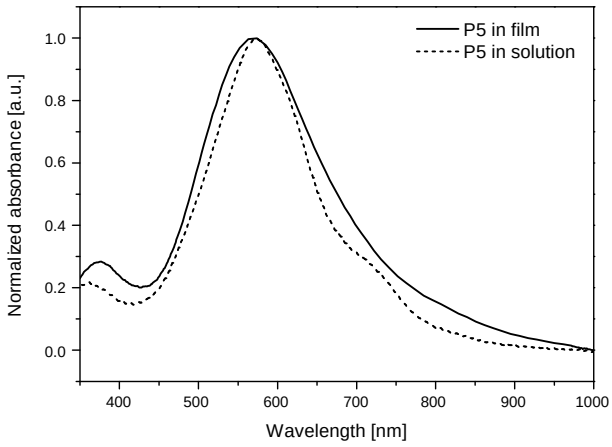

*Figure 2-31: Normalized UV-Vis absorption spectra of **P5** as thin film (solid) and in $CHCl_3$ solution (dash).*

2.6.3.2 Electrochemistry

An estimation of the relative position of HOMO/LUMO levels was determined with cyclic voltammetry (CV). The HOMO/LUMO levels are determined from the onsets of oxidation and reduction, respectively. In the anodic scan, the onset of oxidation of **P5** starts at –0.02 V *vs.* Ag/Ag^+; reduction at –1.46 V *vs.* Ag/Ag^+. This means a HOMO energy level of -4.82 eV and a LUMO energy level of -3.38 eV. Changing the side chains from alkoxy to oligoether on the central core does not affect the HOMO and LUMO energy levels (**P3:** HOMO = -4.83 eV and LUMO = -3.27 eV). Apparently, the influence of the exact nature of the alkoxy side chain has no significant effect on the HOMO and LUMO energy levels.

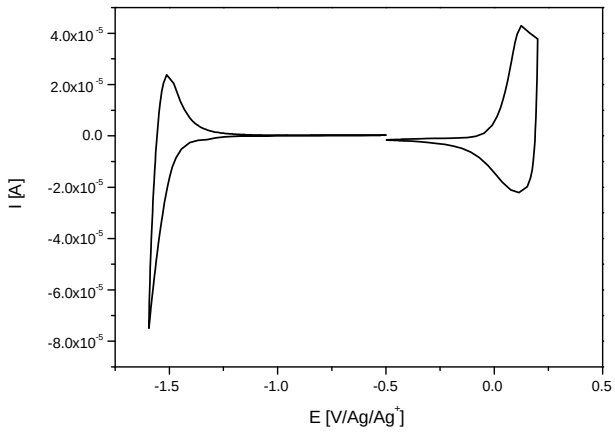

*Figure 2-32: Cyclic voltammograms of the oxidation and reduction behavior of thin films of **P5**.*

2.6.4 Photovoltaic device

A first attempt was made to construct a bulk heterojunction solar cell with polymer **P5** as a donor and PCBM as an acceptor at Konarka by David Muhlbacher from the group of Christoph Brabec. Preliminary solar cell characteristics for the **P5 device** are: I_{sc} = 0.67 mA/cm^2, V_{oc} = 0.20 V, FF = 42 %, η = 0.07 %. The charge carrier mobility measurements were carried out in a field effect transistor. However, the observed hole mobility was below 10^{-6} cm^2/Vs, which may well be an explanation for the low efficiency. These results are in line with the results obtained with polymers **P2** and **P3**.

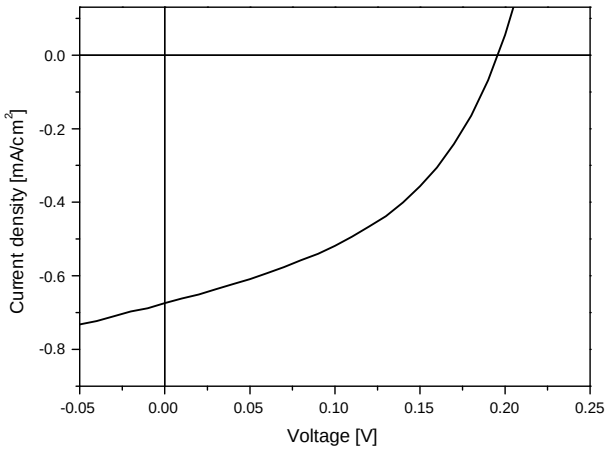

*Figure 2-33: Linear representation of I-V characteristics (AM 1.5, 100 mW/cm^2) of ITO/PEDOT:PSS/**P5**:PCBM/LiF/Al.*

2.7 Low band gap polymer bearing a push-pull molecule

2.7.1 Introduction

In order to improve solar cell efficiencies, the low mobility of the charge carriers must be improved significantly. One of the reasons of this low mobility is the large degree of disorder inherent to organic films deposited by the techniques available at industrial scale. Classical approaches to induce structural order at the nanoscale or molecular level are regioregularity[35], hydrogen bonding[96], liquid crystal groups[73], etc. An alternative principle is based on polar order[14]. When molecules with a large ground-state dipole are grafted onto a conjugated polymer, orientation can be introduced by applying a static electric field. This field can order the so-called DπA-molecules that have electron donor and acceptor groups which are part of the conjugated system *via* a π-conjugated bridge (also called push-pull molecules). If the polymer is heated near the glass transition temperature (T_g), the molecules with a

large ground-state dipole are free to rotate and are oriented in the field. Upon cooling the orientation is frozen and an internal field is stored in the polymeric semi-conductor[15-17].

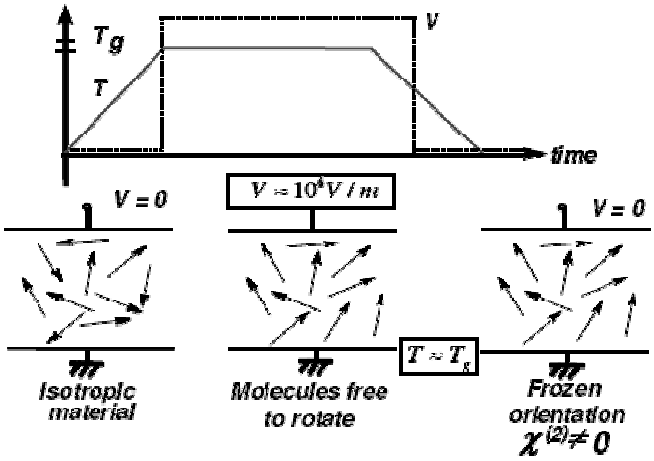

Figure 2-34: Mechanism of the dc-field ordering of the polar molecules covalently linked to a polymer.

The storage of an internal field in a polymeric semi-conductor should be of significant interest for solar cell applications as it will facilitate exciton dissociation. The depletion zone, in which the majority of charge separation or recombination processes take place, extends over the whole polymer film thickness, as opposed to classical p-n junction devices which are limited by a weak extension of the depletion zone (typically 10 to 50 nm). In this work the introduction of a push-pull molecule, *p*-(N-butyl-N-2-hydroxyethyl)-nitrobenzene (Figure 2-35) as side chain on a *bis*-(1-cyano-2-thienyl vinylene)phenylene derivative is described in order to study the molecular orientation concept for plastic solar cells. This study was done in collaboration with the CEA Saclay, France.

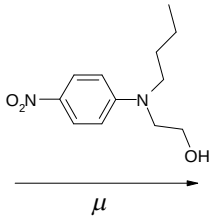

Figure 2-35: Push-pull molecule: p-(N-butyl-N-2-hydroxyethyl)-nitrobenzene.

2.7.2 Synthesis

The synthesis strategy is similar to the synthesis of the previous polymers with only some small adaptations (Figure 2-36). In the first step *p*-(N-butyl-N-2-hydroxyethyl)-nitrobenzene and *p*-hydroxyanisol are coupled using the mild and neutral conditions of the *Mitsunobu* reaction[97-100]. The subsequent compound [2-(2,5-bis-chloromethyl-4-methoxy-phenoxy)-ethyl]-butyl-(4-nitro-phenyl)-amine (**9**) is prepared according to a literature procedure[95]. The aromatic acetonitrile (**10**) is then prepared from **9** *via* nucleophilic substitution with sodium cyanide in DMF. Subsequent *Knoevenagel* condensation[4,84] of 3-octyl-2-thienylaldehyde **(5b)** with **10** in refluxing methanol containing sodium *t*-butoxide yields the monomer **M6**.

The polymer **P6** is prepared by chemical oxidation of the monomers using $FeCl_3$. The result of the polymerization is shown in Table 2-8. The reported overall yield (Y1) was determined after extraction with acetone and the soluble polymer yield (Y2) indicates the soluble fraction of the polymer in chloroform. The polymerization was allowed to continue for 24 h after which the rigorous purification was carried out. The obtained molecular weight is comparable to **P2**.

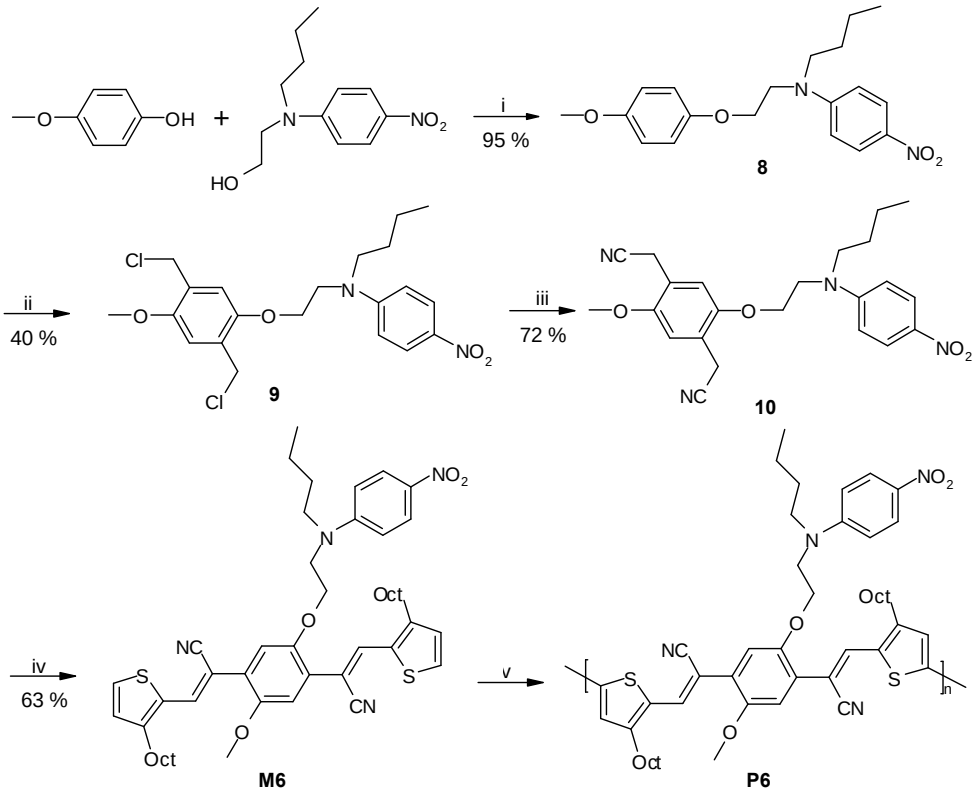

*Figure 2-36: Synthetic route toward the synthesis of monomer **M6** and polymer **P6**. (i) DEAD, PPh_3, Et_2O; p-CH_2O, Ac_2O, HCl, 70°C; (iii) NaCN, DMF, reflux; (iv) **5b**, Na-tBuO, MeOH, reflux; (v) $FeCl_3$, $CHCl_3$.*

*Table 2-8: Polymerization results for monomer **M6**.*

	Time [h]	M_w[a]	M_n[a]	PD[a]	Y1[b] [%]	Y2[c] [%]
P6	24	36000	8000	4.4	46	85

[a] *Determined by means of SEC in DMF against polystyrene standards.*

[b] *Overall yield.*

[c] *Soluble polymer yield with respect to the overall yield.*

2.7.3 Characterization

2.7.3.1 Optical absorption

The spectroscopic properties were measured both as thin film on quartz substrates and in chloroform solution (Figure 2-37). UV-Vis absorption spectroscopy shows that the absorption maximum of **P6** in thin film is 504 nm. In solution the λ_{max} = 481 nm. The absorptionband at 395 nm, both in thin film as in solution, is originating from the absorption of the push-pull molecule. The band gap for **P6** as derived from UV-Vis spectroscopy is 1.8 eV.

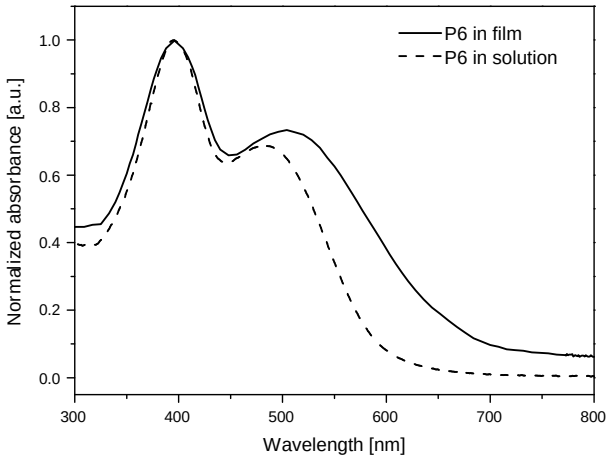

*Figure 2-37: Normalized UV-Vis absorption spectra of **P6** as thin film (solid) and in $CHCl_3$ solution (dash).*

2.7.3.2 Electrochemistry

The electrochemical behavior of **P6** was studied using cyclic voltammetry (CV). Figure 2-38 shows the quasi-reversible electroactivity of **P6** both in oxidation and reduction ranges. The HOMO/LUMO levels are determined from the onsets of oxidation and reduction, respectively. In the anodic scan, the onset of oxidation of **P6** starts at 0.72 V *vs.* Ag/Ag^+; reduction at –1.45 V *vs.* Ag/Ag^+. This means a HOMO energy level of -5.62 eV and a LUMO energy level of -3.45 eV. The incorporation

of a bulky push-pull molecule apparently changes the HOMO energy level as compared to **P2** (HOMO = -5.48 eV, LUMO = -3.36 eV). The LUMO, as seen for all the polymers of this family, is less affected by an adaptation on the central core.

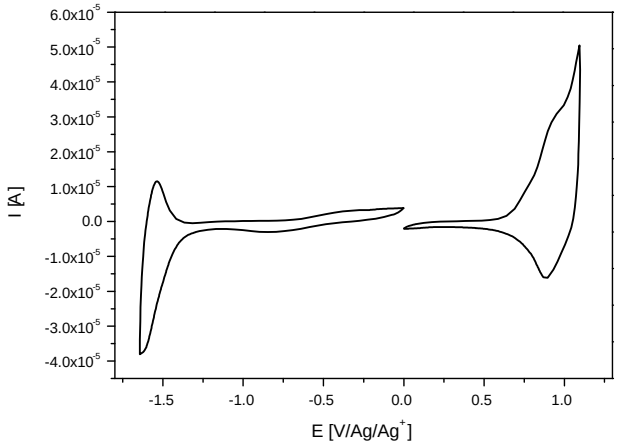

*Figure 2-38: Cyclic voltammograms of the oxidation and reduction behavior of thin films of **P6**.*

2.7.4 Photovoltaic device

In order to study the effect of orientation by applying a static electric field, an attempt to construct a bulk heterojunction solar cell with polymer **P6** as a donor and PCBM as an acceptor before and after orientation was done by Alexandra Apostoluk from the group of Carole Sentein at the CEA in France. However no photovoltaic effect was observed within the limits of the measurement technique. It was also impossible to orient the polymer layer between the two electrodes.

The photocurrent spectrum of the **P6** device shows an onset at about 700 nm (1.77 eV) close to the optical band gap and exhibits a maximum of 0.4 % at 370 nm (Figure 2-39).

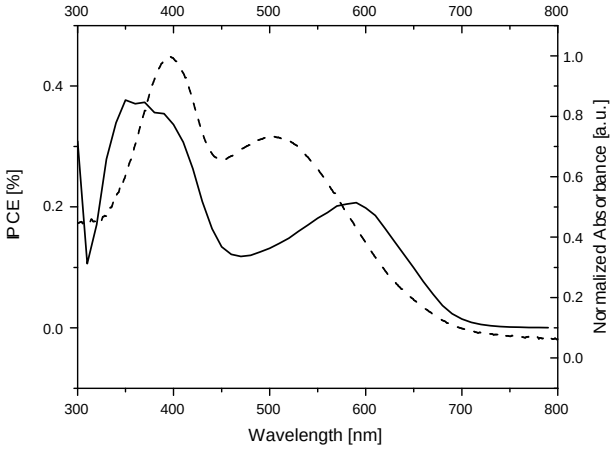

*Figure 2-39: Photocurrent spectrum (solid line) of photovoltaic device ITO/PEDOT:PSS/**P6**:PCBM/LiF/Al and the normalized optical absorption for the corresponding pristine polymer (dashed line).*

2.8 Conclusions

In conclusion, the synthesis of six different soluble low band gap polymers (1.6-2.0 eV) has been demonstrated. The polymers were synthesized by $FeCl_3$-oxidative polymerization. The influence of time on the polymerization was studied. Long reaction times give rise to lower molecular weights and lower yields. The introduction of extra solubilizing chains (**P2** and **P4**) on the thiophene unit or changing the alkoxy side chain on the central core into an oligo(oxyethylene) side chain (**P5**) increases the solubility of the final polymers but also lowers their molecular weights as a result of sterical hindrance during the polymerization. The influence of the electron donor strength of the thiophene units was studied with UV-Vis absorption spectroscopy and cyclic voltammetry. It is shown clearly that in going from **P3** over **P2** to **P1** the HOMO energy level decreases due to a decrease of the electron donor strength in the polymer. As a result hereof the band gap

increases. The introduction of alkyl substituents in **P4** gives rise to a higher band gap. The reason for this behavior is related to the sterical hindrance imparted by the tetradecyl substituents that affect the planarity of the molecule. In this work we were able to show that changing the substituents on the thiophene unit allows the modulation of the HOMO/ionization potential while changing the substituent on the central core has only little effect on the electronic properties. Efficient charge transfer is demonstrated in blends of **P2** and **P3** with PCBM by PL, PIA and LI-EPR measurements. However all solar cells made of the polymers showed only low efficiencies, which is related to the low hole mobilities observed in the pure polymer films. The introduction of a push-pull molecule as side chain on the **P6** derivative is described in order to study the molecular orientation concept for plastic solar cells. Unfortunately, it was impossible to orient the polymer layer between the two electrodes.

2.9 Experimental part

Chemicals

All reagents and chemicals were obtained from commercial sources (Acros, Aldrich and Merck) and used without further purification unless otherwise stated. $SOCl_2$ is distilled prior to use. 3,4-ethylenedioxythiophene, distilled under reduced pressure prior to use, and poly(3,4-ethylenedioxy-thiophene):poly(styrenesulfonate) (PEDOT:PSS) (Baytron® P) were provided by Bayer AG. 2-tetradecyl-2,3-dihydro-thieno[3,4-b][1,4]dioxin was kindly donated by Agfa-Gevaert N.V.. *p*-(N-butyl-N-2-hydroxyethyl)-nitrobenzene was received from CEA, Saclay France. 1,4–bischloromethyl-2,5-bis{2-[2-(2-methoxy-ethoxy)ethoxy]-ethoxy}benzene **6** is synthesized according to a literature procedure[95]. Tetrahydrofuran (THF), acetonitrile, and chloroform were dried by distillation from sodium/benzophenone, CaH_2 and P_2O_5 respectively. Commercial $FeCl_3$ was purified and treated to obtain anhydrous $FeCl_3$[101] and was stored in a Schlenk-type flask under inert atmosphere (Appendix).

Instrumentation

NMR spectra were recorded on a Varian Inova 300 spectrometer at 300 MHz for ^1H NMR and at 75 MHz for ^{13}C NMR using a 5 mm probe. ^1H and ^{13}C chemical shifts are reported in ppm downfield from tetramethylsilane (TMS) reference using the residual protonated solvent resonance as an internal standard.

Melting points (uncorrected) were measured on an Electrothermal IA9100 digital melting point apparatus.

Gas chromatography/mass spectrometry (**GC/MS**) analyses were carried out on TSQ–70 and Voyager mass spectrometers

(Thermoquest); the capillary column was a Chrompack Cpsil5CB or Cpsil8CB. **DIP-MS** measurements were performed at a heating rate of 10 °C/min up to 600 °C. In this technique the material is brought directly on the heating element of the probe as a thin film and this enables to study the products that are liberated in the high vacuum (4.10^{-4} Pa) inside the spectrometer. Liberated products were ionized by electron impact.

Elemental analysis was performed with a Flash EA 1112 Series CHNS-O analyzer.

Analytical Size Exclusion Chromatography (**SEC**) was performed using a Spectra series P100 (Spectra Physics) pump equipped with two mixed-B columns (10 μm, 2 x 30 cm, Polymer Labs) and a Refractive Index detector (Shodex) at 40 °C (THF) or 70 °C (DMF). THF or a DMF solution of oxalic acid ($1.1x10^{-3}$ M) was used as the eluent at a flow rate of 1.0 mL/min. Molecular weight distributions are given relative to polystyrene standards.

Unless stated otherwise, all thin films in the following characterization methods were prepared by spin coating from a $CHCl_3$ solution (10 mg/mL).

UV-Vis spectroscopy was performed on a Varian CARY 500 UV-Vis-NIR spectrophotometer. Samples for thin film UV-Vis characterization were prepared by spin-coating the polymer onto quartz disks. For temperature dependent thin film UV-Vis characterization the disks were heated in a Harrick high temperature cell (heating rate: 2 °C/min), which was positioned in the beam of the UV-Vis spectrometer to allow *in-situ* measurements. Spectra were taken continuously under a continuous flow of N_2 during which the samples were in direct contact with the heating element.

Thin film **electrochemical properties** were measured with an Eco Chemie Autolab PGSTAT 20 Potentiostat/Galvanostat using a conventional three-electrode cell (electrolyte: 0.1 mol/L $TBAPF_6$ in anhydrous CH_3CN) with an Ag/Ag^+ reference electrode (0.01 mol/L $AgNO_3$, 0.1 mol/L $TBAPF_6$ and CH_3CN), a platinum counter electrode and

a platinum wire as working electrode. Cyclic voltammograms were recorded at 50 mV/s under N_2 atmosphere and all potentials were referenced using a known internal standard ferrocene/ferrocinium, which in acetonitrile solution is estimated to have an oxidation potential of –4.98 eV vs. vacuum. The polymers were directly spin coated onto the Pt working electrode.

A Varian Cary Eclipse fluorometer was used for the photoluminescence (**PL**) measurements.

Time-resolved PL spectra were obtained by streak camera detection after excitation with 400 nm laser pulses (1.5 kHz, <2 ps) from the frequency-doubled output of a Ti-sapphire laser amplifier (Spectra Physics Spitfire). These experiments were performed on solutions of either the pure polymer or a mixture of the polymer and PCBM in a 1:1 ratio by weight and on spin-coated films (thickness ~100 nm) prepared from these solutions.

Photoinduced absorption (**PIA**) measurements were performed on the pristine and the blend films with 1:2 weight ratio of polymer/PCBM. The sample film was mounted in a cryostat (Oxford CF 204) and held at 80 K under vacuum higher than 10^{-5} mbar. Photoinduced changes in the absorption spectra were recorded by mechanical chopping the pump beam of an argon laser (514 nm, 40 mW, INNOVA 400) at 218 Hz. The transmission T and the photoinduced changes ΔT in the spectral range of 600–2200 nm were measured using a detector and lock in amplifier technique.

A Bruker ELEXSYS E680 spectrometer in conjunction with a split-coil 6-T superconducting magnet was used for W-band (95 GHz) Light-Induced Electron Paramagnetic Resonance (**LI-EPR**). These measurements were performed at 100 K using an Oxford flow cryostat and with a Bruker cylindrical cavity which allows optical access to the sample *via* an optical fiber. Optical excitation was performed with the 488 nm line of an Ar^+ laser. The results presented here are recorded with a modulation frequency and amplitude of 100 kHz and 3 G respectively and a microwave frequency and microwave power of 94.0795 GHz and $7x10^{-2}$

mW. The samples were prepared from dried drop cast films of the 1:1 ratio polymer/PCBM solution.

Atomic force microscopy (**AFM**) studies were performed by using a Digital Instruments Dimension 3100 in the tapping mode. The AFM characterization was performed in an area of the active layer of the photovoltaic device where the electrode was not deposited.

Solar Cells

Using the bulk heterojunction concept, photovoltaic devices were fabricated from a blend of the polymer as a donor and PCBM as an acceptor. A solution of the polymer and PCBM in a 1:2 ratio (by weight) was prepared in chloroform with a total concentration of 10 mg/mL. Poly(3,4-ethylenedioxythiophene):poly(styrenesulfonate) (PEDOT:PSS) (Baytron® P) was spincoated on top of an indium-tin oxide (ITO) coated glass substrate (~25 Ω/sq) which had been cleaned in an ultrasonic bath with acetone and isopropyl alcohol. Then the active layer (polymer:PCBM blend) was spin coated on the PEDOT:PSS layer (about 80 nm thick). 6 Å of lithium fluoride (LiF) and an 80 nm thick Al electrode were deposited on the blend film by thermal evaporation at ~5x 10^{-6} mbar. Device annealing was carried out inside a glove box at 120 °C for 4 min. All current-voltage (I-V) characteristics of the photovoltaic devices were measured using a Keithley SMU 2400 unit under inert atmosphere (argon) in a dry glove box. A Steuernagel solar simulator under AM 1.5 conditions was used as the excitation source with an input power of 100 $mWcm^{-2}$ white light illumination. A lock-in technique was used to measure the incident photon-to-current efficiency (**IPCE**). With this technique the number of electrons produced from the cell under short-circuit conditions are related to the number of incident photons. Light intensity correction was performed using a calibrated Si photodiode.

Field Effect Transistors

The hole mobility of the polymers was measured in thin film field effect transistor (TF-FET) devices. The measurements were performed on a top-contact parallel transistor (L = 60 μm; W = 9000 μm). It consisted of a highly doped Si substrate on which an isolating oxide (SiO_2) of 100 nm was grown thermally on one side and of which the backside was covered with an aluminum layer as gate electrode. The polymers were spin coated on top of the oxide. Subsequently the gold contacts (source and drain) were evaporated on top of the device.

Synthesis

1-Chloro-3,7-dimethyloctane (1)

To a mixture of 3,7-dimethyl-1-octanol (62 g, 0.39 mol) and pyridine (2 mL) as a catalyst at 15 °C, freshly distilled $SOCl_2$ (62 g, 0.52 mol) is added drop wise over a period of 2 hours, keeping the internal temperature below 30 °C. This mixture is heated at 100 °C for 1.5 hours. After cooling to room temperature, 30 mL of water is carefully added. The organic layer is washed 2 times with water (30 mL) and 2 times with an aqueous solution of $NaHCO_3$ (10 %, 30 mL), after which it is dried over $MgSO_4$. After distillation under reduced pressure (80 °C/10 mbar) a colorless liquid was obtained (62.3 g, 90 % yield); ^1H NMR ($CDCl_3$): 3.55 (m, 2H), 1.77 (m, 1H), 1.53 (m, 3H), 1.30-1.10 (m, 6H), 0.86 (t, 9H); MS (EI, m/e): 176 (M^+), 133, 113, 105.

1,4-Bis[3',7'-dimethyloctyl)oxy]benzene (2)

Hydroquinone (11 g, 0.1 mol), potassium hydroxide (12.3 g, 0.22 mol) and sodium iodide (3.3 g, 0.022 mol) are dissolved in 50 mL absolute ethanol. Compound **1** (39 g, 0.22 mol) is added drop wise and the resulting mixture is stirred for four days at reflux temperature. After

evaporation of the solvent the resulting brown mixture is washed 3 times with an aqueous solution of NaOH (10 %, 50 mL) and 3 times with water (50 mL). The organic layer is dried over $MgSO_4$ and concentrated. The crude mixture is purified by column chromatography (silica, *n*-hexane/ethylacetate 9/1) yielding a light yellow oil (22.6 g, 58 % yield); ^{1}H NMR ($CDCl_3$): 6.81 (s, 4H), 3.92 (m, 4H), 1.77 (m, 2H), 1.53 (m, 6H), 1.30-1.10 (m, 12H), 0.91 (d, 6H), 0.85 (d, 12H); MS (EI, m/e): 390 (M^+), 250 (M^+ - $C_{10}H_{20}$), 110 (M^+ - 2 x $C_{10}H_{20}$).

1,4-Bischloromethyl-2,5-bis[3',7'-dimethyloctyl)-oxy]benzene (3)

To a mixture of **2** (20 g, 0.051 mol) and *p*-formaldehyde (12.6 g, 0.42 mol) placed in an ice bath under argon atmosphere, HCl (37%) (36 g, 0.36 mol) is added drop wise. Afterwards acetic anhydride (156 g, 1.53 mol) is added at such a rate that the internal temperature does not exceed 70 °C. The mixture is than stirred overnight at 90 °C and poured into 500 mL water. The resulting white precipitate (22.45 g, 90 % yield) is collected by filtration and dried under vacuo; ^{1}H NMR ($CDCl_3$): 6.90 (s, 2H), 4.61 (s, 4H), 4.00 (m, 4H), 1.81 (m, 2H), 1.53 (m, 6H), 1.30-1.10 (m, 12H), 0.91 (d, 6H), 0.85 (d, 12H); ^{13}C NMR ($CDCl_3$): 150.72, 118.55, 116.69, 67.51, 40.90, 39.66, 37.12, 35.86, 29.70, 27.56, 24.85, 22.62, 22.55, 19.48; MS (EI, m/e): 486 (M^+), 346 (M^+ - $C_{10}H_{20}$), 206 (M^+ - 2 x $C_{10}H_{20}$), 170 (M^+ - 2 x $C_{10}H_{20}$ - Cl).

1,4-Biscyanomethyl-2,5-bis[3',7'-dimethyloctyl)oxy]benzene (4)

Fine crushed sodium cyanide (8.0 g, 0.164 mol) and 1,4-bischloromethyl-2,5-bis[3',7'-dimethyloctyl)oxy]benzene (**3**) (20 g, 0.041 mol) are dissolved in 100 mL of anhydrous DMF. This mixture is heated at 110 °C for 1 hour. After cooling, the mixture is poured in 150 g of crushed ice upon which a brown solid precipitates. The solid is collected *via* filtration and washed on the filter with hexane.

Recrystallization from hexane yields an off white solid (15.9 g, 83 % yield; mp 83-84 °C); ^{1}H NMR ($CDCl_3$): 6.90 (s, 2H), 4.00 (m, 4H), 3.67 (s, 4H), 1.80 (m, 2H), 1.52 (m, 6H), 1.29-1.15 (m, 12H), 0.92 (d, 6H), 0.85 (d, 12H); ^{13}C NMR ($CDCl_3$): 149.82, 118.85, 117.68, 112.37, 67.08, 39.04, 37.08, 36.01, 29.69, 27.80, 24.52, 22.54, 22.45, 19.51, 18.49; MS (EI, m/e): 468 (M^+), 328 (M^+ - $C_{10}H_{20}$), 188 (M^+ - 2 x $C_{10}H_{20}$).

3-Octyl-2-thienylaldehyde (5b)

Phosphorusoxychloride (5.15 g, 0.033 mol) was added drop wise to ice-cold DMF (35 mL), followed by the addition of 3-octylthiophene (6 g, 0.031 mol). The resulting brown mixture was heated to 55 °C and stirred at this temperature for two hours. Afterwards the reaction mixture was poured into 100 g of crushed ice and the pH of the solution was brought to 14 by adding a concentrated aqueous NaOH-solution (10 N). This mixture is extracted 3 times with 50 mL of CH_2Cl_2. The organic layer is dried over $MgSO_4$ and the solvent evaporated. **5b** was obtained as a yellow oil. The crude mixture was purified by column chromatography (silica, CH_2Cl_2/*n*-hexane 1/1) and a pale yellow oil was obtained (5.88 g, 86 % yield); ^{1}H NMR ($CDCl_3$): 10.01 (s, 1H), 7.62 (d, 1H), 6.98 (d, 1H), 2.93 (t; 2H), 1.64 (qu, 2H), 1.38-1.15 (br, s, 10H), 0.85 (t, 3H); MS (EI, m/e): 224 (M^+), 195 (M^+ - CHO).

3,4-Ethylenedioxy-2-thienylaldehyde (5c)

Compound **5c** was obtained in an analogous way as described for **5b**, starting from 3,4-ethylendioxythiophene (16.76 g, 0.118 mol), phosphorusoxychloride (16,87 g, 0.11 mol). Fine white-gray crystals were filtered off after the addition of NaOH and washed several times with water (19.12 g, 95 % yield); ^{1}H NMR ($CDCl_3$): 9.87 (s, 1H), 6.77 (s, 1H), 4.34 (m, 2H), 4.25 (m, 2H); MS (EI, m/e): 170 (M^+), 141 (M^+ - CHO).

3 or 4-Tetradecyl-2,3-dihydro-thieno[3,4-b][1,4]dioxine-5-carbaldehyde (5d)

Compound **5d** was obtained in an analogous way as described for **5b**. Starting from 2-tetradecyl-2,3-dihydro-thieno[3,4-b][1,4]dioxine (2 g, 5.9 mmol), phosphorusoxychloride (1 g, 6.5 mmol) **8** was obtained as a sticky brown solid. The crude mixture was purified by column chromatography (silica, CH_2Cl_2/*n*-hexane 3/7) and a pale yellow solid was obtained (1.7 g, 83 % yield); ^{1}H NMR ($CDCl_3$): 9.90 (d, 1H), 6.75 (s, 1H), 4.24 (m, 2H), 3.94 (m; 1H), 1.76-1.50 (br, s, 6H), 1.50-1.05 (br, s, 20H), 0.86 (t, 3H); MS (EI, m/e): 367 (M^+), 338 (M^+ - CHO).

1,4-Biscyanomethyl-2,5-bis{2-[2-(2-methoxy-ethoxy)ethoxy]-ethoxy}benzene (7)

Fine crushed sodium cyanide (3.15 g, 0.064 mol) and 1,4-bischloromethyl-2,5-bis{2-[2-(2-methoxy-ethoxy)ethoxy]-ethoxy}-benzene (**6**) (8 g, 0.016 mol) are dissolved in 50 mL of anhydrous DMF. This mixture is heated at 110 °C for 1.5 h. After cooling, the mixture is poured in 150 g of crushed ice to stop the reaction. This mixture is extracted 3 times with 50 mL of CH_2Cl_2. The organic layer is dried over $MgSO_4$ and the solvent evaporated. **7** was obtained as a brown oil. The crude mixture was purified by column chromatography (silica, Ether/MeOH 9/1) and a pale yellow oil was obtained (5.39 g, 69 % yield); ^{1}H NMR ($CDCl_3$): 6.91 (s, 2H), 4.12 (t, 4H), 3.79 (t, 4H), 3.70 (s, 4H), 3.69-3.58 (m, 12H), 3.50 (m, 4H), 3.34 (s, 6H); GC MS (EI, m/e): 480 (M^+), 450, 147.

Butyl-[2-(4-methoxy-phenoxy)-ethyl]-(4-nitro-phenyl)-amine (8)

In a three-necked flask, a mixture of *p*-(N-butyl-N-2-hydroxyethyl)-nitrobenzene (3.6 g, 0.015 mol), *p*-hydroxyanisol (2.8 g, 0.023 mol)

and triphenyl phosphine (4.7 g, 0.018 mol) in diethyl ether (120 mL) is stirred for 1 h under Ar atmosphere. The temperature is decreased to 0 °C and diethyl azodicarboxylate (DEAD; 40 wt. % in toluene) (8.2 mL, 0.018 mol) is added drop wise. The mixture is stirred for 24 h at room temperature after which water is added (150 mL) and an extraction with CH_2Cl_2 is performed (3 x 150 mL). The organic layers are combined and dried over $MgSO_4$. The solvent is evaporated under vacuum to yield crude **8**. After purification by column chromatography (silica, CH_2Cl_2), **8** is obtained as a yellow solid (4.9 g, 95 % yield); ^{1}H NMR ($CDCl_3$): 8.06 (d, 2H), 6.79 (s, 4H), 6.62 (d, 2H), 4.08 (t, 2H), 3.78 (t, 2H), 3.73 (s, 3H), 3.46 (t, 2H), 1.62 (m, 2H), 1.39 (m, 2H), 0.96 (t, 3H); GC MS (EI, m/e): 344 (M^+).

[2-(2,5-Bis-chloromethyl-4-methoxy-phenoxy)-ethyl]-butyl-(4-nitro-phenyl)-amine (9)

To a mixture of **8** (5.0 g, 0.014 mol) and *p*-formaldehyde (1.19 g, 0.040 mol) concentrated HCl (7.2 mL) was added drop wise under N_2 atmosphere. Subsequently, acetic anhydride (15.0 mL) was added at such a rate that the internal temperature did not exceed 70 °C. After the addition was complete, the resulting solution was stirred at 70 °C for 12 h after which it was allowed to cool to room temperature and poured into water (100 mL). The pH is adjusted to 7 with an aqueous solution of sodium *t*-butoxide. The product was extracted with CH_2Cl_2 (3 x 75 mL). The organic layers were combined, dried over $MgSO_4$ and the solvent was evaporated to give the crude product, which was purified by column chromatography (silica, CH_2Cl_2). **9** is obtained as a yellow solid (2.55 g, 40 % yield); ^{1}H NMR ($CDCl_3$): 8.12 (d, 2H), 6.93 (s, 1H), 6.87 (s, 1H), 6.71 (d, 2H), 4.56 (d, 4H), 4.18 (t, 2H), 3.89 (t, 2H), 3.78 (s, 3H), 3.49 (t, 2H), 1.63 (m, 2H), 1.41 (m, 2H), 1.01 (t, 3H); GC MS (EI, m/e): 441 (M^+), 392 (M^+ - CH_2Cl), 207.

[2-(2,5-Bis-cyanomethyl-4-methoxy-phenoxy)-ethyl]-butyl-(4-nitro-phenyl)-amine (10)

Fine crushed sodium cyanide (2.0 g, 0.040 mol) and **9** (3.9 g, 0.009 mol) are dissolved in 80 mL of anhydrous DMF. This mixture is heated at 110 °C for 2 h. After cooling, the mixture is poured in 150 g of crushed ice to stop the reaction. This mixture is extracted 3 times with 50 mL of CH_2Cl_2. The organic layer is dried over $MgSO_4$ and the solvent evaporated. **10** was obtained as a brown slurry. The crude mixture was purified by column chromatography (silica, CH_2Cl_2) and a pale yellow solid was obtained (2.73 g, 72 % yield); ^{1}H NMR ($CDCl_3$): 8.10 (d, 2H), 6.90 (s, 1H), 6.84 (s, 1H), 6.69 (d, 2H), 4.18 (t, 2H), 3.87 (t, 2H), 3.81 (s, 3H), 3.66 (s, 2H), 3.55 (s, 2H), 3.48 (t, 2H), 1.63 (m, 2H), 1.39 (m, 2H), 0.97 (t, 3H); GC MS (EI, m/e): 422 (M^+), 379, 207.

2-(4-(1-Cyano-2-thiophen-2-yl-vinyl)-2,5-bis-(3,7-dimethyloctyl-oxy)-phenyl)-3-thiophen-2-yl-acrylonitrile (M1)

A mixture of **4** (5 g, 11 mmol) and 2-thiophenecarboxaldehyde (**5a**) (2.9 g, 26 mmol) is dissolved in 50 mL MeOH. Sodium *t*-butoxide (10 g, 110 mmol) is added as a solid and this mixture is stirred for 24 hours at reflux temperature. Upon cooling, a bright yellow solid (3.3 g, 46 % yield) precipitates, which is filtered and washed with cold methanol; mp 109–110 °C; ^{1}H NMR ($CDCl_3$): 8.00 (s, 2H), 7.64 (d, 2H), 7.54 (d, 2H), 7.14 (t, 2H), 7.10 (s, 2H), 4.08 (m, 4H), 1.89 (m, 2H), 1.58 (m, 6H), 1.30-1.10 (m, 12H), 0.93 (d, 6H), 0.82 (d, 12H); ^{13}C NMR ($CDCl_3$): 150.53, 138.80, 138.15, 130.12, 129.82, 127.80, 124.05, 118.37, 114.09, 104.67, 67.91, 39.17, 37.29, 36.27, 29.88, 27.91, 24.69, 22.67, 22.51, 19.51; DIP MS (EI, m/e): 656 (M^+), 375 (M^+ - 2 x $C_{10}H_{20}$); Anal. Calcd. for $C_{40}H_{52}N_2O_2S_2$: C 73.13; H 7.98; N 4.26; O 4.87; S 9.76. Found: C 73.26; H 8.38; N 4.01; O 5.03; S 8.85; UV-Vis (film) λ_{max}: 344, 407 nm.

2-(4-(1-Cyano-2-(3-octylthiophen-2-yl)-vinyl)-2,5-bis-(3,7-dimethyloctyloxy)-phenyl)-3-(3-octylthiophen-2-yl)-acrylonitrile (M2)

M2 is prepared in an analogous way as described for **M1**. Starting from **4** (1 g, 2 mmol), 3-octyl-2-thienylaldehyde (**5b**) (1.1 g, 5 mmol) and sodium *t*-butoxide (2 g, 20 mmol). After cooling, 50 mL of water is added and the mixture is extracted 3 times with 50 mL of CH_2Cl_2. The organic layer is dried over $MgSO_4$ and the solvent evaporated. **M2** is obtained as a sticky oil. After purification by column chromatography (silica, CH_2Cl_2/*n*-hexane 1/1) a yellow oil is obtained (1.1 g, 60 % yield); ^{1}H NMR ($CDCl_3$): 8.10 (s, 2H), 7.45 (d, 2H), 7.13 (s, 2H), 6.60 (d, 2H), 4.08 (m, 4H), 2.70 (t, 4H), 1.86 (m, 2H), 1.72-1.42 (br, m, 8H), 1.38-1.00 (br, m, 36H), 0.96-0.74 (br, m, 24H); ^{13}C NMR ($CDCl_3$): 150.39, 148.62, 144.08, 137.67, 131.89, 128.88, 124.36, 118.63, 114.08, 102.98, 68.03, 39.07, 37.17, 36.19, 31.72, 31.06, 29.75, 29.32, 29.12, 28.81, 27.80, 24.52, 22.52 , 19.47, 13.96; DIP MS (EI, m/e): 881 (M^+) 600 (M^+ - 2 x $C_{10}H_{20}$); Anal. Calcd. for $C_{56}H_{84}N_2O_2S_2$: C 76.31; H 9.61; N 3.18; O 3.63; S 7.28. Found: C 76.46; H 10.11; N 3.01; O 3.32; S 6.61; UV-Vis (film) λ_{max}: 337, 392 nm.

2-(4-(1-Cyano-2-(3,4-ethylenedioxythiophen-2-yl)vinyl)-2,5-bis-(3,7-dimethyloctyloxy)-phenyl)-3-(3,4-ethylenedioxythiophen-2-yl)acrylonitrile (M3)

Monomer **M3** is prepared in an analogous way as described for **M1**. Starting from **4** (8 g, 17 mmol), 3,4-ethylenedioxy-2-thienylaldehyde (**5c**) (6.4 g, 38 mmol) and sodium *t*-butoxide (16.3 g, 170 mmol), **M3** is obtained as a bright orange solid (8.3 g, 63 % yield), which is filtered and washed with methanol; mp 157-158 °C; ^{1}H NMR ($CDCl_3$): 8.16 (s, 2H), 7.07 (s, 2H), 6.59 (s, 2H), 4.28 (m, 4H), 4.23 (m, 4H), 4.06 (m, 4H), 1.86 (m, 4H), 1.67 (m, 2H), 1.47 (m, 2H), 1.30-1.10 (m, 12H), 0.92 (d, 6H), 0.82 (d, 12H); ^{13}C NMR ($CDCl_3$): 150.46, 144.24, 141.33,

134.61, 123.82, 118.94, 114.16, 113.90, 104.95, 101.19, 67.87, 65.10, 64.49, 39.21, 37.20, 36.24, 29.70, 27.93, 24.57, 22.68, 22.55, 19.61; DIP MS (EI, m/e): 772 (M^+), 632 (M^+ - $C_{10}H_{20}$), 491 (M^+ - 2 x $C_{10}H_{20}$); Anal. Calcd. for $C_{44}H_{56}N_2O_6S_2$: C 68.36; H 7.30; N 3.62; O 12.42; S 8.30. Found: C 68.76; H 7.51; N 3.88; O 11.85; S 8.04; UV-Vis (film) λ_{max}: 348, 425 nm.

2-(4-(1-Cyano-2-(3 or 4 tetradecyl-2,3-dihydro-thieno(3,4-b)(1,4)dioxin-5-yl)-vinyl)-2,5-bis-(3,7-dimethyloctyloxy)-phenyl)-3-(3 or 4 tetradecyl-2,3-dihydro-thieno(3,4-b)(1,4)dioxin-5-yl)-acrylonitrile (M4)

Monomer **M4** is prepared in an analogous way as described for **M2**. Starting from **4** (1 g, 2 mmol), 3 or 4-tetradecyl-2,3-dihydro-thieno[3,4-b][1,4]dioxine-5-carbaldehyde (**5d**) (1.7 g, 5 mmol) and sodium *t*-butoxide (2 g, 20 mmol), **M4** is obtained as a sticky oil. After purification by column chromatography (silica, CH_2Cl_2/*n*-hexane 9/1) a yellow-orange oil is obtained (1.7 g, 72 % yield); ^{1}H NMR ($CDCl_3$): Very complex mixture of 4 isomers and thus very difficult to analyze in detail; Anal. Calcd. for $C_{72}H_{112}N_2O_6S_2$: C 74.18; H 9.68; N 2.40; O 18.23; S 5.50. Found: C 74.64 H 9.90; N 2.06; O 8.33; S 4.89; DIP MS (EI, m/e): 1165 (M^+); UV-Vis (film) λ_{max}: 334, 397 nm.

2-(4-(1-Cyano-2-(3,4-ethylenedioxythiophen-2-yl)vinyl)-2,5-bis{2-[2-(2-methoxy-ethoxy)ethoxy]-ethoxy}phenyl)-3-(3,4-ethylenedi-oxythiophen-2-yl)acrylonitrile (M5)

Monomer **M5** is prepared in an analogous way as described for **M1**. Starting from **7** (4.6 g, 9.6 mmol), 3,4-ethylenedioxy-2-thienylaldehyde (**5c**) (3.6 g, 21 mmol) and sodium *t*-butoxide (9,2 g, 96 mmol), **M5** is obtained as a bright orange solid (6.6 g, 88 % yield), which is filtered and washed with methanol; mp 137-138 °C; ^{1}H NMR ($CDCl_3$): 7.96 (s, 2H), 7.03 (s, 2H), 6.59 (s, 2H), 4.30 (m, 4H), 4.22 (m, 8H), 3.90 (t,

4H), 3.71 (m, 4H), 3.66-3.58 (m, 8H), 3.49 (m, 4H), 3.33 (s, 6H); ^{13}C NMR ($CDCl_3$): 150.49, 144.37, 141.36, 134.60, 124.79, 118.72, 114.45, 113.93, 105.21, 101.02, 71.83, 70.86, 70.48 (2C) 69.54, 69.33, 65.12, 64.50, 58.95; DIP MS (EI, m/e): 784 (M^+).

2-{5-{2-[Butyl-(4-nitro-phenyl)-amino]-ethoxy}-4-[1-cyano-2-(3-octyl-thiophen-2-yl)-vinyl]-2-methoxy-phenyl}-3-(3-octyl-thiophen-2-yl)-acrylonitrile (M6)

M6 is prepared in an analogous way as described for **M1**. Starting from **10** (1 g, 2,4 mmol), 3-octyl-2-thienylaldehyde (**5b**) (1.2 g, 5,3 mmol) and sodium *t*-butoxide (2,3 g, 24 mmol). After cooling, 50 mL of water is added and the mixture is extracted 3 times with 50 mL of CH_2Cl_2. The organic layer is dried over $MgSO_4$ and the solvent evaporated. **M6** is obtained as an oil. After purification by column chromatography (silica, CH_2Cl_2) a yellow oil is obtained (1.26 g, 63 % yield); ^1H NMR ($CDCl_3$): 8.12 (s, 2H), 8.00 (d, 2H), 7.48 (d, 2H), 6.97 (d, 2H), 6.95 (s, 1H), 6.86 (s, 1H), 6.60 (d, 2H), 4.24 (t, 2H), 4.10 (t, 2H), 3.90 (s, 3H), 3.45 (t, 2H), 2.66 (m, 4H), 1.66-1.48 (br, m, 6H), 1.38-1.16 (br, m, 22H), 0.87 (m, 9H); DIP MS (EI, m/e): 835 (M^+); UV-Vis (film) λ_{max}: 394 nm.

General procedure of polymerization

The polymers are prepared by chemical oxidation of the monomers using $FeCl_3$ according to a procedure adapted from Sugimoto *et al.*.[59] Anhydrous $FeCl_3$ (4 mmol) is suspended in 50 mL of dry $CHCl_3$ under Ar atmosphere to which a solution of the monomer (1 mmol **M1**, **M2**, **M3, M4, M5 or M6**) in 20 mL of dry $CHCl_3$ is added drop wise under fast stirring. The mixture is further stirred for 3h, 24h, 48h or 72h at room temperature under a gentle Ar flow. The dark solution is poured into methanol (1 L) and the black precipitate is collected on a 0,45 micron Teflon® filter. The precipitate is then immersed into 1 L of a 1 v/v% solution of hydrazine in methanol and stirred for 12 h. The polymer is

then filtered and washed with methanol. The polymer is transferred into a *Soxhlet* extraction apparatus and than extracted two times for 72 h, first with methanol and than with acetone to remove residual monomer and oligomer fractions. After this step the solvent is changed into $CHCl_3$ and the soluble fraction is collected. The $CHCl_3$ solution is than concentrated and precipitation into methanol yields the polymer as a black, shining powder. The polymer is then redissolved in $CHCl_3$ and filtered over a 0,45 micron Teflon® filter to remove dust and other solid particles, the solvent is than removed and the product is dried under vacuum. The yields of the polymers are reported in Table 2-3, Table 2-7 and Table 2-8.

Polymer P1. ^{1}H NMR ($CDCl_3$): 8.20-8.05 (br, 1H); 8.00-7.80 (br, 2H); 7.60-7.30 (br, 1H); 7.20-7.00 (br, 2H); 7.00-6.55 (br, 2H); 4.22-3.75 (br, 4H); 2.02-1.00 (br, 16H); 1.00-0.68 (br, 18H); Anal. Calcd. for $C_{40}H_{50}N_2O_2S_2$: C 73.36; H 7.70; N 4.28; O 4.89; S 9.77. Found: C 72.45; H 8.22; N 3.76; O 5.15; S 9.13.

Polymer P2. ^{1}H NMR ($CDCl_3$): 8.20-8.05 (br, 1H); 8.00-7.80 (br, 1H); 7.60-7.30 (br, 1H); 7.20-7.00 (br, 2H); 7.00-6.55 (br, 1H); 4.22-3.75 (br, 4H); 2.98-2.28 (br, 4H); 2.02-1.00 (br, 36H); 1.00-0.68 (br, 24H); Anal. Calcd. for $C_{56}H_{82}N_2O_2S_2$: C 76.49; H 9.41; N 3.19; O 3.64; S 7.28. Found: C 76.01; H 9.68; N 3.28; O 3.59; S 7.39.

Polymer P3. ^{1}H NMR ($CDCl_3$): 8.2 (br, 2H), 7.1 (br, 2H), 4.3 (br m, 8H), 4.1 (br, 4H), 1.9 (br, 2H), 1.6 (br, 6H), 1.4-1.0 (br, 12), 0.9 (br, 6H), 0.8 (br, 12H); Anal. Calcd. for $C_{44}H_{54}N_2O_6S_2$: C 68.54; H 7.07; N 3.64; O 12.46; S 8.30. Found: C 67.17; H 7.49 N 3.24; O 12.92; S 7.52.

Polymer P4. ^{1}H NMR ($CDCl_3$): As this polymer comes from a polymerization of a mixture of 4 isomers, the material has a very

complex spectrum; Anal. Calcd. for $C_{72}H_{110}N_2O_6S_2$: C 74.30; H 9.54; N 2.41; O 8.25; S 5.50. Found: C 73.15; H 10.12; N 1.99; O 8.97; S 4.70.

Polymer P5. ^{1}H NMR ($CDCl_3$): 8.1 (br, 2H), 7.0 (br, 2H), 4.4 (br, 4H), 4.2 (br, 8H), 3.90 (br, 4H), 3.7 (br, 4H), 3.6 (br, 8H), 3.5 (br, 4H), 3.3 (br, 6H).

Polymer P6. ^{1}H NMR ($CDCl_3$): 8.23-8.08 (br, 2H), 8.08-7.90 (br, 2H), 7.57-7.38 (br, 2H), 7.13-6.91 (br, 2H), 6.72-6.56 (br, 2H), 4.31-4.09 (br, 2H), 3.99-3.71 (br, 2H), 3.54-3.42 (br, 3H), 3.39-3.28 (br, 2H), 2.78-2.47 (br, 4H), 1.80-1.45 (br, 6H), 1.35-1.00 (br, m, 22H), 1.00-0.80 (br, 9H).

2.10 References

1. Colladet K., Fourier S., Cleij T. *et al.* "Low Band Gap Donor-Acceptor Conjugated Polymers toward Organic Solar Cells Applications", *Macromolecules* 40, (1), **2007**, 65.
2. Colladet K., Nicolas M., Goris L. *et al.* "Low-band gap polymers for photovoltaic applications", *Thin Solid Films* 451-52, **2004**, 7.
3. van Mullekom H. A. M., Vekemans J. A. J. M., Havinga E. E. *et al.* "Developments in the chemistry and band gap engineering of donor-acceptor substituted conjugated polymers", *Mater. Sci. Eng. R-Rep.* 32, (1), **2001**, 1.
4. Sotzing G. A., Thomas C. A., Reynolds J. R. *et al.* "Low band gap cyanovinylene polymers based on ethylenedioxythiophene", *Macromolecules* 31, (11), **1998**, 3750.
5. Wagner P., Aubert P-H., Lutsen L. *et al.* "Conjugated polymers based on new thienylene - PPV derivatives for solar cell applications", *Electrochem. Commun.* 4, (11), **2002**, 912.
6. Seshadri V. and Sotzing G. A. "Polymerization of two unsymmetrical isomeric monomers based on thieno[3,4-b]thiophene containing cyanovinylene spacers", *Chem. Mat.* 16, (26), **2004**, 5644.
7. Thomas C. A., Zong K. W., Abboud K. A. *et al.* "Donor-mediated band gap reduction in a homologous series of conjugated polymers", *J. Am. Chem. Soc.* 126, (50), **2004**, 16440.
8. Cho N. S., Hwang D. H., Lee J. K. *et al.* "Synthesis and color tuning of new fluorene-based copolymers", *Macromolecules* 35, (4), **2002**, 1224.
9. Xue C. H. and Luo F. T. "Novel p-phenylene-vinylene-dithienylene type copolymer: potential red-emitting materials", *Synth. Met.* 145, (1), **2004**, 67.

10. Chang C. P., Huang W. T. and Lin M. S. "Syntheses and optical properties of alpha- and beta-cyano-poly(p-phenylene vinylene) derivatives", *J. Polym. Res.* 11, (4), **2004**, 257.
11. Gordon K. C., MacArthur S., David G. *et al.* "Experimental and computational studies of substituted terthiophene oligomers as electroluminescent materials", *Synth. Met.* 153, (1-3), **2005**, 225.
12. Thompson B. C., Kim Y. G. and Reynolds J. R. "Spectral broadening in MEH-PPV : PCBM-based photovoltaic devices via blending with a narrow band gap cyanovinylene-dioxythiophene polymer", *Macromolecules* 38, (13), **2005**, 5359.
13. Lee S. K., Cho N. S., Kwak J. H. *et al.* "New low band-gap alternating polyfluorene derivatives for photovoltaic cells", *Thin Solid Films* 511, **2006**, 157.
14. Sentein C., Fiorini C., Lorin A. *et al.* "Molecular rectification in oriented polymer structures", *Adv. Mater.* 9, (10), **1997**, 809.
15. Singer K. D., Kuzyk M. G. and Sohn J. E. "2nd-Order Nonlinear-Optical Processes in Orientationally Ordered Materials - Relationship between Molecular and Macroscopic Properties", *J. Opt. Soc. Am. B-Opt. Phys.* 4, (6), **1987**, 968.
16. Sentein C., Fiorini C., Lorin A. *et al.* "Poling induced improvement of organic polymer device efficiency", *Synth. Met.* 102, (1-3), **1999**, 989.
17. Sicot L., Fiorini C., Lorin A. *et al.* "Improvement of the photovoltaic properties of poly(thiophene)-based cells", *Sol. Energy Mater. Sol. Cells* 63, (1), **2000**, 49.
18. Feast W. J., Tsibouklis J., Pouwer K. L. *et al.* "Synthesis, processing and material properties of conjugated polymers", *Polymer* 37, (22), **1996**, 5017.
19. McCullough R. D. "The chemistry of conducting polythiophenes", *Adv. Mater.* 10, (2), **1998**, 93.
20. Perepichka I. F., Perepichka D. F., Meng H. *et al.* "Light-emitting polythiophenes", *Adv. Mater.* 17, (19), **2005**, 2281.

21. Roncali J. "Synthetic principles for bandgap control in linear pi-conjugated systems", *Chem. Rev.* 97, (1), **1997**, 173.
22. Van Geneugden D. "Poly(1,3-dithienylisothianaphtene) derivatives; synthesis, characterisation and possible applications of a new class of low bandgap materials", *Ph. D. dissertation*, **1999,** Limburgs Universitair Centrum, Diepenbeek.
23. Roncali J. "Conjugated Poly(Thiophenes) - Synthesis, Functionalization, and Applications", *Chem. Rev.* 92, (4), **1992**, 711.
24. Dietrich M., Heinze J., Heywang G. *et al.* "Electrochemical and Spectroscopic Characterization of Polyalkylenedioxythiophenes", *J. Electroanal. Chem.* 369, (1-2), **1994**, 87.
25. Sankaran B. and Reynolds J. R. "High-contrast electrochromic polymers from alkyl-derivatized poly(3,4-ethylenedioxythiophenes)", *Macromolecules* 30, (9), **1997**, 2582.
26. Sotzing G. A., Reynolds J. R. and Steel P. J. "Electrochromic conducting polymers via electrochemical polymerization of bis(2-(3,4-ethylenedioxy)thienyl) monomers", *Chem. Mat.* 8, (4), **1996**, 882.
27. Kumar A., Buyukmumcu Z. and Sotzing G. A. "Poly(thieno 3,4-b furan). A new low band gap conjugated polymer", *Macromolecules* 39, (8), **2006**, 2723.
28. Lee B., Yavuz M. S. and Sotzing G. A. "Poly(thieno[3,4-b]thiophene)s from three symmetrical thieno[3,4-b]thiophene dimers", *Macromolecules* 39, (9), **2006**, 3118.
29. Schroter S., Stock C. and Bach T. "Regioselective cross-coupling reactions of multiple halogenated nitrogen-, oxygen-, and sulfur-containing heterocycles", *Tetrahedron* 61, (9), **2005**, 2245.
30. Tamao K., Sumitani K. and Kumada M. "Selective Carbon-Carbon Bond Formation by Cross-Coupling of Grignard-Reagents with Organic Halides - Catalysis by Nickel-Phosphine Complexes", *J. Am. Chem. Soc.* 94, (12), **1972**, 4374.

31. Yamamoto T., Sanechika K. and Yamamoto A. "Preparation of Thermostable and Electric-Conducting Poly(2,5-Thienylene)", *J. Polym. Sci. Pol. Lett.* 18, (1), **1980**, 9.

32. Lin J. W. P. and Dudek L. P. "Synthesis and Properties of Poly(2,5-Thienylene)", *J. Polym. Sci. Pol. Chem.* 18, (9), **1980**, 2869.

33. Tamao K., Kodama S., Nakajima I. *et al.* "Nickel-Phosphine Complex-Catalyzed Grignard Coupling .2. Grignard Coupling of Heterocyclic-Compounds", *Tetrahedron* 38, (22), **1982**, 3347.

34. McCullough R. D., Lowe R. D., Jayaraman M. *et al.* "Design, Synthesis, and Control of Conducting Polymer Architectures - Structurally Homogeneous Poly(3-Alkylthiophenes)", *J. Org. Chem.* 58, (4), **1993**, 904.

35. McCullough R. D., Williams S. P., Tristramnagle S. *et al.* "The First Synthesis and New Properties of Regioregular, Head-to-Tail Coupled Polythiophenes", *Synth. Met.* 69, (1-3), **1995**, 279.

36. Loewe R. S., Khersonsky S. M. and McCullough R. D. "A simple method to prepare head-to-tail coupled, regioregular poly(3-alkylthiophenes) using grignard metathesis", *Adv. Mater.* 11, (3), **1999**, 250.

37. Iovu M. C., Jeffries-El M., Sheina E. E. *et al.* "Regioregular poly(3-alkylthiophene) conducting block copolymers", *Polymer* 46, (19), **2005**, 8582.

38. Iovu M. C., Sheina E. E., Gil R. R. *et al.* "Experimental evidence for the quasi-"living" nature of the grignard metathesis method for the synthesis of regioregular poly(3-alkylthiophenes)", *Macromolecules* 38, (21), **2005**, 8649.

39. Sheina E. E., Khersonsky S. M., Jones E. G. *et al.* "Toward Poly(3- and 3,4-alkoxythiophenes)", *Polymer Preprints* 44, (1), **2003**, 843.

40. Sheina E. E., Khersonsky S. M., Jones E. G. *et al.* "Highly conductive, regioregular alkoxy-functionalized polythiophenes: A new class of stable, low band gap materials", *Chem. Mat.* 17, (13), **2005**, 3317.

41. Chen T. A. and Rieke R. D. "Polyalkylthiophenes with the Smallest Bandgap and the Highest Intrinsic Conductivity", *Synth. Met.* 60, (2), **1993**, 175.

42. Chen T. A., Wu X. M. and Rieke R. D. "Regiocontrolled Synthesis of Poly(3-Alkylthiophenes) Mediated by Rieke Zinc - Their Characterization and Solid-State Properties", *J. Am. Chem. Soc.* 117, (1), **1995**, 233.

43. Chen T. A. and Rieke R. D. "The 1st Regioregular Head-to-Tail Poly(3-Hexylthiophene-2,5-Diyl) and a Regiorandom Isopolymer - Ni Vs Pd Catalysis of 2(5)-Bromo-5(2)-(Bromozincio)-3-Hexylthiophene Polymerization", *J. Am. Chem. Soc.* 114, (25), **1992**, 10087.

44. Zhu L., Wehmeyer R. M. and Rieke R. D. "The Direct Formation of Functionalized Alkyl(Aryl)Zinc Halides by Oxidative Addition of Highly Reactive Zinc with Organic Halides and Their Reactions with Acid-Chlorides, Alpha,Beta-Unsaturated Ketones, and Allylic, Aryl, and Vinyl Halides", *J. Org. Chem.* 56, (4), **1991**, 1445.

45. Dai J., Sellers J. L. and Noftle R. E. "An efficient method for the synthesis of 3-alkylthiophenes bearing functional groups on the side chain: imides and amides", *Synth. Met.* 139, (1), **2003**, 81.

46. Miyaura N. and Suzuki A. "Palladium-Catalyzed Cross-Coupling Reactions of Organoboron Compounds", *Chem. Rev.* 95, (7), **1995**, 2457.

47. Svensson M., Zhang F. L., Veenstra S. C. *et al.* "High-performance polymer solar cells of an alternating polyfluorene copolymer and a fullerene derivative", *Adv. Mater.* 15, (12), **2003**, 988.

48. Perzon E., Wang X. J., Zhang F. L. *et al.* "Design, synthesis and properties of low band gap polyfluorenes for photovoltaic devices", *Synth. Met.* 154, (1-3), **2005**, 53.

49. Perzon E., Wang X. J., Admassie S. *et al.* "An alternating low band-gap polyfluorene for optoelectronic devices", *Polymer* 47, (12), **2006**, 4261.

50. Beaupre S. and Leclerc M. "Optical and electrical properties of pi-conjugated polymers based on electron-rich 3,6-dimethoxy-9,9-dihexylfluorene unit", *Macromolecules* 36, (24), **2003**, 8986.

51. Xia Y. J., Luo J., Deng X. Y. *et al.* "Novel random low-band-gap fluorene-based copolymers for deep red/near infrared light-emitting diodes and bulk heterojunction photovoltaic cells", *Macromol. Chem. Phys.* 207, (5), **2006**, 511.

52. Guillerez S. and Bidan G. "New convenient synthesis of highly regioregular poly(3-octylthiophene) based on the Suzuki coupling reaction", *Synth. Met.* 93, (2), **1998**, 123.

53. Milstein D. and Stille J. K. "General, Selective, and Facile Method for Ketone Synthesis from Acid-Chlorides and Organotin Compounds Catalyzed by Palladium", *J. Am. Chem. Soc.* 100, (11), **1978**, 3636.

54. Bundgaard E. and Krebs F. C. "Low-band-gap conjugated polymers based on thiophene, benzothiadiazole, and benzobis(thiadiazole)", *Macromolecules* 39, (8), **2006**, 2823.

55. Dhanabalan A., van Duren J. K. J., van Hal P. A. *et al.* "Synthesis and characterization of a low bandgap conjugated polymer for bulk heterojunction photovoltaic cells", *Adv. Funct. Mater.* 11, (4), **2001**, 255.

56. Zen A., Pflaum J., Hirschmann S. *et al.* "Effect of molecular weight and annealing of poly (3-hexylthiophene)s on the performance of organic field-effect transistors", *Adv. Funct. Mater.* 14, (8), **2004**, 757.

57. Kline R. J., McGehee M. D., Kadnikova E. N. *et al.* "Controlling the field-effect mobility of regioregular polythiophene by changing the molecular weight", *Adv. Mater.* 15, (18), **2003**, 1519.

58. Kossmehl G. and Chatzitheodorou G. "Electrical-Conductivity of Poly(2,5-Thiophenediyl)-AsF_5-Complexes", 2, (9-10), **1981**, 551.

59. Sugimoto R., Takeda S., Gu H.B. *et al. Chem. Express* 1, **1986**, 635.

60. Niemi V. M., Knuuttila P., Osterholm J. E. *et al.* "Polymerization of 3-Alkylthiophenes with $FeCl_3$", *Polymer* 33, (7), **1992**, 1559.

61. Barbarella G., Zambianchi M., DiToro R. *et al.* "Regioselective oligomerization of 3-(alkylsulfanyl)thiophenes with ferric chloride", *J. Org. Chem.* 61, (23), **1996**, 8285.

62. Andersson M. R., Selse D., Berggren M. *et al.* "Regioselective Polymerization of 3-(4-Octylphenyl)Thiophene with Fecl3", *Macromolecules* 27, (22), **1994**, 6503.

63. Leclerc M., Martinez Diaz F. and Wegner G. "Structural analysis of poly(3-alkylthiophene)s", *Makromol. Chem.* 190, **1989**, 3105.

64. Pomerantz M., Tseng J. J., Zhu H. *et al.* "Processable Polymers and Copolymers of 3-Alkylthiophenes and Their Blends", *Synth. Met.* 41, (3), **1991**, 825.

65. Abdou M. S. A., Lu X. T., Xie Z. W. *et al.* "Nature of Impurities in Pi-Conjugated Polymers Prepared by Ferric-Chloride and Their Effect on the Electrical-Properties of Metal-Insulator-Semiconductor Structures", *Chem. Mat.* 7, (4), **1995**, 631.

66. Chen F., Mehta P. G., Takiff L. *et al.* "Improved electroluminescence performance of poly(3-alkylthiophenes) having a high head-to-tail (HT) ratio", *J. Mater. Chem.* 6, (11), **1996**, 1763.

67. Taka T., Nyholm P., Laakso J. *et al.* "Determination of Impurity Effects on Solubility and Processability of Poly(3-Octyl Thiophene)", *Synth. Met.* 41, (3), **1991**, 899.

68. Laakso J., Jarvinen H. and Skagerberg B. "Recent Developments in the Polymerization of 3-Alkylthiophenes", *Synth. Met.* 55, (2-3), **1993**, 1204.

69. Reynolds J. R., Kumar A., Reddinger J. L. *et al.* "Unique variable-gap polyheterocycles for high-contrast dual polymer electrochromic devices", *Synth. Met.* 85, (1-3), **1997**, 1295.

70. Kumar A. and Reynolds J. R. "Soluble alkyl-substituted poly-(ethylenedioxythiophenes) as electrochromic materials", *Macromolecules* 29, (23), **1996**, 7629.

71. Bizzarri P. C., Andreani F., DellaCasa C. *et al.* "Ester-functionalized poly(3-alkylthienylene)s: Substituent effects on the polymerization with FeCl3", *Synth. Met.* 75, (2), **1995**, 141.

72. Chittibabu K. G., Balasubramanian S., Kim W. H. *et al.* "Synthesis and properties of a soluble polythiophene derivative with a urethane side chain", *J. Macromol. Sci.-Pure Appl. Chem.* A33, (9), **1996**, 1283.

73. Kijima M., Akagi K. and Shirakawa H. "Synthesis and characterization of poly(3-substituted thiophene)s having liquid crystalline moiety", *Synth. Met.* 84, (1-3), **1997**, 237.

74. Della-Casa C., Fraleoni-Morgera A., Lanzi M. *et al.* "Preparation and Characterization of thiophene copolymers with second order non-linear optical properties", *Eur. Polym. J.* 41, (10), **2005**, 2360.

75. Costa-Bizzarri P., Lanzi M., Paganin L. *et al.* "Poly [3-hexyl-4-(6-bromohexyl)thiophene]: a key-intermediate for the synthesis of self-plastifying multifunctional polythiophenes", *Polymer* 45, (26), **2004**, 8629.

76. Fraleoni-Morgera A., Della-Casa C., Lanzi M. *et al.* "Investigation on different procedures in the oxidative copolymerization of a dye-functionalized thiophene with 3-hexylthiophene", *Macromolecules* 36, (23), **2003**, 8617.

77. Ng S. C., Fu P., Yu W. L. *et al.* "Electrically conducting poly[3-(omega-hydroxyalkyl)thiophenes]", *Synth. Met.* 87, (2), **1997**, 119.

78. Ong B. S., Wu Y. L., Liu P. *et al.* "High-performance semiconducting polythiophenes for organic thin-film transistors", *J. Am. Chem. Soc.* 126, (11), **2004**, 3378.

79. Jayakannan M., Van Hal P. A. and Janssen R. A. J. "Synthesis and structure-property relationship of new donor- acceptor-type conjugated monomers and polymers on the basis of thiophene and benzothiadiazole", *J. Polym. Sci. Pol. Chem.* 40, (2), **2002**, 251.

80. Catellani M., Boselli B., Luzzati S. *et al.* "Dithienothiophene and dithienothiophene-S,S-dioxide copolymers for photovoltaics", *Thin Solid Films* 403, **2002**, 66.

81. Catellani M., Destri S., Porzio W. *et al.* "Thiazole-Based Polymers - Synthesis, Characterization and Electronic-Structure", *Synth. Met.* 26, (3), **1988**, 259.

82. Becker H., Spreitzer H., Ibrom K. *et al.* "New insights into the microstructure of GILCH-polymerized PPVs", *Macromolecules* 32, (15), **1999**, 4925.

83. Meth-Cohn O. and Ashton M. "Regioselective electrophilic formylation - 3-substituted thiophenes as a case study", *Tetrahedron Lett.* 41, (15), **2000**, 2749.

84. Moratti S. C., Cervini R., Holmes A. B. *et al.* "High Electron-Affinity Polymers for Leds", *Synth. Met.* 71, (1-3), **1995**, 2117.

85. Kesters E., Vanderzande D., Lutsen L. *et al.* "Study of the thermal elimination and degradation processes of n-alkylsulfinyl-PPV and -OC1C10-PPV precursor polymers with in situ spectroscopic techniques", *Macromolecules* 38, (4), **2005**, 1141.

86. Note: It is our experience that the thermal stability of conjugated polymers is limited by the stability of the conjugated system rather than by the thermal stability of the polymer itself. For a detailed study of the stability of the conjugated system measured with an in-situ UV-Vis technique we refer to the previous reference.

87. Aguirre A., Janssen G., Goovaerts E. *et al.* "Optical and EPR spectroscopy in pure and blended films of a novel low band gap polymer", *Eur. Phys. J.-Appl. Phys* 36, (3), **2006**, 285.

88. Nguyen L. H., Gunes S., Neugebauer H. *et al.* "Side chain effects on photoinduced absorption and photovoltaic performance of low bandgap thienylene vinylene and phenylene vinylene copolymers", *Eur. Phys. J.-Appl. Phys* 36, (3), **2006**, 219.

89. Sariciftci N. S., Smilowitz L., Heeger A. J. *et al.* "Photoinduced Electron-Transfer from a Conducting Polymer to Buckminsterfullerene", *Science* 258, (5087), **1992**, 1474.

90. Smilowitz L., Sariciftci N. S., Wu R. *et al.* "Photoexcitation Spectroscopy of Conducting-Polymer-C(60) Composites - Photoinduced Electron-Transfer", *Phys. Rev. B* 47, (20), **1993**, 13835.

91. Lee K., Miller E. K., Sariciftci N. S. *et al.* "Photoinduced absorption and photoinduced reflectance in conducting polymer methanofullerene films: Nonlinear-optical changes in the complex index of refraction", *Phys. Rev. B* 54, (15), **1996**, 10525.

92. De Ceuster J., Goovaerts E., Bouwen A. *et al.* "High-frequency (95 GHz) electron paramagnetic resonance study of the photoinduced charge transfer in conjugated polymer-fullerene composites", *Phys. Rev. B* 64, (19), **2001**, 195206.

93. Brabec C. J., Sariciftci N. S. and Hummelen J. C. "Plastic solar cells", *Adv. Funct. Mater.* 11, (1), **2001**, 15.

94. Scharber M. C., Mühlbacher D., Koppe M. *et al.* "Design Rules for Donors in Bulk-Heterojunction Solar Cells - Towards 10 % Energy-Conversion Efficiency", *Adv. Mat.* 18, (6), **2006**, 789.

95. Motmans F. "Synthesis and Characterisation of Polar PPV Derivatives through the Sulfinyl Precursor Route", *Ph. D dissertation*, **2004,** Limburgs Universitair Centrum, Diepenbeek.

96. Benjamin I., Hong H. P., Avny Y. *et al.* "Poly(phenylenevinylene) analogs with ring substituted polar side chains and their use in the formation of hydrogen bonding based self-assembled multilayers", *J. Mater. Chem.* 8, (4), **1998**, 919.

97. Hughes D. L., Reamer R. A., Bergan J. J. *et al.* "A Mechanistic Study of the Mitsunobu Esterification Reaction", *J. Am. Chem. Soc.* 110, (19), **1988**, 6487.

98. Hughes D. L. "Progress in the Mitsunobu reaction. A review", *Org. Prep. Proced. Int.* 28, (2), **1996**, 127.

99. Mitsunobu O. "The Use of Diethyl Azodicarboxylate and Triphenylphosphine in Synthesis and Transformation of Natural-Products", *Synthesis* (1), **1981**, 1.

100. Hughes D. L. "The Mitsunobu Reaction", *Org. Reactions* 42, **1992**, 335.

101. Pray A. R., in: T. Moeller (Eds.), "Inorganic Synthesis" 5, Mcgraw-Hill Book company, New York, **1957**, 153-155.

Chapter Three

Low Band Gap Polymers based on the Precursor Approach[1]

Abstract: *The precursor approach is discussed in this chapter and in particular the new dithiocarbamate precursor route. Two poly(2,5-thienylene vinylene) derivatives are synthesized. Several polymerization conditions have been studied, including the change of base from LDA to LHMDS. Both polymers have a low band gap (1.7-1.8 eV) and primary solar cell measurements gave promising results. An effort to synthesize the electron poor poly(thiazolo[5,4-*d*]thiazole vinylene) was made. Unfortunately, for this material, the polymerization via the dithiocarbamate precursor route failed.*

3.1 Introduction

3.1.1 The precursor approach

In chapter two the direct synthesis toward low band gap polymers was described. Introduction of side chains was necessary to keep the final polymers soluble and thus processable. A second route toward processable polymers is the precursor approach, which involves the formation of an intermediate non-conjugated, soluble and thus processable, precursor polymer which can be converted into the fully conjugated polymer after processing[2-6]. The use of such a precursor approach implies the formation of a double bond between the aromatic

parts. In this aspect, poly(2,5-thienylene vinylene) (PTV) can be seen as the alternating copolymer of thiophene and acetylene and thus should have properties of both PT and PA[7]. Due to the extra vinylene double bond in PTV, compared to PT, the band gap of PTV is smaller. This is the result of two effects (i) a decrease in the overall aromatic character of the π-conjugated system, allowing a better delocalization of π-electrons over the whole polymer chain, and (ii) a limitation in rotational disorder due to the presence of ethylenic linkages of defined configuration[8]. Since these routes were already well reviewed for poly(*p*-phenylene vinylene) derivatives[9-11], only PTV will be discussed here.

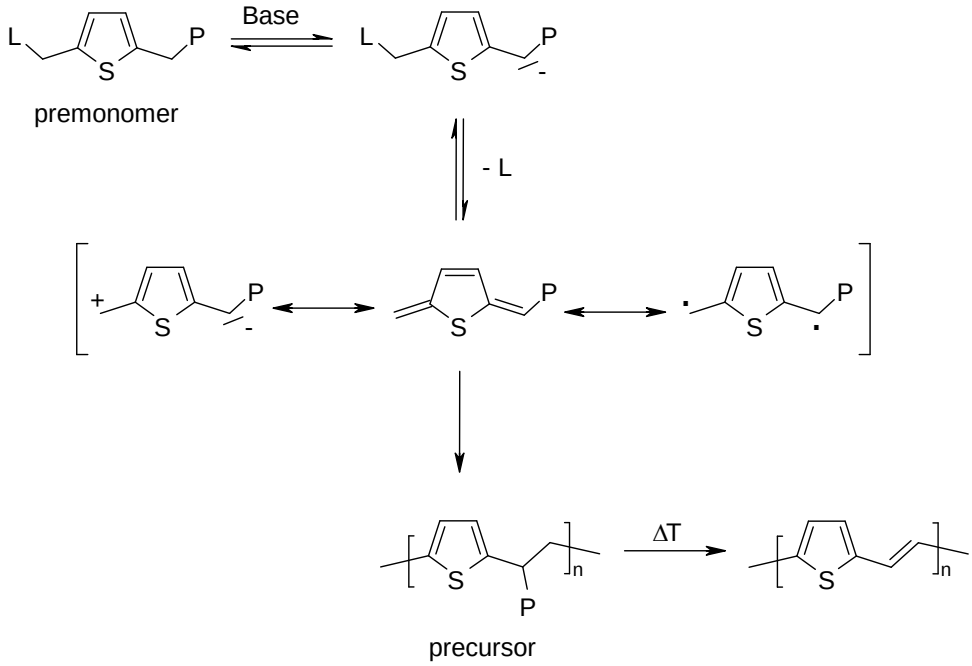

Figure 3-1: General reaction scheme of a precursor route toward PTV.

In Figure 3-1 the general reaction scheme toward PTV *via* a precursor route is depicted. The first step is a base induced 1,6-elimination from the premonomer leading to the in situ formation of the actual monomer, a quinodimethane system. This quinodimethane system can be drawn both under its diamagnetic and paramagnetic

resonance form. The polymerization of the highly reactive quinodimethane intermediate toward the precursor polymer occurs spontaneously. The mechanism (either radical or anionic) is still subject to an ongoing discussion, however, the high molecular weights suggest that a radical mechanism is more favorable. In the last step the precursor polymer is converted to its conjugated analogue *via* thermal treatment.

The first reports on the synthesis of PTV via a precursor route were published in 1987 by Elsenbaumer *et al.*[12-14]. They polymerized, in a ***Wessling*** type of polymerization, 2,5-bis(tetrahydrothiophenonium methyl)thiophene dichloride in water. However the obtained precursor polymer was not stable and a spontaneous elimination to the conjugated form could occur. To overcome this problem, an adaptation of this route was independently reported by Saito *et al.*[15,16] and Murase *et al.*[17]. They treated the water soluble precursor with MeOH to obtain a precursor polymer bearing methoxy leaving groups. (Figure 3-2)

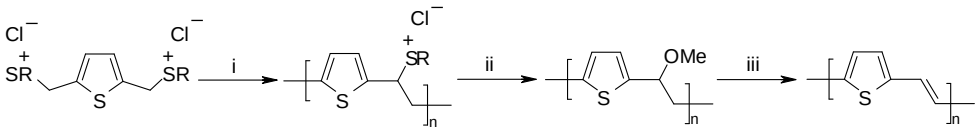

Figure 3-2: Synthesis of PTV via the Wittig precursor route (R = Me_2 or $(CH_2)_4$): (i) NaOH, H_2O; (ii) MeOH, H_2O; (iii) ΔT, HCl.

This adapted *Wessling* route is not ideal however. The synthesis is difficult and the reproducibility is rather poor. Due to the high reactivity, originating from the electron rich thiophene ring, monomer and thus polymer synthesis is difficult. Additionally, an alkoxy leaving group precursor polymer requires acid catalysis for the conversion process. Since this is incompatible with device fabrication, this PTV is not a suitable candidate for device applications.

This high reactivity of (substituted)-2,5-bis(chloromethyl)-thiophene derivatives makes also a ***Gilch*** type polymerization impossible[18, 19].

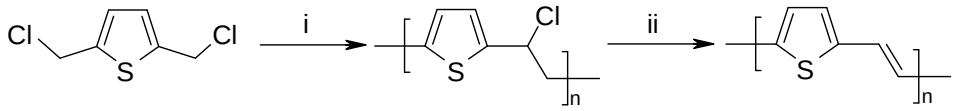

Figure 3-3: Synthesis of PTV via the Gilch precursor route: (i) t-BuOK, THF; (ii) t-BuOK, ΔT.

To overcome these problems, an effort to develop the synthesis of PTV via the **sulphinyl** precursor route was made in our lab[20]. However major difficulties in the synthesis of the sulphinyl monomer were encountered. Solvent substitution and instability of the intermediary products, caused by the high reactivity of the "benzylic" chlorine atoms, were the main problems. Due to these synthetical problems it was almost impossible to apply the sulphinyl route in the synthesis of PTV. Only derivatives with electron withdrawing groups at the 3 and 4 positions were accessible[21].

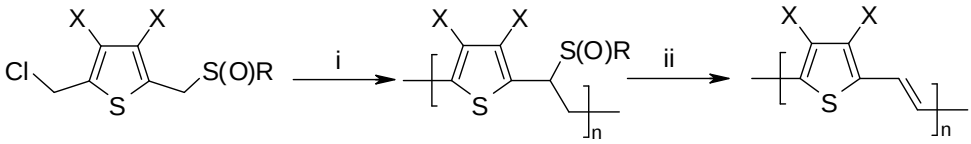

Figure 3-4: Synthesis of PTV via the sulphinyl precursor route (R = octyl and X = Br or Cl): (i) Na-tBuO, s-BuOH; (ii) ΔT.

The **xanthate** route was another option to obtain this polymer but very high polydispersities of the precursor polymers and a quite low λ_{max} value (520 nm) for the corresponding conjugated polymers were found. This resulted in developing another precursor route for PTV synthesis. Given that substituted PTV derivatives could be synthesized via the xanthate precursor route[20], a small change on the level of the leaving group was made. The xanthate group was changed into a **dithiocarbamate** group[1,6,22]. The first results were very promising for PTV; high molecular weight polymers with a high λ_{max} value (570 nm) were obtained. This is an indication of an improved conjugation of the π-

electron system, which means less defects in the polymer chain. The next challenge in further developing this dithiocarbamate route is to try to polymerize more electron rich PTV derivatives and expanding the scope of this polymerization toward other conjugated systems as shown in this chapter.

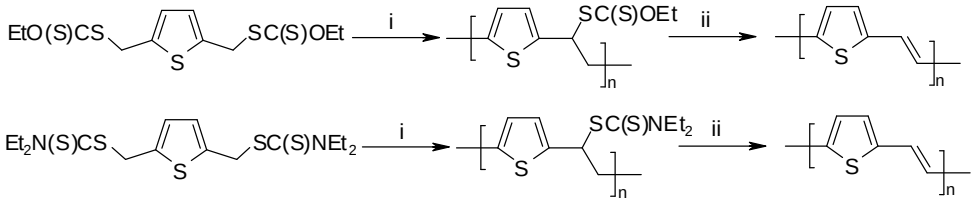

Figure 3-5: Synthesis of PTV via the xanthate (above) and dithiocarbamate (below) precursor route: (i) LDA, THF; (ii) ΔT.

3.1.2 Structures

Of all heteropolymers, thiophene derivatives seem to be the most promising as semi-conducting materials in photovoltaic devices. When looking into literature the majority of the research toward materials for plastic solar cells involves thiophene based conductive polymers and the record efficiency of 5 % was reached with solar cells made of poly(3-hexylthiophene) (P3HT)[23]. In this aspect PTV and especially substituted derivatives can be suitable candidates for the next generation of polymeric solar cells. An example of such a substituted PTV derivative is poly(3,4-diphenyl-2,5-thienylene vinylene) (DP-PTV, **5a**). It is anticipated that in this particular derivative, the sterical hindrance of the reactive 3- and 4-position by the two phenyl rings will lead to a higher stability than its unsubstituted analogue, which is advantageous for applications. Additionally, it is expected that the introduction of phenyl substituents will lead to a decrease in the band gap yielding an even broader absorption of visible light, which would increase the applicability of this class of conjugated materials in photovoltaic applications. In spite of these promising features, surprisingly only limited reports exist on the synthesis and use of DP-PTV. These few reports focus on the

modification of the optical properties of DP-PTV *via* near-field optical microscopy[24,25]. However, the DP-PTV employed in those studies was synthesized *via* the chlorine precursor or Gilch route[26, 27], a route which inherently is characterized by gel formation and the instability of the precursor polymer. Hence, a pathway toward DP-PTV *via* a more suitable route is desirable. One of the major factors causing the limited processability of PTV is the general insolubility of this type of polymers. This problem can be partially circumvented by working *via* a soluble precursor polymer. Notwithstanding, the synthesis of a soluble, conjugated PTV derivative could be a substantial additional advantage. Therefore in a second derivative additional alkyl side chains onto the DP-PTV were introduced leading to a novel soluble derivative of DP-PTV, poly(3,4-bis(4-butylphenyl)-2,5-thienylene vinylene) **5b**.

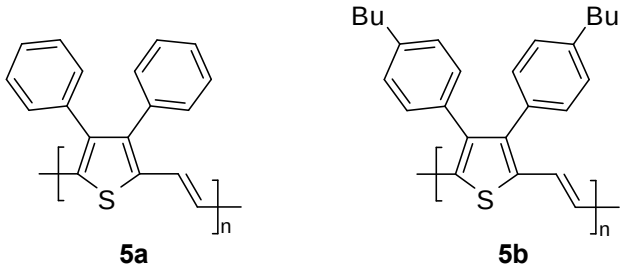

*Figure 3-6: Poly(3,4-diphenyl-2,5-thienylene vinylene) (DP-PTV, **5a**) and poly(3,4-bis(4-butylphenyl)-2,5-thienylene vinylene) **5b**.*

In the second part, the thiophene unit is replaced by a thiazolo[5,4-*d*]thiazole unit. It is reported that this replacement is effective to reduce the sterical interactions due to the absence of hydrogen atoms[28]. In addition, thiazole is an electron-withdrawing heterocycle and the replacement enhances stability to oxygen. Furthermore, the planar geometry induces efficient intermolecular π–π interactions[29-31]. Recently, Ando et al.[32-34] have found that field effect transistors fabricated from thiazolothiazole–thiophene co-oligomers show good p-type characteristics with high stability to oxygen and high field-effect mobilities (2×10^{-2} cm^2 V^{-1} s^{-1}) which are comparable with those of the corresponding alpha-sexithiophenes[35]. This result implies

that the thiazolothiazole ring is a promising candidate as a core unit for high performance semiconductors. Earlier Catellani *et al.*[36] tried to polymerize thiazolo[5,4-*d*]thiazole *via* oxidative coupling which resulted in brown insoluble powders. In this context, and to circumvent the solubility problem (there are no flexible side chains), an attempt was made to synthesize poly(thiazolo[5,4-*d*]thiazole vinylene) **14** *via* the dithiocarbamate precursor route (Figure 3-7).

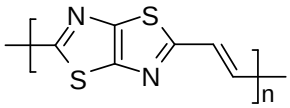

14

Figure 3-7: Poly(thiazolo[5,4-d]thiazole vinylene) ***14****.*

3.2 Poly(3,4-diphenyl-2,5-thienylene vinylene) and poly(3,4-bis(4-butylphenyl)-2,5-thienylene vinylene)

3.2.1 Monomer synthesis

In view of the advantages compared to the other routes, the dithiocarbamate precursor route has been picked as the precursor method of choice to obtain the PTV derivatives. The monomers used in the dithiocarbamate precursor route are synthesized from a dihalogenide in a single step reaction[6]. In the past, two different synthetic pathways toward the required dihalogenide, *i.e.* 3,4-diphenyl-2,5-bischloromethylthiophene **2a**, have been described[37]. The first route involves the reduction of two carboxylic groups with lithium aluminum hydride ($LiAlH_4$) followed by chlorination of the diol with thionyl chloride ($SOCl_2$) to yield the desired dichloride **2a**. Upon purification by column chromatography of **2a** prepared *via* this first route, degradation occurred as a result of its instability.

In the second route toward dichloride **2a**, first 3,4-diphenylthiophene **1a** has been synthesized *via* the method developed

by Nakayama *et al*.[38, 39]. The latter involves a three step synthesis of thiophenes with two substituents on the 3- and 4-positions. However the yield over the three steps to obtain **1a** is only 30 %.

Upon the commercialization of a lot of boronic acid compounds, a new route to obtain the monomer was accessible. Compound **1** is now directly synthesized *via* a *Suzuki* coupling reaction between the commercially available phenylboronic acid and 3,4-dibromothiophene in 77 % yield. Having obtained **1a** *via* this *Suzuki* coupling, the desired dichloride **2a** is prepared *via* a typical chloromethylation reaction[40]. It should be noted that **2a** prepared *via* this route does not require purification by column chromatography which can lead to degradation. Instead, the dithiocarbamate monomer **3a** forms directly from the bischloromethyl compound **2a** by reaction with sodium diethyldithiocarbamate trihydrate.

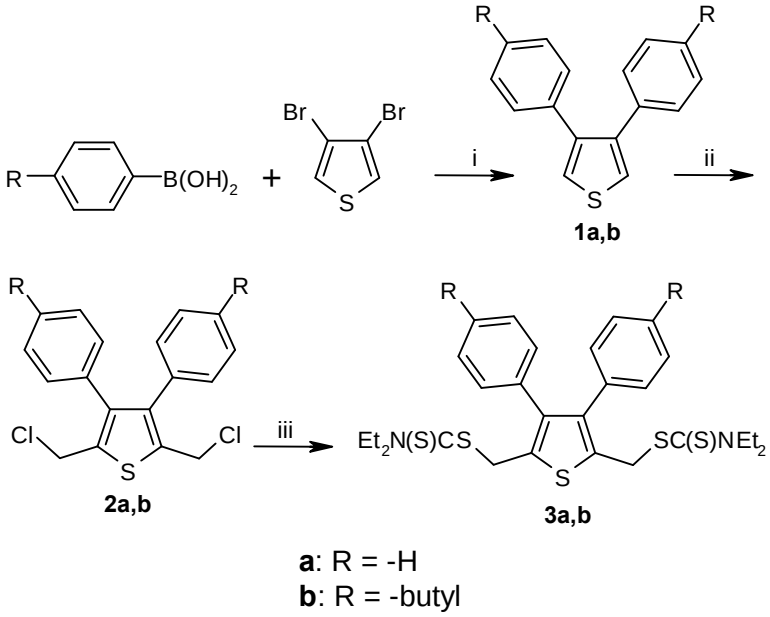

*Figure 3-8: Synthetic route toward the dithiocarbamate monomers **3a,b**. (i) $Pd(PPh_3)_4$, KF, toluene/H_2O; (ii) CH_2O, HCl, Ac_2O; (iii) $NaSC(S)NEt_2.3H_2O$, MeOH.*

In view of the better overall monomer yields, the straightforward preparation and conversion of **2a** without degradation as well as the

lowest number of reaction steps, the third route involving the *Suzuki* coupling of the phenyl with the thiophene ring has been chosen to prepare **3a**. The overall yield from the starting compounds toward **3a** is 53 %. Similar considerations have motivated our choice to prepare the butyl substituted monomer **3b** *via* this route. This synthesis is straightforward and the overall yield from the starting compounds toward **3b** is 39 %.

Structural characterization of the monomers

Structural characterization of the monomers **3a** and **3b** was performed using standard ^{1}H and ^{13}C NMR techniques. Chemical shift assignment can be found in Table 3-1 and the spectra (Figure 3-9).

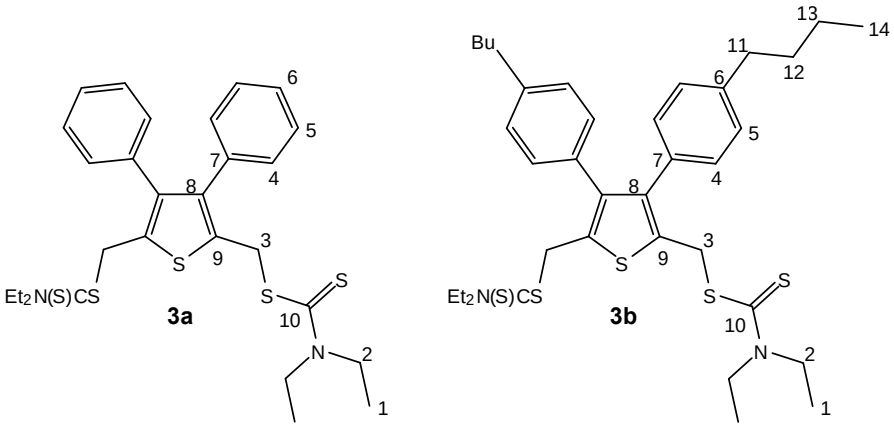

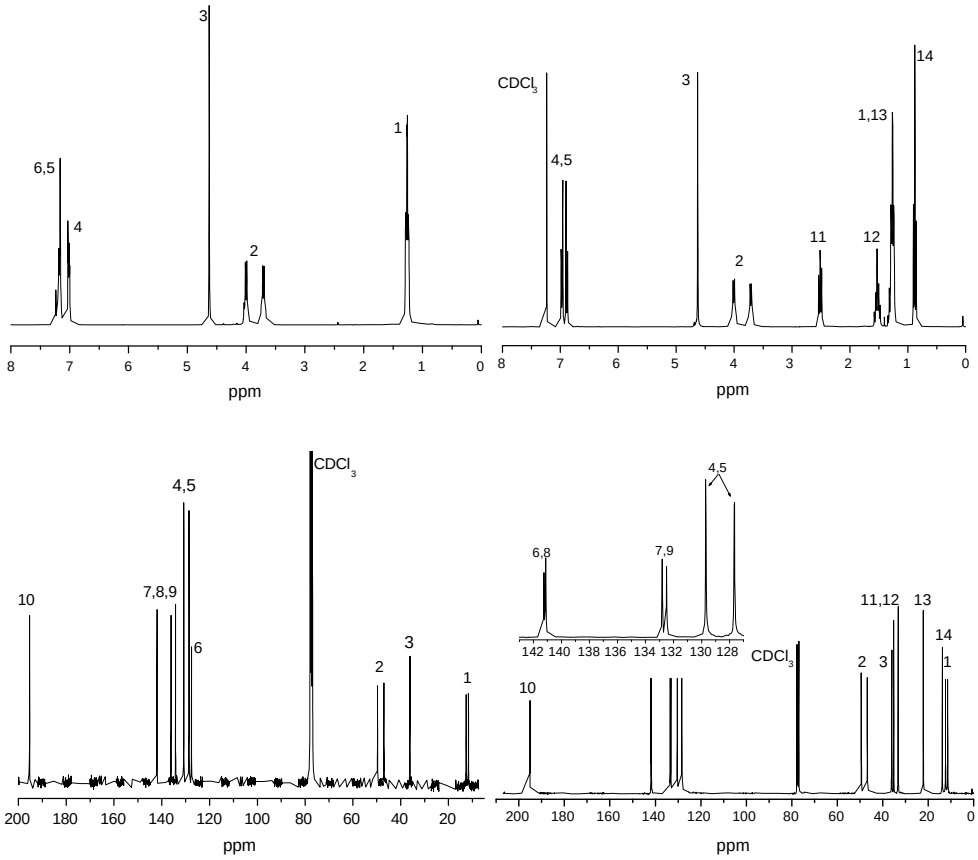

*Figure 3-9: ^{1}H and ^{13}C NMR spectra of monomers **3a** (left) and **3b** (right)*

*Table 3-1: ^{1}H and ^{13}C chemical shift values of **3a** and **3b**.*

#3a	^{1}H δ (ppm)	^{13}C δ (ppm)	#3b	^{1}H δ (ppm)	^{13}C δ (ppm)
1	1.26	11.4-12.4	1	1.27	11.4-12.4
2	3.69-4.01	46.6-49.3	2	3.71-4.01	46.6-49.2
3	4.62	35.8	3	4.63	35.9

*Table 3-1: ^{1}H and ^{13}C chemical shift values of **3a** and **3b** (con't.).*

#3a	^{1}H δ (ppm)	^{13}C δ (ppm)	#3b	^{1}H δ (ppm)	^{13}C δ (ppm)
4	1.47	127.8-130.0	4	6.97-6.90	127.7-129.8
5	7.02-7.19		5		
6		126.7	6		141.1-141.2
7		133.4-	8		
8		135.3-	7		132.5-132.8
9		141.14	9		
10		194.2	10		194.2
11			11	2.52	33.1-35.1
12			12	1.53	
13			13	1.27	22.1
14			14	0.88	13.8

3.2.2 Polymerization

3.2.2.1 Influence of temperature

The polymerization of monomer **3a** has been performed using three different reaction conditions (cf. entries 1-3, Table 3-2), deviating in the temperatures employed. For monomer **3b** only one procedure has been selected (cf. entry 4, Table 3-2). For all reactions, lithium diisopropyl amide (LDA) is used as the base and dried THF as the solvent (Figure 3-10).

After the polymerization was allowed to proceed for 90 minutes, termination of the reaction is achieved by pouring the polymerization mixture in ice water followed by acidification with hydrochloric acid (1 M) to pH = 7. To avoid possible side reactions, the polymerizations performed at -78 °C are first quenched with ethanol at -78 °C prior to this acidification step (only entries 2 and 4, Table 3-2). After extraction, the polymers are purified using reprecipitation. The isolated yields range from 20 to 40 % (Table 3-2), with the highest yields being associated with the low polymerization temperatures.

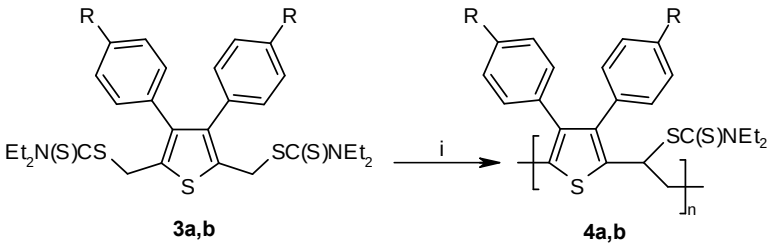

3a,b **4a,b**

a: R = -H
b: R = -butyl

*Figure 3-10: Polymerization of the monomers **3a,b** toward the precursor polymers **4a,b**. (i) LDA, THF.*

The weight-average molecular weights (M_w) of **4a** and **4b** have been determined by analytical SEC in DMF and THF respectively against polystyrene standards. The observed molecular weight distributions for **4a** are monomodal with M_w values ranging from 24.6 x 10^3 to 50.4 x 10^3 and low polydispersities (cf. entries 1-3, Table 3-2). In contrast, polymer **4b** exhibits a bimodal weight distribution with a lower apparent M_w (M_W = 16.2 x 10^3 and 3.3 x 10^3; cf. entry 4, Table 3-2). However, it should be noted that since all molecular weights are referenced to polystyrene standards, the actual value for M_w will differ from the apparent M_w observed with analytical SEC.

*Table 3-2: Polymerization results for monomer **4a** (entry 1-3) and **4b** (entry 4).*

	Entry	Polymerization temperature	M_w [x 10^{-3}]	PD	Yield [%]
4a[a]	1	0°C	50.4	1.4	20
	2	-78°C	29.8	1.2	40
	3	-78°C → 0°C	24.6	1.2	35
4b[b]	4	-78°C	16.2, 3.3[c]	1.2, 1.1[b]	38

[a] *Determined by means of SEC in DMF against polystyrene standards.*

[b] *Determined by means of SEC in THF against polystyrene standards.*

[c] *Bimodal molecular weight distribution*

3.2.2.2 Influence of the base used

The molecular weights of the polymers obtained *via* the polymerization with LDA were promising but still rather low. Furthermore, polymerization of the soluble derivative proved to be very difficult. Since LDA is a very reactive compound the decision was made to use a less reactive base but still with a similar structure. Therefore lithium hexamethyldisilazane (LHMDS) was chosen. LHMDS is less basic, more stable and much less sensitive to air as compared to LDA.

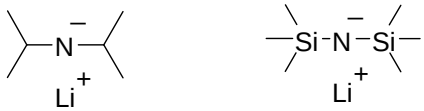

Figure 3-11: Lithium diisopropyl amide (LDA) (left) and lithium hexamethyldisilazane (LHMDS) (right).

In Table 3-3 the polymerization results are summarized. The weight-average molecular weights (M_w) of **4a** and **4b** have been determined by analytical SEC in DMF and THF respectively against polystyrene standards. The observed molecular weight distributions for **4a** are monomodal with M_w values ranging from 82.9 x 10^3 to 708.3 x 10^3 for polymerization with LHMDS. The same trend is observed for the soluble analogue **4b** with M_w values ranging from 138.2 x 10^3 to 592.3 x 10^3.

It is clear from these values that polymerization with LHMDS as base gives rise to polymers with much higher molecular weights as compared to the results obtained with LDA. As a result, even at 25 °C polymerization occurred where polymerization at ambient temperatures with LDA did not yield any polymer. Both the higher polymerization temperature and the higher molecular weights are significant advantages from an industrial application point of view. High M_w polymers have better film forming properties which is crucial for device preparation. Furthermore, recent papers[41,42] correlate the charge carrier mobility in devices to the molecular weight of the polymer. It has been shown that high molecular weight polymers exhibit better mobility.

*Table 3-3: Polymerization results for monomer **4a** and **4b** with LHMDS as base.*

Entry	Polymerization Temperature	4a[a]			4b[b]		
		Yield [%]	M_w [x 10^{-3}]	PD	Yield [%]	M_w [x 10^{-3}]	PD
1	-78°C	60	708.3	3.3	74	592.3	2.5
2	-78°C → 0°C	55	625.7	3.1	66	402.7	2.4
3	0°C	68	82.9	3.4	67	241.8	2.2
4	25°C	56	89.8	3.5	63	138.2	2.1

[a]*Determined by means of SEC in DMF against polystyrene standards.*

[b]*Determined by means of SEC in THF against polystyrene standards.*

3.2.3 Conversion of the polymer into the conjugated structure

The synthesized precursor polymers can be transformed into the conjugated polymer by a thermal treatment. Upon heating, the dithiocarbamate group of polymer **4a,b** is eliminated to form the corresponding conjugated polymer **5a,b** (Figure 3-12). The thermal conversion can be performed in a thin film or in solution, depending on the type and solubility of the polymer used. Thin film processes have the extra advantage that the thermal elimination reaction and the thermal stability of the polymer can be followed by means of *in-situ* UV-Vis and *in-situ* FT-IR spectroscopy. In this way one can deduce a reproducible protocol to convert the precursor into the conjugated form, which is essential for device applications.

The thin film conversion process was used to obtain both **5a** and **5b**. In contrast to the thin film elimination, the solution elimination process can be accomplished on a large scale, although this is only of interest when the conjugated polymer obtained is soluble. Hence, the solution elimination was only performed to obtain the butyl substituted DP-PTV **5b**.

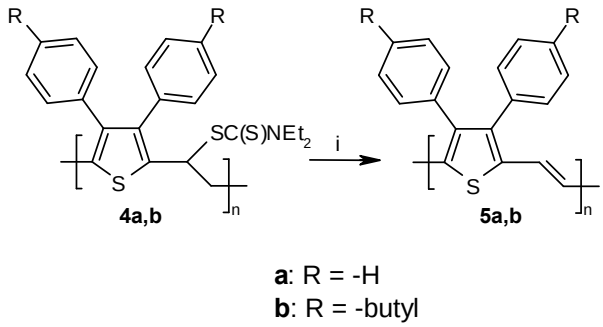

*Figure 3-12: Formation of the conjugated polymers **5a,b**. (i) ΔT in film or dichlorobenzene.*

3.2.3.1 Formation of **5a** in a thin film

The results shown in this part are originating from films made of the polymer with characteristics shown in Table 3-2, entry 2. Films of the other polymers showed exactly the same optical properties. Upon heating a thin film of **4a**, the gradual formation of the conjugated structure of polymer **5a** is observed. This is well visible in the temperature dependent UV-Vis absorption spectrum by the development of a band with λ_{max} = 550-600 nm and the decrease of the absorption of **4a** at λ_{max} = 247 nm (Figure 3-13, left). The thermal process can be better analyzed using the absorbance profiles (Figure 3-13, right). In these profiles, an increase in the absorbance at 590 nm can be seen between 110 and 160 °C, reflecting the formation of the conjugated system. Furthermore, in the region between 80 and 160 °C, the formation and disappearance of partially conjugated segments (λ_{max} = 403 nm) is visible.

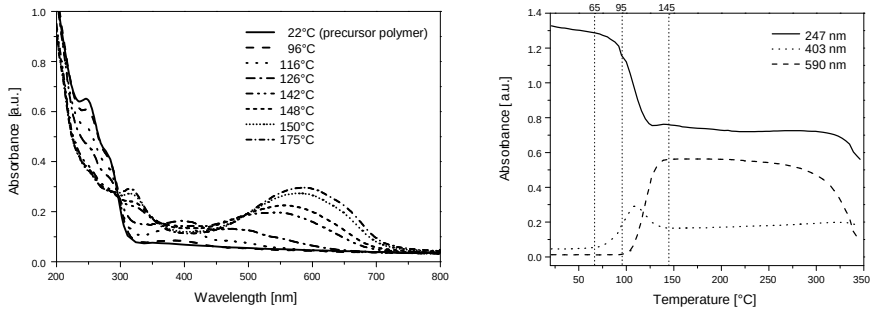

*Figure 3-13: Temperature dependent UV-Vis spectra of the elimination of **4a** giving **5a** (left). UV-Vis absorbance profiles at 247, 403 and 590 nm as a function of temperature during the elimination of **4a** (right).*

The conversion process is also readily observed using temperature dependent FT-IR spectroscopy (Figure 3-14, left). The absorption bands at 1486, 1416, 1267 and 1206 cm^{-1} all arise from the dithiocarbamate group. From the profiles in Figure 3-14 (right), it is clear that the increase in double bond absorption (934 cm^{-1}) starts just above 100 °C and the conversion process is complete around 130 °C for the applied temperature program (heating rate at 2 °C/min).

This small difference as compared to the temperature dependent UV-Vis data is a result of the increased sensitivity of FT-IR, *viz.* any double bond formed will be visible in FT-IR, whereas only longer conjugated systems will be visible in the UV-Vis spectra. Hence, temperature dependent FT-IR spectroscopy is an excellent method to study the start and nature of the elimination process, whereas temperature dependent UV-Vis spectroscopy is the most suitable method to determine the end-point of the elimination process. It is noteworthy that the thermal stability of **5a** is 300 °C. This is higher than unsubstituted PTV, which already displays a notable decrease in intensity of the UV-Vis absorption maximum around 275 °C[6].

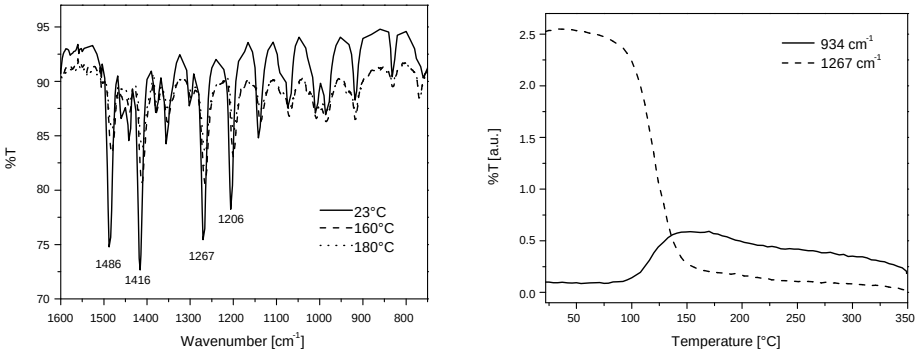

*Figure 3-14: Temperature dependent FT-IR spectra of the elimination of **4a** giving **5a** (left). IR absorption profiles at 934 and 1267 cm^{-1} as a function of temperature during the elimination of **4a** (right).*

The room temperature absorption maximum λ_{max} of a thin film of **5a** is 600 nm (Figure 3-15). This is notably higher than λ_{max} observed by previous researchers for thin films of the same polymer (*i.e.* 546[26] and 540 nm[27]). These anomalous results are possibly the result of either the presence of polymer defects or the occurrence of incomplete conversion in the previous studies; *viz.* only comparatively short conjugated systems were present. This is in agreement with our observations in the temperature dependent UV-Vis measurements (Figure 3-13, left), in which the λ_{max} of a thin film of **5a** gradually shifts to higher wavelength upon increase of temperature. In our experiments, all films are heated until no increase of λ_{max} occurs, *i.e.* full conjugation is achieved. Upon heating **5a**, a blue-shift of λ_{max} is observed as a result of the thermochromic effect (175°C: λ_{max} = 590 nm). This thermochromic shift of 10 nm is smaller than the shift observed for unsubstituted PTV (*i.e.* 25 nm), possibly reflecting the reduced mobility of the phenyl substituted PTV main chain[6]. The band gap of **5a** at room temperature can be derived from its UV-Vis characteristics by drawing the tangent on the low energetic edge of the absorption spectrum. The intersection with the abscissa is at 730 nm which corresponds to a band gap of 1.70 eV. This is almost identical to the band gap observed for PTV, *i.e.* 1.67 eV[6].

Apparently, no reduction in band gap is observed as a result of phenyl substitution, possibly as a result of competing sterical effects. In agreement to unsubstituted PTV as well as other substituted PTV derivatives[43], thin films and solutions of polymer **5a** do not exhibit photoluminescence at room temperature.

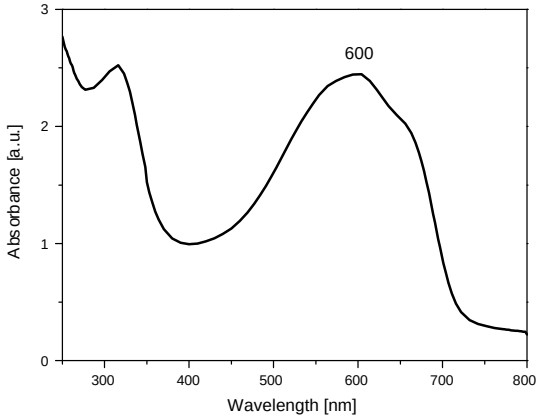

*Figure 3-15: Room temperature absorbance spectrum of **5a**.*

3.2.3.2 Formation of **5b** in a thin film

Precursor polymer **4b** was converted in a thin film toward **5b** under similar conditions as **4a**. Temperature dependent UV-Vis and FT-IR measurements (Figure 3-16 and Figure 3-17) indicate that the introduction of butyl groups surprisingly has only a small impact on the elimination process, *i.e.* the elimination process starts at *circa* 90 °C. However, it should be noted that the profiles (Figure 3-16, right and Figure 3-17, right) indicate that degradation of the conjugated system commences around 275 °C. Apparently the introduction of the butyl side chains somewhat reduces the thermal stability. Notwithstanding, thermal stability up to 275 °C is sufficiently high for virtually all applications. The shoulder observed in the profile at 1266 cm^{-1} of the in situ FT-IR measurement is inherent to the measurement technique. Since the profile is measured at a fixed wavenumber, even a slight shift

of the absorption peak results in a shoulder in the profile, especially for the rather narrow peaks in the FT-IR spectra. In this particular case the original peak at 1266 cm^{-1} shifts toward 1264 cm^{-1} at higher temperature.

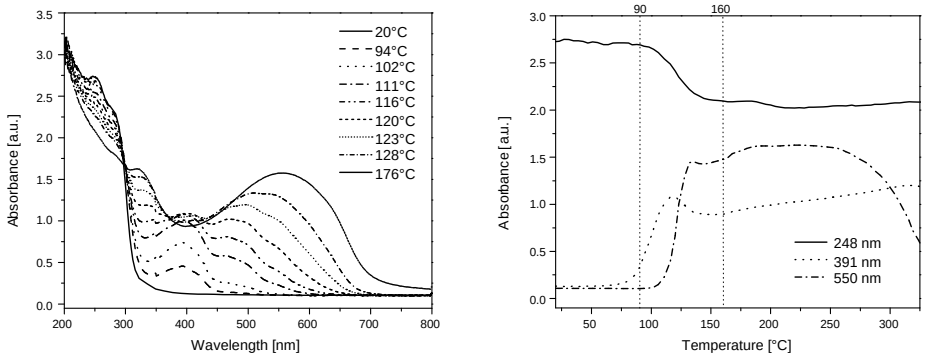

*Figure 3-16: Temperature dependent UV-Vis spectra of the elimination of **4b** giving **5b** (left). UV-Vis absorbance profiles at 247, 403 and 590 nm as a function of temperature during the elimination of **4b** (right).*

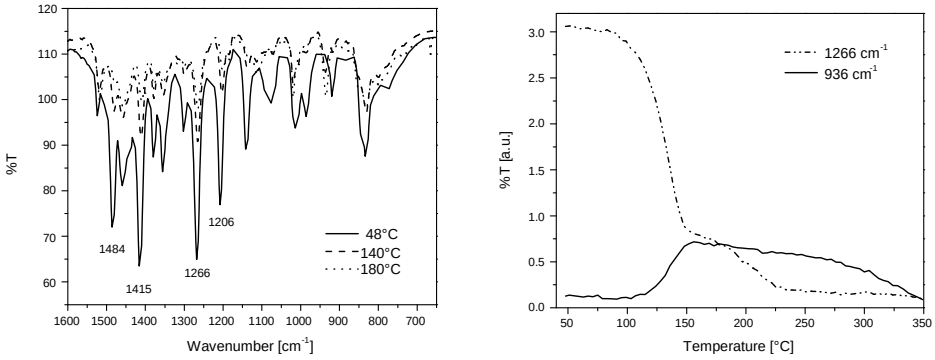

*Figure 3-17: Temperature dependent FT-IR spectra of the elimination of **4b** giving **5b** (left). IR absorption profiles at 936 and 1266 cm^{-1} as a function of temperature during the elimination of **4b** (right).*

The introduction of alkyl side chains has also an impact on the room temperature UV-Vis absorption properties (Figure 3-18). In this case however, in contrast to the elimination process, there is a

significant difference between the low M_w polymer (Entry 4; Table 3-2) and the higher M_w polymers obtained from the polymerization with LHMDS (Entry 1; Table 3-3).

Low M_w polymer 5b

The room temperature absorption maximum λ_{max} of a thin film of low M_w **5b** is 590 nm (Figure 3-18, dashed line). This is slightly blue-shifted with respect to the absorption maximum observed for **5a** (λ_{max} = 600 nm, Figure 3-15). This shift is also observed for the band gap. The low energetic edge of the absorption spectrum of low M_w **5b** is at 701 nm which corresponds to a band gap of 1.77 eV.

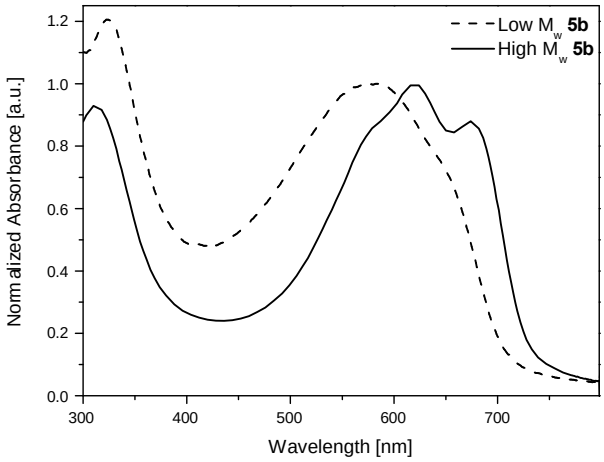

*Figure 3-18: Room temperature absorbance spectrum of low M_w **5b** (dashed line) and high M_w **5b** (solid line).*

High M_w polymer 5b

For thin films of higher M_w **5b** the room temperature absorption maximum λ_{max} is 620 nm (Figure 3-18, solid line). This is a red shift of 30 nm as compared to low M_w **5b**. This is a strong evidence that,

besides the increase in M_w of the polymers, also the quality of the conjugated system, *i.e.* less defects, is much better when polymerizing with LHMDS as base. Furthermore this high M_w **5b** exhibits a distinct shoulder at 674 nm which could be related to strong $\pi-\pi$ interactions in the solid state inducing ordering. The low energetic edge of the absorption spectrum of high M_w **5b** is at 730 nm which corresponds to a band gap of 1.70 eV which is the same as the band gap of **5a**.

3.2.3.3 Formation of **5b** in solution

In addition to the thin film conversion, highly soluble **4b** has also been converted into **5b** in solution. Dichlorobenzene was used as the solvent and the solution was heated to 150 °C. It is noteworthy that conjugated **5b** is soluble in a wide variety of common organic solvents, including $CHCl_3$, CH_2Cl_2, toluene and (di)chlorobenzene. Hence, **5b** can be analyzed in solution as well as spin-coated from a solution, thus considerably increasing the applicability of this polymer for electronic applications. The apparent molecular weight (M_w) observed with analytical SEC of low M_w **5b** prepared in this way is 9.0 x 10^3 (solvent THF; polydispersity PD = 1.7). For high M_w **5b** this is 23 x 10^3 (solvent THF; polydispersity PD = 2.6). These molecular weights are low as compared to the precursor polymer. This is probably due to the (lack of) solubility of the polymers in THF. Apparently, only the lower molecular weight fraction passes through the filter prior to the SEC measurement.

Low M_w polymer 5b

The observed absorption maximum (λ_{max}) of a thin film of low M_w **5b** spin-coated from a $CHCl_3$ solution is 592 nm. The UV-Vis absorption spectrum of a solution of low M_w **5b** in $CHCl_3$ exhibits an absorption maximum λ_{max} = 577 nm (Figure 3-19, left). This is 15 nm blue shifted with respect to the absorption maximum of a thin film of **5b** as a result of electronic interchain interactions in the solid state.

High M_w polymer 5b

The same difference between high and low M_w **5b**, as seen for the conversion in film, is noticed in the absorption spectra obtained from the conversion in solution. In thin film, the observed absorption maximum (λ_{max}) of high M_w **5b** is 620 nm. In $CHCl_3$ solution, high M_w **5b** exhibits an absorption maximum λ_{max} of 593 nm (Figure 3-19, right). In this case, there is a 27 nm blue shift with respect to the absorption maximum of a thin film of **5b**.

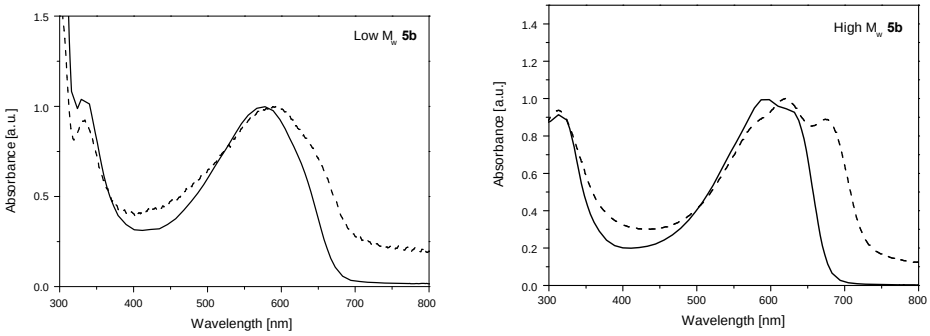

*Figure 3-19: UV-Vis absorption spectra of low M_w **5b** (left) and high M_w **5b** (right) in a $CHCl_3$ solution (solid) and as a thin film spin coated from a $CHCl_3$ solution (dashed).*

Similarly to **5a**, solutions and thin films of polymer **5b** do not exhibit photoluminescence at room temperature. The thermal stability of the conjugated system of spin-coated thin films of **5b** formed in solution was investigated using temperature dependent UV-Vis spectroscopy (Figure 3-20). The onset of degradation occurs around 180 °C as compared to 275 °C in the films of **5b** formed directly in a thin film. The origin of this difference is not certain, but may be related to the exposure of the, in solution formed, **5b** to ambient conditions after conversion and during spin-coating.

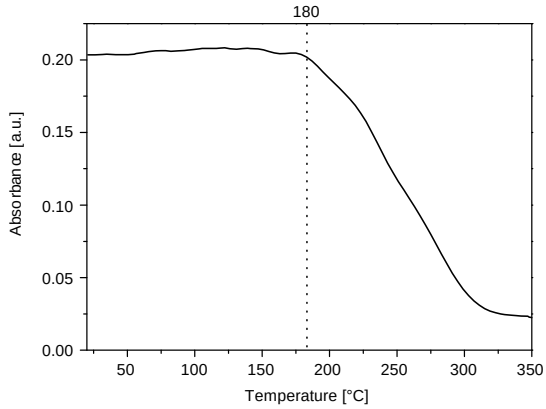

*Figure 3-20: UV-Vis absorbance profile of **5b** at λ_{max} as a function of temperature.*

3.2.4 Electrochemistry

Cyclic voltammetry (CV) was employed to investigate the electrochemical behavior of polymers **5a** and **5b** and to estimate their energy levels. No significant difference was observed between the high and low M_w polymers. The cyclic voltammograms of **5a** and **5b** display distinct quasi reversible oxidation and reduction processes (Figure 3-21). The oxidation potential of **5a** is 0.43 V *vs.* Ag/Ag^+. However, the HOMO energy level is more accurately determined from the onset of oxidation. In the anodic scan the onset of oxidation of **5a** occurs at 0.24 V *vs.* Ag/Ag^+, which corresponds to a HOMO energy level of -5.19 eV. The reduction potential of **5a** is -1.91 V *vs.* Ag/Ag^+, but the onset of reduction is at -1.62 V *vs.* Ag/Ag^+. This corresponds to a LUMO energy level of -3.33 eV. The p-doping for **5b** is also reversible (oxidation potential is 0.63 V *vs.* Ag/Ag^+), although not as well defined as for **5a**. The onset of oxidation of **5b** occurs at 0.29 V *vs.* Ag/Ag^+, which corresponds to a HOMO energy level of –5.24 eV. The LUMO energy level of -3.26 eV was determined from the onset of reduction (-1.69 V *vs.* Ag/Ag^+, reduction potential -1.8 V *vs.* Ag/Ag^+). For comparison, the oxidation potential of PTV is 0.39 V *vs.* Ag/Ag^+ with an onset of

oxidation at 0.15 V *vs.* Ag/Ag^+, which corresponds to a HOMO energy level of −5.08 eV.

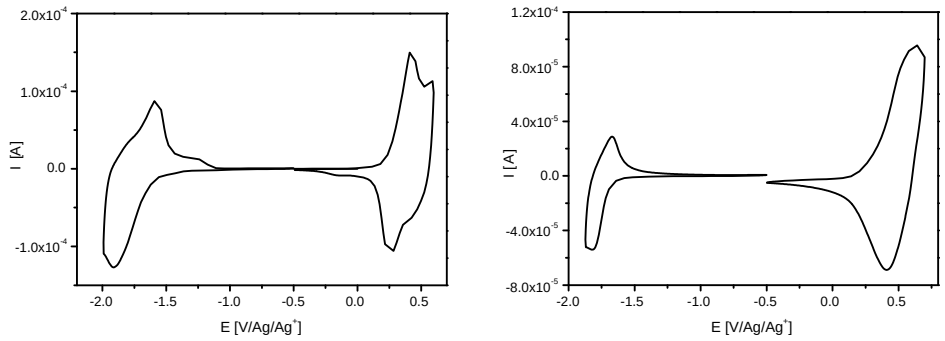

*Figure 3-21: Cyclic voltammograms of the oxidation and reduction behavior of thin films of **5a** (left) and **5b** (right).*

It should be noted that the oxidation process can also be observed visually. For both **5a** and **5b** a color change of the films from blue to light yellow was observed upon oxidation. Subsequently, in the reverse process upon dedoping, the color of the film returned to blue. This observation further confirms the reversibility of the p-doping process. It is noteworthy that upon application of increased bias (*i.e.* scanning to 1.0 V *vs.* Ag/Ag^+), a second and a third oxidation process can be observed for **5a** (Figure 3-22). Similarly to the first oxidation process, which is associated with the HOMO energy level, the second oxidation process with an oxidation potential of *circa* 0.7 V *vs.* Ag/Ag^+ (-5.4 eV) is reversible. This process is possibly associated with the oxidation of the phenyl rings. In contrast, the third oxidation process with an oxidation potential of *circa* 0.9 V *vs.* Ag/Ag^+ (-5.6 eV) is irreversible and results in the irreversible degradation of the conjugated system.

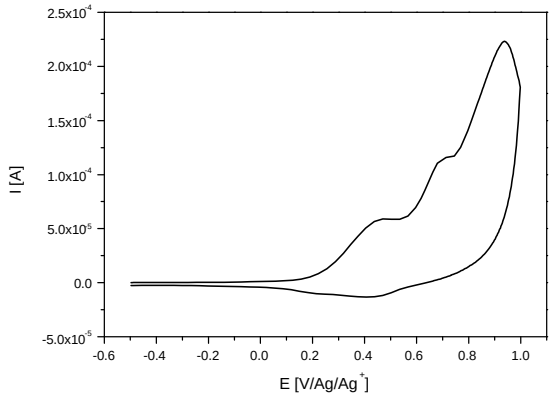

*Figure 3-22: Cyclic voltammogram of the oxidation behavior of a thin film of **5a**.*

Figure 3-23 exhibits the resulting energy band diagram in relation to the relative energy levels of the most frequently employed acceptor in organic solar cells, PCBM, and the workfunctions of indium tin oxide (ITO) and aluminum (Al), which are usually applied as electrodes in polymer solar cells. The HOMO of the polymers **5a** and **5b** is distinctively higher in energy than that of PCBM. However, not only the HOMO energy levels but also the relative positions of the donor LUMO and the acceptor LUMO are important for the intended charge transfer. The difference between the LUMOs of **5a**, **5b** and PCBM is in the range of 0.6 eV, which is sufficiently high to enable an unrestricted and directed charge transfer.

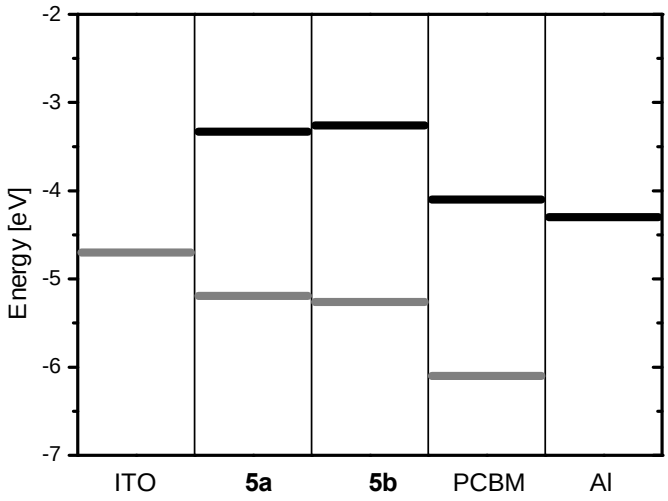

*Figure 3-23: Energy band diagram with HOMO/LUMO levels of **5a**, **5b** and PCBM in relation to the work function of the common electrode materials ITO and Al.*

3.2.5 Photovoltaic device

Exploratory photovoltaic studies on solar cell devices were performed by Le Huong Nguyen and Helmut Neugebauer from the group of Serdar Sariciftci at the Linz Institute for Organic Solar Cells (LIOS) in Austria.

Typical I-V characteristics of ITO/PEDOT:PSS/**5b**:PCBM/LiF/Al (named **5b** device) is shown in Figure 3-24, both in dark (dotted line) and under AM 1.5 illumination (solid line). The **5b** device performance shows open circuit voltages (V_{OC}) of 650 mV, short circuit currents (I_{SC}) of 0.97 mA/cm^2, fill factors (FF) of 0.34 and the conversion efficiency (η) of about 0.27 %. The polymer used in this device was the low M_w **5b**. The high M_w **5b** was still under investigation at the time of writing.

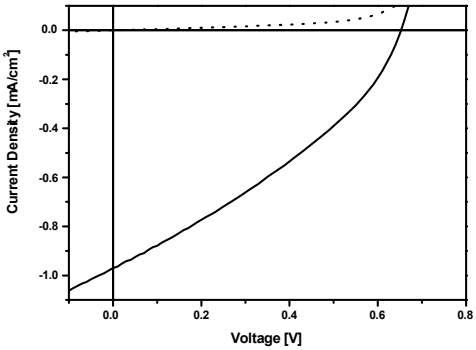

*Figure 3-24: Linear representations of I-V characteristics (AM 1.5, 100 mW/cm^2) of ITO/PEDOT:PSS/**5b**:PCBM/LiF/Al. The solid line represents data obtained under illumination, while the dotted line is measured in the dark.*

3.3 Poly(thiazolo[5,4-d]thiazole vinylene)

3.3.1 Monomer synthesis

Two different synthetic routes toward the required intermediate diethyl thiazolo[5,4-*d*]thiazole-2,5-dicarboxylate (**10**) have been successfully tested[44,45]. The first route (Figure 3-25, A) starts with the formation of *N*-formylglycine ethyl ester **(6)** in good yield (73 %) from the commercial available glycine ethyl ester hydrochloride and methyl formate under basic conditions. Next, **6** is reacted with phosphorus oxychloride to yield ethyl isocyanoacetate (**7**) (yield: 82 %). The synthesis toward **7** is adapted from a literature procedure[46]. In the next step the thiazolo[5,4-*d*]thiazole-2,5-dicarboxylate (**10**) is formed from **7** and dichlorodisulfane. A possible reaction mechanism of this step, proposed by Bossio *et al.*[44], is depicted in Figure 3-26. The yield obtained in literature was 52 %, however in our case only 19 % was achieved.

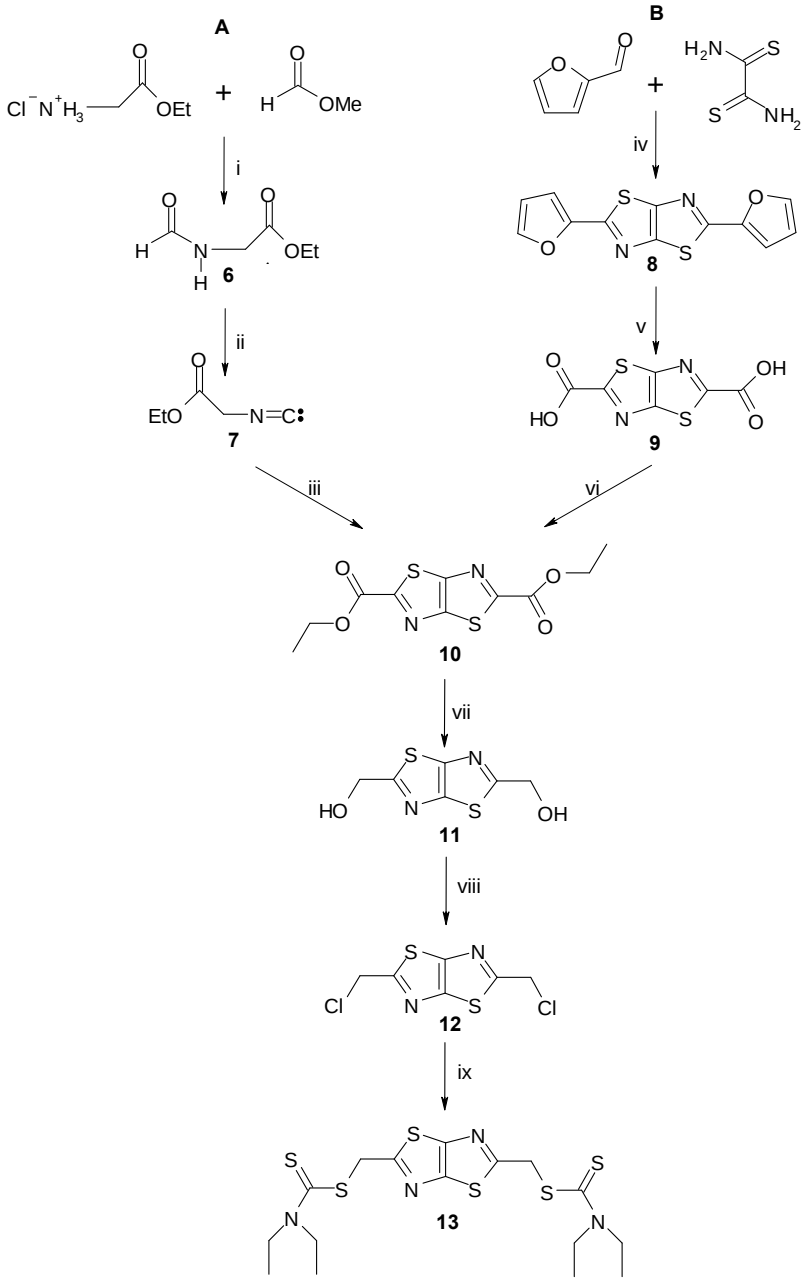

Figure 3-25: General scheme of the monomer synthesis. (i) Et_3N; (ii) Et_3N, CH_2Cl_2, $POCl_3$; (iii) S_2Cl_2, CH_2Cl_2, Et_3N; (iv) ΔT; (v) pyridine, $KMnO_4$, HCl; (vi) EtOH, H_2SO_4; (vii) $NaBH_4$, MeOH; (viii) $SOCl_2$; (ix) $NaSC(S)NEt_2.3H_2O$, EtOH.

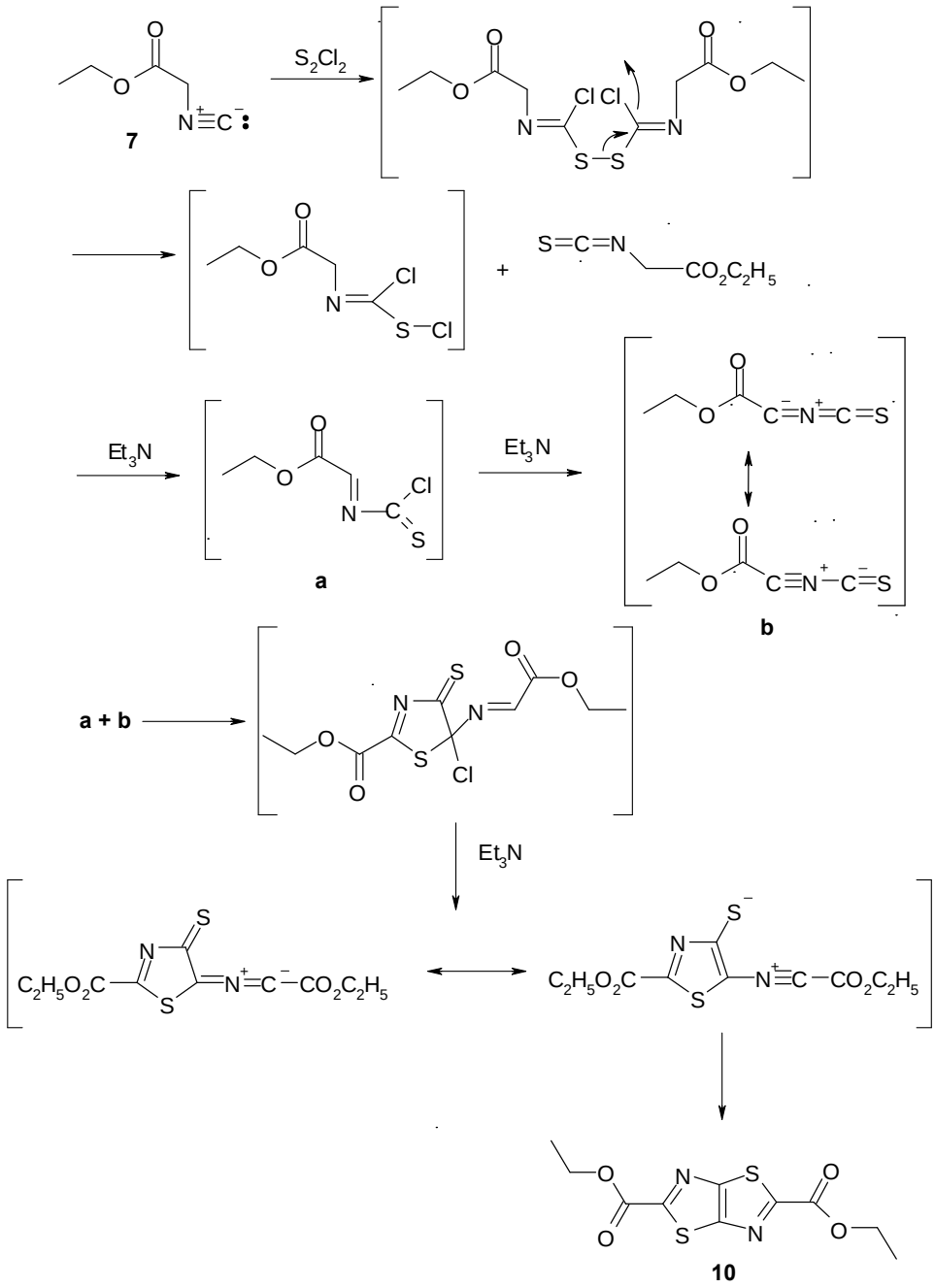

*Figure 3-26: Possible reaction mechanism toward **10**[44].*

In the second route (Figure 3-25, B) toward diester **10**, first the thiazolo[5,4-*d*]thiazole ring has been synthesized *via* the method developed by Johnson *et al*[45,47]. The latter involves the condensation between commercially available dithiooxamide and furfural at high temperature (180 °C) in moderate yield (51 %). Subsequently, 2,5-bis(2-furyl)thiazolothiazole (**8**) is oxidized using $KMnO_4$ to yield the corresponding acid **9** which is esterified with ethanol to yield the desired thiazolo[5,4-*d*]thiazole-2,5-dicarboxylate (**10**). The overall yield from the starting compounds toward **10** is 11 % for route A and 30 % for route B. In view of the better overall yield and the straightforward preparation, the second route, involving the condensation between dithiooxamide and furfural is the preferential route toward **10**.

In the next step the obtained diester **10** is reduced to its alcohol derivative **11** with $NaBH_4$. It is generally accepted that $NaBH_4$, a powerful reducing agent for aldehydes and ketones, will not reduce carboxylic esters for which normally $LiAlH_4$ is used. However in this case, and in some others[9,48], esters of heterocyclic compounds can be reduced by a large excess of $NaBH_4$ in methanol, especially with electron poor ring systems. First trials revealed that reduction with $LiAlH_4$ leads to simultaneous reduction of the thiazolo[5,4-*d*]thiazole ring. With $NaBH_4$ however a yield of 70 % was achieved.

The bishydroxymethyl **11** is than converted into the bischloromethyl **12** *via* nucleophilic substitution with thionyl chloride. Without further purification, the dithiocarbamate monomer **13** is formed directly from the bischloromethyl compound **12** by reaction with sodium diethyldithiocarbamate trihydrate. The yield from **11** to **13** is 44 %.

Structural characterization of monomer 13

Structural characterization of the monomer **13** was performed using standard ^{1}H and ^{13}C NMR techniques. Full chemical shift assignment can be found in the spectra (Figure 3-27) and confirm the expected structure.

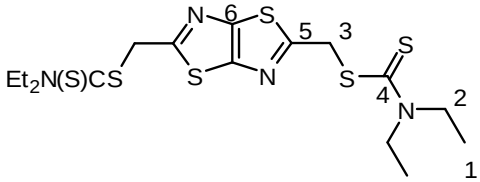

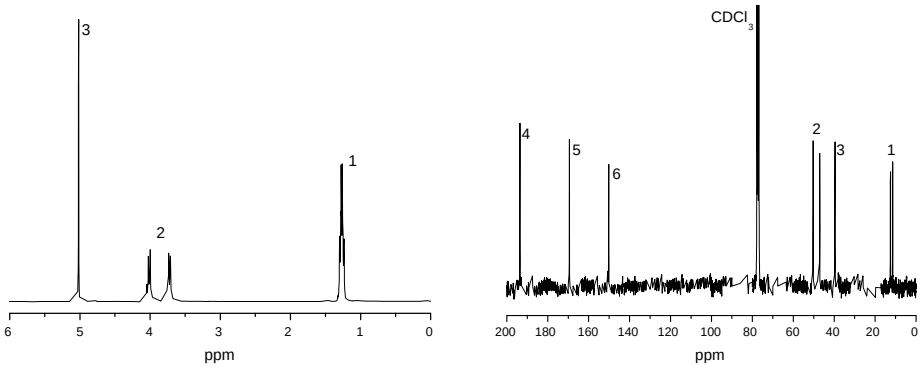

*Figure 3-27: ^{1}H and ^{13}C NMR spectra of monomer **13**.*

*Table 3-4: ^{1}H and ^{13}C chemical shift values of **13**.*

# 13	^{1}H δ (ppm)	^{13}C δ (ppm)
1	1.28	11.4-12.5
2	3.72-4.01	46.8-50.1
3	5.02	39.4
4		192.6
5		168.6
6		149.5

3.3.2 Polymerization

The polymerization of monomer **13** has been performed using four different reaction conditions, deviating in the base used (LDA, LHMDS, Na-*t*BuO and 1,8-diazabicyclo[5.4.0]undec-7-ene (DBU)). pK_a values of the conjugate acids are given in Table 3-5. All polymerizations were performed at room temperature since monomer **13** is not soluble in THF at lower temperatures.

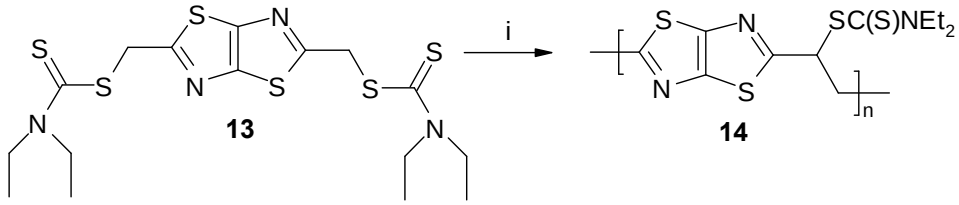

*Figure 3-28: Polymerization of the monomer **13** toward the precursor polymer **14**. (i) LDA, LHMDS; Na-tBuO or DBU, THF.*

Upon addition of the base, the solution immediately becomes black. After the polymerization was allowed to proceed for 90 minutes, termination of the reaction is achieved by pouring the polymerization mixture in ice water followed by acidification with hydrochloric acid to pH = 7. After extraction, the polymers are precipitated in MeOH. Purification of the polymers was done using a *Biobeads*® separation column and this yielded the "polymers" as black solids. The isolated yields range from 10 to 27 %, with still a large fraction of unreacted monomer left.

The weight-average molecular weights (M_w) of **14** have been determined by analytical SEC in DMF using polystyrene standards. The observed molecular weight distributions for **14** are monomodal with M_w values ranging from 6.6×10^3 to 27.6×10^3. Unfortunately only very low molecular weight polymers were obtained. The reaction with DBU did not yield any polymer at all, only unreacted monomer was found. Furthermore, structural characterization revealed partial degradation of the precursor polymer possibly by ring opening[36].

*Table 3-5: Polymerization results for monomer **13**.*

	Entry	Base (pKa)[a]	M_w [x 10^{-3}][b]	PD[b]	Yield [%]
14	1	LDA (35)	6.6	2.2	22
	2	LHMDS (26)	27.6	3.9	27
	3	Na *t*-BuO (19)	3.2	1.7	10
	4	DBU (12)	/	/	/

[a]*pKa values measured in DMSO, except for LDA in THF.*

[b]*Determined by means of SEC in DMF against polystyrene standards.*

3.3.3 Conversion of the polymer into the conjugated structure

The synthesized precursor polymer can be converted into the conjugated polymer by a thermal treatment. Upon heating, the dithiocarbamate group of polymer **14** is eliminated to form the corresponding conjugated polymer **15** (Figure 3-29). The thermal elimination reaction and the thermal stability of the polymer can be followed by means of *in-situ* UV-Vis spectroscopy.

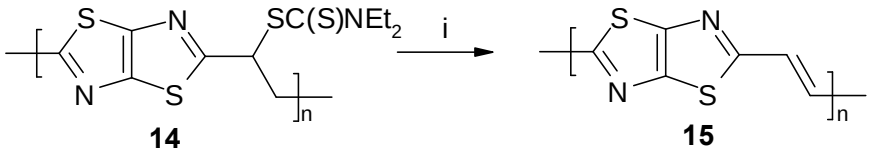

*Figure 3-29: Formation of the conjugated polymer **15** (i) ΔT in film.*

Upon heating a thin film of **14**, a small increase of absorbance is seen at 500 nm, which is related to the formation of the conjugated structure **15**. Simultaneously, there is a decrease of the absorption at 284 nm *i.e.* the precursor polymer **14**. However, from the start of the measurement there is an absorption peak at 410 nm which remains unchanged during the conversion process (Figure 3-30, left). The origin of this absorption is not completely clear but is most likely related to degradation products. The thermal process can be better analyzed using

the absorbance profiles (Figure 3-30, right). In these profiles, an increase in the absorbance at 500 nm can be seen between 110 and 160°C, reflecting the formation of some conjugated system.

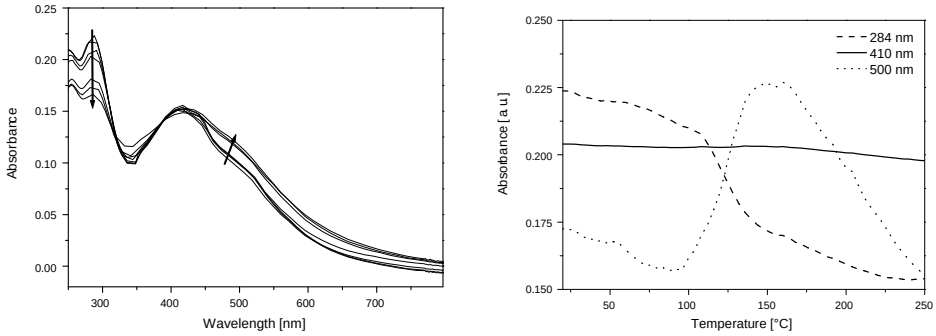

*Figure 3-30: Temperature dependent UV-Vis spectra of the elimination of **14** giving **15** (left). UV-Vis absorbance profiles at 284, 410 and 500 nm as a function of temperature during the elimination of **14** (right).*

Further investigation of the reaction conditions of the dithiocarbamate precursor route needs to be done in order to fully understand the synthesis toward electron-poor conjugated polymers.

3.4 Conclusion

In conclusion, the dithiocarbamate precursor route proved to be an excellent synthetic route toward electron rich PTV-derivatives. The monomer preparation procedures have been optimized and DP-PTV **4a** is readily accessible. Several polymerization conditions have been studied, including the change of base from LDA to LHMDS. The latter gives rise to higher molecular weight polymers. As a result of the introduction of phenyl substituents, **4a** demonstrates an enhanced thermal stability as compared to PTV. Furthermore, **4a** exhibits a significantly improved λ_{max} value as compared to previous reports, indicating its improved purity and lower defect levels. In addition to DP-PTV, a substituted DP-PTV **4b** has been prepared, which is soluble in

common organic solvents. This allows the solution processing of DP-PTV derivatives for applications. Primary solar cell measurements gave promising results. Both polymers have a low band gap (1.7 - 1.8 eV) and can be reversibly p-doped.

In an attempt to synthesize the electron poor poly(thiazolo[5,4-*d*]thiazole vinylene), monomer **13** was synthesized. Unfortunately, the polymerization *via* the dithiocarbamate precursor route failed.

Despite this last result, the dithiocarbamate precursor route still remains the best approach to synthesize PTV-derivatives and further research in our lab will disclose the scope and limitations of this route.

3.5 Experimental part

Chemicals

All reagents and chemicals were obtained from commercial sources (Acros, Aldrich and Merck) and used without further purification unless otherwise stated. Tetrahydrofuran (THF) and acetonitrile (ACN), were dried by distillation from sodium/benzophenone and CaH_2 respectively.

Instrumentation

NMR spectra were recorded on a Varian Inova 300 spectrometer at 300 MHz for ^{1}H NMR and at 75 MHz for ^{13}C NMR using a 5 mm probe. ^{1}H and ^{13}C chemical shifts are reported in ppm downfield from tetramethylsilane (TMS) reference using the residual protonated solvent resonance as an internal standard.

Gas chromatography/mass spectrometry (**GC/MS**) analyses were carried out on TSQ–70 and Voyager mass spectrometers (Thermoquest); the capillary column was a Chrompack Cpsil5CB or Cpsil8CB. DIP-MS measurements were performed at a heating rate of 10 °C/min up to 600 °C. In this technique the material is brought directly on the heating element of the probe as a thin film and this enables to study the products that are liberated in the high vacuum (4.10^{-4} Pa) inside the spectrometer. Liberated products were ionized by electron impact.

Analytical Size Exclusion Chromatography (**SEC**) was performed using a Spectra series P100 (Spectra Physics) pump equipped with two mixed-B columns (10 μm, 2 x 30 cm, Polymer Labs) and a Refractive Index detector (Shodex) at 40 °C (THF) or 70 °C (DMF). THF or a DMF solution of oxalic acid (1.1×10^{-3} M) was used as the eluent at a flow rate of 1.0

mL/min. Molecular weight distributions are given relative to polystyrene standards.

Unless stated otherwise, all thin films in the following characterization methods were prepared by spin coating from a $CHCl_3$ solution (10 mg/mL).

FT-IR spectra were collected with a Perkin Elmer Spectrum One FT-IR spectrometer (nominal resolution 4 cm^{-1}, summation of 16 scans). **UV-Vis spectroscopy** was performed on a VARIAN CARY 500 UV-Vis-NIR spectrophotometer (scan rate: 600 nm/min). Samples for temperature dependent thin film FT-IR and UV-Vis characterization were prepared by spin-coating the precursor polymer onto NaCl disks (IR) or quartz disks (UV). The disks were heated in a Harrick high temperature cell (heating rate: 2 °C/min), which was positioned in the beam of either the FT-IR or the UV-Vis spectrometer to allow *in-situ* measurements. Spectra were taken continuously under a flow of N_2 during which the samples were in direct contact with the heating element. **Photoluminescence** spectra were obtained with a Perkin Elmer LS-5B luminescence spectrometer.

Thin film **electrochemical properties** were measured with an Eco Chemie Autolab PGSTAT 20 Potentiostat/Galvanostat using a conventional three-electrode cell (electrolyte: 0.1 mol/L $LiClO_4$ in anhydrous CH_3CN) with an Ag/Ag^+ reference electrode (0.01 mol/L $AgNO_3$, 0.1 mol/L $LiClO_4$ and CH_3CN), a platinum counter electrode and an Indium-Tin Oxide (ITO) coated glass substrate as working electrode. Cyclic voltammograms were recorded at 50 mV/s under N_2 atmosphere and all potentials were referenced using a known internal standard ferrocene/ferrocinium, which in acetonitrile solution is estimated to have an oxidation potential of –4.98 eV *vs.* vacuum. Precursor polymers were spin-coated from a $CHCl_3$ solution (5 mg/mL) onto the ITO working electrode and subsequently converted to the conjugated polymers by thermal treatment under a continuous flow of N_2. Soluble conjugated polymers were directly spin-coated from a $CHCl_3$ solution (5 mg/mL) onto the ITO working electrode. Solution electrochemistry was

performed using the same setup (electrolyte: 0.1 mol/L TBAPF6 in anhydrous CH_2Cl_2) and a Pt working electrode.

Solar Cells

Using the bulk heterojunction concept, photovoltaic devices were fabricated from a blend of the polymer as a donor and PCBM as an acceptor. A solution of the polymer and PCBM in a 1:2 ratio (by weight) was prepared in chloroform with a total concentration of 10 mg/mL. Poly(3,4-ethylenedioxythiophene):poly(styrenesulfonate) (PEDOT:PSS) (Baytron® P) was spin coated on top of an indium-tin oxide (ITO) coated glass substrate (~25 Ω/sq) which had been cleaned in an ultrasonic bath with acetone and isopropyl alcohol. Then the active layer (polymer:PCBM blend) was spin coated on the PEDOT:PSS layer (about 80 nm thick). 6 Å of lithium fluoride (LiF) and an 80 nm thick Al electrode were deposited on the blend film by thermal evaporation at ~5x 10^{-6} mbar. Device annealing was carried out inside a glove box at 120 °C for 4 min. All current-voltage (I-V) characteristics of the photovoltaic devices were measured using a Keithley SMU 2400 unit under inert atmosphere (argon) in a dry glove box. A Steuernagel solar simulator under AM 1.5 conditions was used as the excitation source with an input power of 100 mW/cm^2 white light illumination. A lock-in technique was used to measure the incident photon-to-current efficiency (**IPCE**). With this technique the number of electrons produced from the cell under short-circuit conditions are related to the number of incident photons. Light intensity correction was performed using a calibrated Si photodiode.

Field Effect Transistors

The hole mobility of the polymers was measured in thin film field effect transistor (TF-FET) devices. The measurements were performed on a top-contact parallel transistor (L = 60 μm; W = 9000 μm). It consisted

of a highly doped Si substrate on which an isolating oxide (SiO_2) of 100 nm was grown thermally on one side and of which the backside was covered with an aluminum layer as gate electrode. The polymers were spin coated on top of the oxide. Subsequently the gold contacts (source and drain) were evaporated on top of the device.

Synthesis

3,4-Diphenylthiophene (1a)

Phenylboronic acid (5 g, 41.0 mmol), 3,4-dibromothiophene (2.14 g, 8.85 mmol) and KF (2.10 g, 36.2 mmol) were dissolved in water (40 mL) and toluene (40 mL). $Pd(PPh_3)_4$ (730 mg, 0.63 mmol) was added as a catalyst. After refluxing the mixture for 18 hours, an extraction with CH_2Cl_2 (3 x 50 mL) was performed and the combined organic phases were dried over $MgSO_4$. The crude reaction product was purified by column chromatography (silica, n-hexane) and a white solid was obtained (1.6 g, 77 % yield); ^{1}H NMR ($CDCl_3$): 7.30 (s, 2H), 7.25-7.21 (m, 6H), 7.19-7.16 (m, 4H); MS (EI, m/e): 236 (M+).

3,4-Diphenyl-2,5-bischloromethylthiophene (2a)

To a mixture of paraformaldehyde (343 mg, 11.4 mmol) and **1a** (1 g, 4.24 mmol), concentrated HCl (2.35 g, 24.2 mmol) and acetic anhydride (4.32 g, 42.4 mmol) were added dropwise under N_2 atmosphere at 0 °C. The mixture was heated at 70 °C for 4.5 hours after which a cold (0 °C) saturated aqueous solution of sodium acetate (10 mL) and a 25% aqueous solution of sodium hydroxide (10 mL) were added. The mixture was extracted with CH_2Cl_2 (3 x 50 mL) and dried over $MgSO_4$. After evaporation of the solvent a light brown solid was obtained (1.38 g, 98% yield); ^{1}H NMR ($CDCl_3$): 7.24-7.21 (m, 6H), 7.08-7.05 (m, 4H), 4.67 (s, 4H); MS (EI, m/e): 332 (M+), 297 (M+ - Cl), 261 (M+ – 2 Cl).

3,4-Diphenylthiophene-2,5-diylbismethylene-N,N-diethyl-dithiocarbamate (3a)

A mixture of **2a** (3 g, 8.89 mmol) and sodium diethyldithiocarbamate trihydrate (4.6 g, 20.4 mmol) in 10 mL of methanol was stirred for three hours at ambient temperature. Subsequently, the mixture was extracted with diethyl ether (3 x 50 mL) and dried over $MgSO_4$. The crude reaction mixture was purified by column chromatography (silica, n-hexane/CH_2Cl_2 3/7) after which the dithiocarbamate monomer was obtained as a white solid (3.47 g, 70 % yield); ^{1}H NMR ($CDCl_3$): 7.24-7.14 (m, 6H), 7.03-7.00 (m, 4H), 4.62 (s, 4H), 4.01 (q, 4H), 3.69 (q, 4H), 1.26 (2t, 12H); 13C NMR ($CDCl_3$): 194.22 (2C), 141.14 (2C), 135.33 (2C), 133.39 (2C), 129.99 (4C), 127.82 (4C), 126.77 (2C), 49.31 (2C), 46.63 (2C), 35.82 (2C), 12.39 (2C), 11.43 (2C).

3,4-Bis(4-butylphenyl)thiophene (1b)

Compound **1b** was obtained in an analogous way as described for **1a**, starting from 4-butylphenylboronic acid (2.5 g, 14.0 mmol) and 3,4-dibromothiophene (0.885 g, 3.66 mmol). A colorless oil was obtained (730 mg, 60 % yield); ^{1}H NMR ($CDCl_3$): 7.26 (s, 2H), 7.08 (m, 8H), 2.58 (t, 4H), 1.59 (m, 4H), 1.35 (m, 4H), 0.92 (t, 6H); MS (EI, m/e): 348 (M+), 262 (M+ - 2 C_3H_7), 248 (M+ - C_3H_7 - C_4H_9), 234 (M+ - 2 C_4H_9).

3,4-Bis(4-butylphenyl)thiophene-2,5-diylbismethylene-N,N-diethyldithiocarbamate (3b)

Compound **3b** was obtained in an analogous way as described for **3a**. Starting from **1b** (730 mg, 2.09 mmol), paraformaldehyde (170 mg, 5.66 mmol), concentrated HCl (1.18 g, 12.0 mmol) and acetic anhydride (2.14 g, 20.9 mmol), **2b** was obtained. Without further isolation **2b** was reacted with sodium diethyldithiocarbamate trihydrate (1.09 g, 4.84

mmol). The dithiocarbamate monomer **3b** was obtained as an orange oil (900 mg, 64 % yield); ^{1}H NMR ($CDCl_3$): 7.01-6.94 (AA'BB', 4H), 6.93-6.86 (AA'BB', 4H), 4.63 (s, 4H), 4.01 (q, 4H), 3.71 (q, 4H), 2.52 (t, 4H), 1.53 (qu, 4H), 1.27 (m, 16H), 0.88 (t, 6H); ^{13}C NMR ($CDCl_3$): 194.21 (2C), 141.24 (2C), 141.11 (2C), 132.85 (2C), 132.54 (2C), 129.76 (4C), 127.73 (4C), 49.23 (2C), 46.58 (2C), 35.93 (2C), 35.08 (2C), 33.11 (2C), 22.07 (2C), 13.78 (2C), 12.36 (2C), 11.41 (2C).

Polymerization of 3a (4a)

The polymerization of **3a** was performed using four different reaction conditions (cf. entries 1-4, Table 3-2 and Table 3-3). A solution of monomer **3a** (400 mg, 0.716 mmol) in dry THF (3.6 mL, 0.2 M) at –78 °C (entries 2 and 3), 0 °C (entry 1) or 25 °C (entry 4) was degassed for 15 minutes by passing through a continuous stream of N_2 after which LDA (360 μL of a 2 M solution in THF/n-heptane) or LHMDS (720 μL of a 1 M solution in THF) was added in one portion. The mixture was kept at –78 °C (entries 2 and 3), 0 °C (entry 1) or 25 °C (entry 4) for 90 minutes during which time the passing of N_2 was continued. Subsequently depending on the polymerization procedure, ethanol (6 mL) was added at -78 °C to stop the reaction (entry 2) or the solution was allowed to come to 0 °C (entry 3). The reaction mixture was quenched in ice water (100 mL), after which it was neutralized with HCl (1 M in H_2O). Subsequently, the aqueous phase was extracted with CH_2Cl_2 (3 x 60 mL). The organic layers were combined after which the solvents were removed by evaporation under reduced pressure. The resulting crude polymer was redissolved in $CHCl_3$ (2 mL) and a precipitation was performed in MeOH (100 mL) at 0 °C. The polymer was collected and dried in vacuo and further purified to remove traces of monomer by reprecipitation in diethyl ether/n-hexane (3/1; 100 mL) at 0 °C. A white solid was obtained (yields are shown in Table 3-2 and Table 3-3). ^{1}H NMR (CD_2Cl_2): 7.21-6.94 (br m, 6H), 6.84-6.60 (br m, 4H), 5.20-5.10 (br s, 1H), 4.10-3.85 (br s, 2H), 3.85-3.55 (br s, 2H),

3.55-3.10 (br s, 2H), 1,42-1.13 (br s, 6H); ^{13}C NMR (CD_2Cl_2): 193.40, 140.48, 139.84, 137.81, 136.33 (2C), 135.76, 130.43 (4C), 127.88 (4C), 126.62 (2C), 51.63, 49.25, 47.03, 38.25, 12.89, 11.63. The residual fractions contained low molecular weight oligomers and monomer residues.

Polymerization of 3b (4b)

Compound **4b** was obtained in an analogous way as described for **4a** starting from **3b** (575 mg, 0.857 mmol) and LDA (429 μL of a 2 M solution in THF/n-heptane) or LHMDS (860 μL of a 1 M solution in THF). A white solid was obtained (yields are shown in Table 3-2 and Table 3-3)). ^{1}H NMR (CD_2Cl_2): 7.01-6.76 (br m, 4H), 6.76-6.53 (br m, 4H), 5.51-5.15 (br s, 1H), 4.14-3.84 (br s, 2H), 3.84-3.54 (br s, 2H), 3.42-3.16 (br s, 2H), 2.63-2.39 (br t, 4H), 1.64-1.40 (br m, 4H), 1,40-1.07 (br m, 10H), 0.99-0.78 (br t, 6H); ^{13}C NMR (CD_2Cl_2): 193.82, 141.48, 140.90 (3C), 137.31, 136.02, 133.78 (2C), 130.45 (4C), 127.81 (4C), 51.87, 49.13, 47.06, 38.30, 35.62 (2C), 33.75 (2C), 22.66 (2C), 14.08 (2C), 12.89, 11.63.

Thermal conversion of 4b in solution (5b)

A solution of **4b** (200 mg) in dichlorobenzene (10 mL) was heated to 150 °C and stirred for 20 hours. After cooling to 50 °C, the resulting blue solution was precipitated in methanol (300 mL). The polymer was filtered off and dried at room temperature under vacuo. A black solid was obtained (140 mg, 95 % yield); ^{1}H NMR ($CDCl_3$): 7.07-6.92 (m, 4H), 6.92-6.73 (m, 6H), 2.70-2.36 (t, 4H), 1.68-1.41 (m, 4H), 1.41-1.11 (m, 4H), 0.99-0.78 (t, 6H); ^{13}C NMR ($CDCl_3$): 141.88 (2C), 141.40 (2C), 136.52 (2C), 132.58 (2C), 130.41 (4C), 127.82 (4C), 121.80 (2C), 35.35 (2C), 33.30 (2C), 22.28 (2C), 13.99 (2C).

_N_-Formylglycine ethyl ester (6)

A 1-L, three-necked, round-bottomed flask fitted with a stirrer, a pressure-equalizing dropping funnel, and a reflux condenser bearing a calcium chloride drying tube is charged with 69.5 g (0.495 mol) of glycine ethyl ester hydrochloride and 250 mL of methylformate. The suspension is stirred and heated at reflux while 55.0 g (0.544 mol) of Et_3N is added. The resulting mixture is stirred and heated under reflux for 20 h, cooled to room temperature, and filtered through a *Büchner* funnel, removing $Et_3N.HCl$. The filtrate is concentrated, and the remaining oil is distilled under reduced pressure (bp 105 °C/0.1 mbar), yielding 47 g (73 % yield) of *N*-formylglycine ethyl ester as a light yellow oil; ^1H NMR ($CDCl_3$): 8.18 (s, 1H), 4.15 (q, 2H), 4.05 (d, 2H), 1.22 (t, 3H); ^{13}C NMR ($CDCl_3$): 169.40, 161.26, 61.50, 39.76, 13.90; MS (EI, m/e): 131 (M^+), 103 (M^+-C_2H_5), 86 (M^+-OC_2H_5), 58 (M^+-$C(O)OC_2H_5$).

Ethyl isocyanoacetate (7)

A mixture of *N*-formylglycine ethyl ester **6** (48.24 g, 0.37 mol), Et_3N (91.79 g, 0.91 mol), and 500 mL of dry CH_2Cl_2 under Ar atmosphere is cooled to 0 °C in an ice–salt bath. $POCl_3$ (55.75 g, 0.37 mol) is added drop wise over 15–20 minutes while the temperature is kept at 0 °C. The mixture becomes reddish brown as it is stirred and cooled at 0° for an additional 1 h. The ice–salt bath is removed and replaced by an ice-water bath. Stirring is continued as an aqueous solution of sodium carbonate (25 %, 400 mL) is added drop wise at a rate such that the temperature of the mixture is maintained at 25–30 °C. The two-phase mixture is stirred for another 30 minutes, after which 600 mL water is added. The aqueous layer is separated and extracted two times with 250 mL of CH_2Cl_2. The combined organic layers are washed with saturated NaCl solution, and dried over anhydrous $MgSO_4$. Evaporation of the solvent under reduced pressure and distillation of the remaining brown

oil (bp 80 °C/0.1 mbar) afford 34 g (82 % yield) of ethyl isocyanoacetate **7** as a light yellow oil; ^{1}H NMR ($CDCl_3$): 4.24 (q, 2H), 4.19 (s, 2H), 1.28 (t, 3H); MS (EI, m/e): 114 (M^+), 69 (M^+-OC_2H_5).

2,5-Bis(2-furyl)thiazolothiazole (8)

Dithioxamide (20 g, 0.167 mol), 60 g of phenol, and 200 g (2.08 mol) of freshly distilled furfural were heated in an oil bath at 200 – 205 °C for 45 min after the dark solution had reached its boiling point. After standing overnight the dark crystalline product was collected on a *Büchner* filter and washed with several portions of EtOH, ether and hexane untill the filtrate is colorless. The crude product was dispersed in 1 L of $CHCl_3$ and refluxed for 1 h. After filtration, the filtrate is concentrated and allowed to cool. The formed greenish crystals are filtered (23.3 g, 51 % yield). Without further purification, compound **8** is used directly in the next step.

Thiazolo[5,4-*d*]thiazole-2,5-dicarboxylic acid (9)

2,5-Bis(2-furyl)thiazolothiazole (**8**) (17 g, 0.062 mol) and 475 mL of pyridine were heated with rapid stirring until the solid had dissolved almost completely. After cooling to 70 °C, 75 mL of water was added to produce a uniform suspension of fine crystals. The mixture was cooled to 15-20 °C and held at this temperature while 104 g (0.66 mol) of finely powdered potassium permanganate in 70 mL of water was added, with continued rapid stirring. After the permanganate had been added, the temperature of the mixture was allowed to rise slowly to 40 °C and maintained there for 12 hr with stirring. The mixture was cooled and 1 g of sodium bisulfite and 100 mL of water were introduced. The black precipitate, consisting of manganese dioxide and the potassium salt of the acid was collected on a *Büchner* funnel and washed sparingly with water. The filter cake was boiled with 1 L of water and the extract filtered hot. Two further extractions with smaller amounts of water were

made. The almost colorless filtrates were acidified with concentrated HCl and the precipitated acid was collected. Washing with water, dioxane and ether yielded the product as colorless crystals (10.5 g, 62 % yield); ^{1}H NMR (DMSO): 9.28 (s); ^{13}C NMR (DMSO): 161.32, 157.66, 150.40; MS (EI, m/e): 230 (M^+), 186 (M^+-CO_2), 142 (M^+-2 CO_2).

Diethyl thiazolo[5,4-*d*]thiazole-2,5-dicarboxylate (10)

Compound **10** was prepared *via* two different synthetic methods. (*Method A*) Under dry conditions, a solution of dichlorodisulfane (S_2Cl_2) (11.4 g, 84.44 mmol) in 40 mL CH_2Cl_2 is added to a solution of ethyl isocyanate (**7**) (19 g, 0.168 mol) in 180 mL CH_2Cl_2 maintaining the temperature at -50 °C. The resulting mixture is allowed to stand without removing the cooling bath, until the temperature has risen to 10 °C, and is then cooled again to -50 °C. Dry Et_3N (16.97 g, 0.168 mol) is added drop wise and the mixture is stirred, without removing the cooling bath, until the temperature has risen to 10 °C, and than filtered. Evaporation of the filtrate leaves a residue which is recrystallized from EtOH to give **10** as off white crystals (2.23 g, 19 %).
(Method B) The dicarboxylic acid **9** (7.4 g, 0.032 mol), 14 mL of concentrated H_2SO_4 and 250 mL EtOH were refluxed for 3 h. The acid dissolved slowly and dense colorless crystals of the ester separated. After cooling, this mixture was neutralized with aqueous Na_2CO_3 (20 %). The crystals were filtered and recrystallized from EtOH to give **10** as white crystals (8.3 g, 91 % yield); ^{1}H NMR ($CDCl_3$): 4.45 (q, 4H), 1.37 (t, 6H); ^{13}C NMR ($CDCl_3$): 162.03 (2C), 159.37 (2C), 154.19 (2C), 63.25 (2C), 14.00 (2C); MS (EI, m/e): 286 (M^+), 271 (M^+-CH_3), 241 (M^+-OC_2H_5), 214 (M^+-$C(O)OC_2H_5$) (100), 142 (M^+- 2 $C(O)OC_2H_5$), 114 (M^+-2 $CH_2C(O)OC_2H_5$).

2,5-Bis-hydroxymethylthiazolo[5,4-*d*]thiazole (11)

1 g (3.49 mmol) diethyl thiazolo[5,4-*d*]thiazole-2,5-dicarboxylate **(10)** and 80 mL MeOH are cooled in an ice bath. 2.62 g (0.07 mol) $NaBH_4$ is added at such a rate that the reaction is not too violent. The temperature is than rised and kept at reflux for 2 h. After cooling, 80 mL of water is added carefully and the excess of methanol is removed. This mixture is extracted 5 times with 50 mL EtOAc and the combined organic layers are dried over $MgSO_4$. After evaporation of the solvent product **11** is obtained as a greenish solid (0.478 g, 68 % yield); ^{1}H NMR (CD_3OD): 4.92 (s); ^{13}C NMR: 176.84 (2C), 150.43 (2C), 63.01 (2C); MS (EI, m/e): 202 (M^+), 173 (M^+ - CH_2OH), 143 (M^+ - $2CH_2OH$), 88, 70, 44.

Thiazolo[5,4-*d*]thiazole-2,5-diylbismethyleen-*N,N*-diethyldithio-carbamate (13)

100 mL $SOCl_2$ is added drop wise to 0.9 g (4.45 mmol) of 2,5-bishydroxymethylthiazolo[5,4-*d*]thiazole **(11)**. This mixture is than stirred overnight at room temperature. Afterwards a saturated aqueous solution of Na_2CO_3 is added drop wise till the pH is neutral. This mixture is extracted three times with CH_2Cl_2 (50 mL) and dried over $MgSO_4$. After careful evaporation of the solvent the highly reactive dichloride **(12)** is used immediately, without further purification in the subsequent reaction.

12 is dissolved in 130 ml EtOH and 2,31 g (10.23 mmol) sodium *N,N*-diethyldithiocarbamate trihydrate is added as a solid to the stirred solution. This mixture is stirred overnight at room temperature. Extraction with Et_2O (3 x 50 mL) drying over $MgSO_4$ and evaporation of the solvent yields the crude product. Recrystallization from MeOH yields the monomer as a green solid (0.9 g, 44 % yield); ^{1}H NMR ($CDCl_3$): 5.02 (s, 4H), 4.01 (q, 4H), 3.72 (q, 4H), 1.28 (t, 12H); ^{13}C NMR: 192.63 (2C), 168.56 (2C), 149.50 (2C), 50.08 (2C), 46.83 (2C), 39.44 (2C),

12.45 (2C), 11.37 (2C); MS (EI, m/e): 465 (M^+), 318 (M^+ - $SC(S)NEt_2$), 171 (M^+ - 2 $SC(S)NEt_2$), 150.

Polymerization of 13 (14)

The polymerization of **13** was performed using four different reaction conditions (cf. entries 1-4, Table 3-5). A solution of monomer **13** (300 mg, 0.646 mmol) in dry THF (3.2 mL, 0.2 M) at room temperature was degassed for 15 minutes by passing through a continuous stream of N_2 after which LDA (420 μL of a 2 M solution in THF/n-heptane), LHMDS (840 μL of a 1 M solution in THF), Na-*t*BuO (0,080 g, 0.840 mmol) or DBU (0.128 g, 0.840 mmol) was added in one portion. The mixture was kept at room temperature for 90 minutes during which time the passing of N_2 was continued. Subsequently the reaction mixture was quenched in ice water (100 mL), after which it was neutralized with HCl (1 M in H_2O). Subsequently, the aqueous phase was extracted with CH_2Cl_2 (3 x 60 mL). The organic layers were combined after which the solvents were removed by evaporation under reduced pressure. The resulting crude polymer was redissolved in $CHCl_3$ (2 mL) and a precipitation was performed in MeOH (100 mL) at 0 °C. The polymer was collected and dried in vacuo and further purified to remove unreacted monomer by passing a solution of the polymer in DMF through a *Biobeads*® separation column. A black solid was obtained (yields are shown in Table 3-5); ^{1}H NMR ($CDCl_3$): 7.59 (s, 0.3H), 6.15 (s, 0.3H), 5.10-4.95 (br s, 0.6H), 4.21-3.72 (br s, 2H), 3.75-3.58 (br s, 2H), 1.39-1.13 (br s, 6H).

3.6 References

1. Henckens A., Colladet K., Fourier S.*, et al.*, "Synthesis of 3,4-diphenyl-substituted poly(thienylene vinylene) low-band-gap polymers via the dithiocarbamate route" *Macromolecules* 38, (1), **2005**, 19.
2. Gilch H.G. and Wheelwright W.L., "Polymerisation of α-halogenated *p*-xylenes with base" *J. Polymer Science* (4), **1966**, 1337.
3. Wessling R. A., "The Polymerization of Xylylene Bisdialkyl Sulfonium Salts" *J. Polymer Science* (72), **1985**, 55.
4. Son S., Dodabalapur A., Lovinger A.J.*, et al.*, "Luminesence enhancement by the introduction of disorder into poly(p-phenylene vinylene)" *Science* 269, (5222), **1995**, 376.
5. Vanderzande D. J., Issaris A. C., VanderBorght M. J.*, et al.*, "A general approach to precursors for poly(arylene vinylene) derivatives: Mechanism, scope and modifications" *Macromol. Symp.* 125, **1998**, 189.
6. Henckens A., Lutsen L., Vanderzande D.*, et al.*, "Synthesis of PTV via the dithiocarbamate route, a new precursor route towards conjugated polymers" *Proc. SPIE Int. Soc. Opt. Eng.* 5464, **2004**, 52.
7. Kaeriyama K., in: H. S. Nalwa (Eds.), "Handbook of Organic Conductive Molecules and Polymers" Vol. 2, John Wiley & Sons, Chichester, **1997**, 271.
8. Roncali J., "Synthetic principles for bandgap control in linear pi-conjugated systems" *Chem. Rev.* 97, (1), **1997**, 173.
9. Gillissen S., "New Poly(arylene vinylene) derivatives via the sulphinyl precursor route" *Ph. D dissertation*, **2002,** Limburgs Universitair Centrum, Diepenbeek.
10. Motmans F., "Synthesis and Characterisation of Polar PPV Derivatives through the Sulfinyl Precursor Route" *Ph. D dissertation*, **2004,** Limburgs Universitair Centrum, Diepenbeek.

11. Van Severen I., "Design, Synthesis and Evaluation of Functionalized Poly(p-Phenylene Vinylene) derivatives: From Existing Structures to Novel Materials" *Ph. D. dissertation*, **2006,** Hasselt University, Diepenbeek.
12. Jen K. Y., Jow R., Shacklette L. W.*, et al.*, "The Optical, Electrochemical and Structure Property Relationships of Poly(Heteroaromatic Vinylenes)" *Mol. Cryst. Liq. Cryst.* 160, **1988**, 69.
13. Jen K. Y., Jow T. R., Eckhardt H.*, et al.*, "Highly Conductive High-Molecular-Weight Poly(Heteroaromatic Vinylene)" *Polym. Mater. Sci. Eng.* 56, **1987**, 49.
14. Jen K. Y., Maxfield M., Shacklette L. W.*, et al.*, "Highly-Conducting, Poly(2,5-Thienylene Vinylene) Prepared Via a Soluble Precursor Polymer" *J. Chem. Soc.-Chem. Commun.* (4), **1987**, 309.
15. Murata H., Tokito S., Tsutsui T.*, et al.*, "Preparation of High-Quality Poly(2,5-Thienylenevinylene) Films" *Synth. Met.* 36, (1), **1990**, 95.
16. Yamada S., Tokito S., Tsutsui T.*, et al.*, "New Conducting Polymer Film - Poly(2,5-Thienylenevinylene) Prepared Via a Soluble Precursor Polymer" *J. Chem. Soc.-Chem. Commun.* (19), **1987**, 1448.
17. Murase I., Ohnishi T., Noguchi T.*, et al.*, "Highly Conducting Poly(2,5-Thienylene Vinylene) Via a Precursor Route" 28, (8), **1987**, 229.
18. Bicknell L. K., Marsella M. J. and Swager T. M., "Designing Ion Responsive Materials - Conductive Crown-Ether Containing Thiophene Polymers" *Polymer Preprints* 35, **1994**, 269.
19. Cheng H. and Elsenbaumer R. L., "New Precursors and Polymerization Route for the Preparation of High-Molecular-Mass Poly(3,4-Dialkoxy-2,5-Thienylenevinylene)S - Low-Band-Gap Conductive Polymers" *J. Chem. Soc.-Chem. Commun.* (14), **1995**, 1451.
20. Gillissen S., Henckens A., Lutsen L.*, et al.*, "Synthesis of a processible high molecular weight poly(thienylene vinylene). Polymerisation and thin-film transistor properties" *Synth. Met.* 135, (1-3), **2003**, 255.

21. Henckens A., Knipper M., Polec I.*, et al.*, "Poly(thienylene vinylene) derivatives as low band gap polymers for photovoltaic applications" *Thin Solid Films* 451-52, **2004**, 572.

22. Vanderzande D., Lutsen L., Henckens A. and Colladet K., "Method of preparing derivatives of polyarylene vinylene and method of preparing an electronic device including same" EP1529794, **2005**.

23. Reyes-Reyes M., Kim K. and Carroll D. L., "High-efficiency photovoltaic devices based on annealed poly(3-hexylthiophene) and 1-(3-methoxycarbonyl)-propyl-1-phenyl-(6,6)C-61 blends" *Appl. Phys. Lett.* 87, (8), **2005**, 083506.

24. Wei P. K., Hsu J. H., Hsieh B. R.*, et al.*, "Surface modification and patterning of conjugated polymers with near-field optical microscopy" *Adv. Mater.* 8, (7), **1996**, 573.

25. Wei P. K., Hsu J. H., Fann W. S.*, et al.*, "Surface modification of conjugated polymers: An application of near-field optical microscopy in sub-micron photochemistry" *Synth. Met.* 85, (1-3), **1997**, 1421.

26. Hsieh B.R., Johnson G.E., Antoniadis H.*, et al.*, "Electroluminescent devices containing a conjugated polymer obtained via halogen precursor route chemistry" US5558904, **1996**.

27. Tan C. H., Inigo A. R., Hsu J. H.*, et al.*, "Mesoscale structures in luminescent conjugated polymer thin films studied by near-field scanning optical microscopy" *J. Phys. Chem. Solids* 62, (9-10), **2001**, 1643.

28. Mitschke U., Debaerdemaeker T. and Bauerle P., "Structure-property relationships in mixed oligoheterocycles based on end-capped oligothiophenes" *Eur. J. Org. Chem.* (3), **2000**, 425.

29. Li W. J., Katz H. E., Lovinger A. J.*, et al.*, "Field-effect transistors based on thiophene hexamer analogues with diminished electron donor strength" *Chem. Mat.* 11, (2), **1999**, 458.

30. Hong X. M., Katz H. E., Lovinger A. J.*, et al.*, "Thiophene-phenylene and thiophene-thiazole oligomeric semiconductors with high field-effect transistor on/off ratios" *Chem. Mat.* 13, (12), **2001**, 4686.

31. Cao J., Kampf J. W. and Curtis M. D., "Synthesis and characterization of bis(3,4-ethylene-dioxythiophene)-(4,4 '-dialkyl-2,2 '-bithiazole) co-oligomers for electronic applications" *Chem. Mat.* 15, (2), **2003**, 404.

32. Ando S., Nishida J., Inoue Y.*, et al.*, "Synthesis, physical properties, and field-effect transistors of novel thiophene/thiazolothiazole co-oligomers" *J. Mater. Chem.* 14, (12), **2004**, 1787.

33. Ando S., Nishida J., Fujiwara E.*, et al.*, "Characterization and field-effect transistor performance of heterocyclic oligomers containing a thiazolothiazole unit" *Chem. Lett.* 33, (9), **2004**, 1170.

34. Ando S., Nishida J., Fujiwara E.*, et al.*, "Physical properties and field-effect transistors based on novel thiazolothiazole/heterocyclic and thiazolothiazole/phenylene co-oligomers" *Synth. Met.* 156, (2-4), **2006**, 327.

35. Halik M., Klauk H., Zschieschang U.*, et al.*, "Relationship between molecular structure and electrical performance of oligothiophene organic thin film transistors" *Adv. Mater.* 15, (11), **2003**, 917.

36. Catellani M., Destri S., Porzio W.*, et al.*, "Thiazole-Based Polymers - Synthesis, Characterization and Electronic-Structure" *Synth. Met.* 26, (3), **1988**, 259.

37. Henckens A., "Synthesis, characterisation and application in electronic devices of low-bandgap materials based on thiophene derivatives" *Ph. D dissertation*, **2003,** Limburgs Universitair Centrum, Diepenbeek.

38. Nakayama J. and Hasemi R., "First synthesis of aromatic compounds carrying two 1-adamantyls on adjacent positions: 3,4-di-1-adamantylthiphene, *o*-di-1-adamantylbenzene, and 4,5-di-1-adamantylpyridazine" 112, **1990**, 5654.

39. Nakayama J., Hasemi R., Yoshimura K.*, et al.*, "Preparation of congested thiophenes carrying bulky substituents on the 3- and 4-positions and their conversion to the benzene drivatives" 63, **1998**, 4912.

40. Becker H., Spreitzer H., Ibrom K.*, et al.*, "New insights into the microstructure of GILCH-polymerized PPVs" *Macromolecules* 32, (15), **1999**, 4925.

41. Kline R. J., McGehee M. D., Kadnikova E. N.*, et al.*, "Controlling the field-effect mobility of regioregular polythiophene by changing the molecular weight" *Adv. Mater.* 15, (18), **2003**, 1519.

42. Zen A., Pflaum J., Hirschmann S.*, et al.*, "Effect of molecular weight and annealing of poly (3-hexylthiophene)s on the performance of organic field-effect transistors" *Adv. Funct. Mater.* 14, (8), **2004**, 757.

43. Goldini F., Janssen R.A.J. and Meijer E.W., "Synthesis and characterization of new copolymers of thiophene and vinylene: poly(thienylenevinylene)s and poly(terthienylenevinylene)s with thioether side chains" 37, **1999**, 4629.

44. Bossio R., Marcaccini S., Pepino R.*, et al.*, "An Unusual and Simple One-Pot Synthesis of Thiazolo[5,4-d]Thiazoles" *Synthesis* (12), **1987**, 1138.

45. Johnson J. R., Rotenberg D. H. and Ketcham R., "Thiazolothiazoles. II. The parent heterocycle and its carboxylic and amino derivatives." *J. Am. Chem. Soc.* 92, (13), **1970**, 4046.

46. Hartman G. D. and Weinstock L.M., "Thiazoles from ethyl isocyanoacetate and thiono esters: ethyl thiazole-4-carboxylate" *Org. Syn.* Coll. Vol. 6, 620.

47. Johnson J. R. and Ketcham R., "Thiazolothiazoles. I. The reaction of Aromatic Aldehydes with dithioöxamide" *J. Am. Chem. Soc.* 82, **1959**, 2719.

48. Brown M. S. and Rapoport H., "The reduction of esters with sodium borohydride" *J. Org. Chem.* 28, **1963**, 3261.

Appendix

Purification of $FeCl_3$

4.1 Introduction

One of the problems regarding the polymerization with $FeCl_3$ is that, under the same conditions, the method often gives variable results in yield, molecular weight and polydispersity. In that aspect and with the help of Dr. Marinella Catellani from the CNR in Milan (IT), we optimized the procedure to purify commercial $FeCl_3$. This method is based on a literature procedure to obtain anhydrous metal chlorides[1]. It consists of the treatment of commercial $FeCl_3$ with $SOCl_2$ followed by a washing step with pentane. In this way we were able to improve the reproducibility of the polymerizations. The following is a detailed guide of the purification of $FeCl_3$ for future reference.

4.2 Purification of $SOCl_2$

It is of crucial importance that during all the steps of the purification, all glassware is clean and dried in the oven for at least 24 h. Further, all handlings must be carried out at a vacuum/argon (or nitrogen) line and one must be sure to constantly work under inert atmosphere or flow.

The setup was brought under vacuum, as depicted in Figure 4-1, dried using a *Bunsen* burner and was than flushed with Ar 3 times (Ar in setup, apply vacuum, Ar in setup, … , end with Ar). Under Ar flow, $SOCl_2$ was added and distilled (bp=76-78 °C, colorless liquid). After distillation the flask containing the purified $SOCl_2$ is removed from the distillation set up, making sure to keep it under inert atmosphere and stored in the dark.

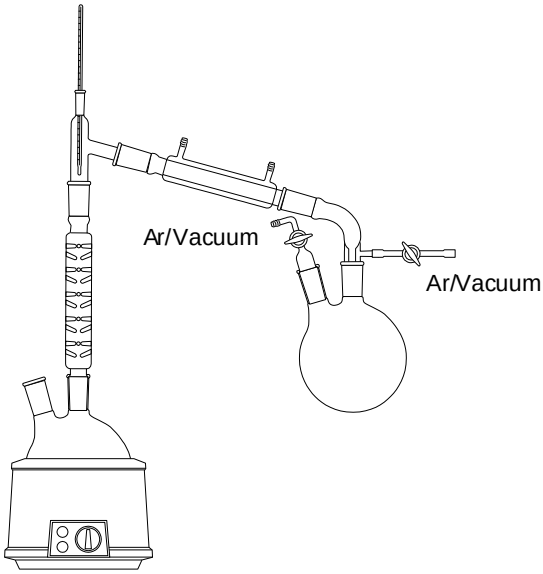

Figure 4-1: Distillation set up for the purification of $SOCl_2$.

4.3 Purification of $FeCl_3$

The setup (Figure 4-2, left) is first dried and flushed with Ar as described above. 50 g of finely ground $FeCl_3$ is put into the 3-necked round-bottomed flask equipped with a valve (in this way an Ar stream can be applied when adding the products in the flask) and 100 ml of freshly distilled thionyl chloride is added at room temperature. Evolution of sulfur dioxide and hydrogen chloride begins at once. The slurry is refluxed for 1 h under inert atmosphere (without a stirring bar). After cooling down the setup is arranged for distillation in order to remove the excess of $SOCl_2$ (Figure 4-2, right). When building the setup an Ar-flow is running through the 3-necked flask. During the distillation Ar is applied at the cold end of the distillation setup and for obvious reasons the valve at the 3-necked flask is closed.

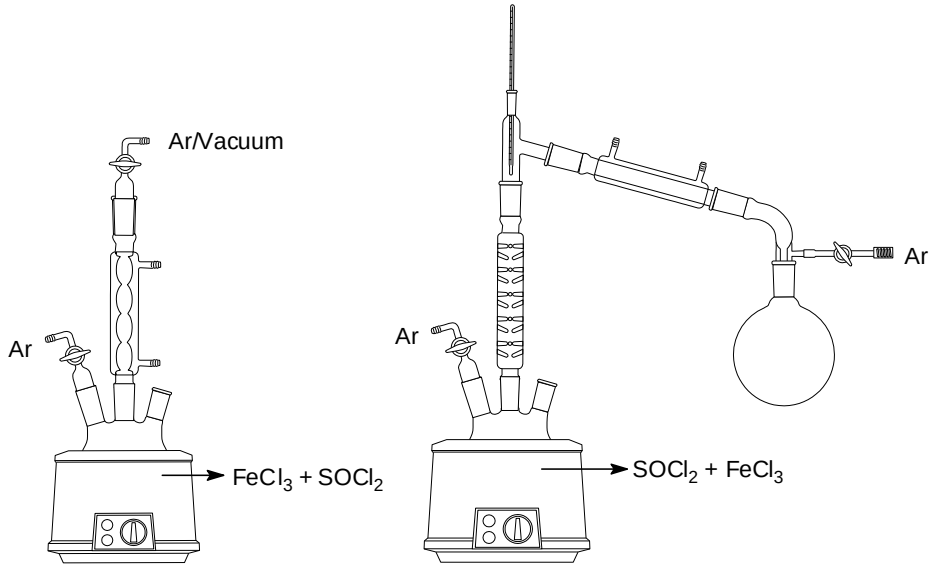

Figure 4-2: Purification of $FeCl_3$ with $SOCl_2$ (left), removing excess $SOCl_2$ (right).

4.4 Washing of $FeCl_3$

After the partial removal of $SOCl_2$ the mixture is transferred under Ar flow into an adapted chromatography column with a glass porous filter using glass cannulas as shown in Figure 4-3. Ar is applied at the 3-necked flask and at the round-bottomed flask. The second Ar inlet is used when changing the upper flask toward the next step. Make sure that the lowest Ar inlet is closed than because otherwise the $FeCl_3$ will be blown out of the dropping funnel. As long as Ar is applied the lower flask (containing $SOCl_2$) can be changed.

In the next step, using the same set-up and procedure, the $FeCl_3$ is washed with freshly dried pentane (dried over Na wire) to remove the remaining $SOCl_2$ (Figure 4-4). Make sure you use new clean/dry glass cannulas. Close the valve at the dropping funnel, add some pentane by twisting the 3-necked flask, shake carefully the entire setup, and remove the pentane by opening the valve. This handling must be done at least 3 times. (Ar 2 is again only used when adding/removing the

upper 3-necked flask). After washing, the upper three-necked flask is removed, as well as the lower round-bottomed flask containing the pentane. A clean round-bottomed flask and glass stopper is added (make sure the $FeCl_3$ always remain under inert atmosphere). Than apply a vacuum for a few hours to dry the $FeCl_3$.

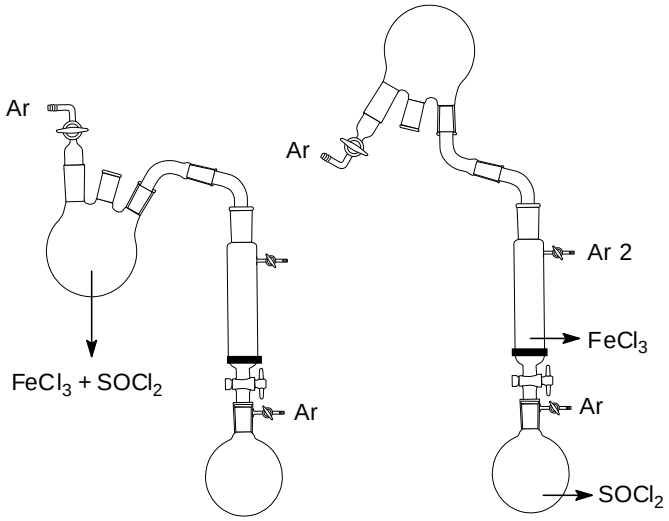

Figure 4-3: Transfer of $FeCl_3$ into the adapted chromatography column.

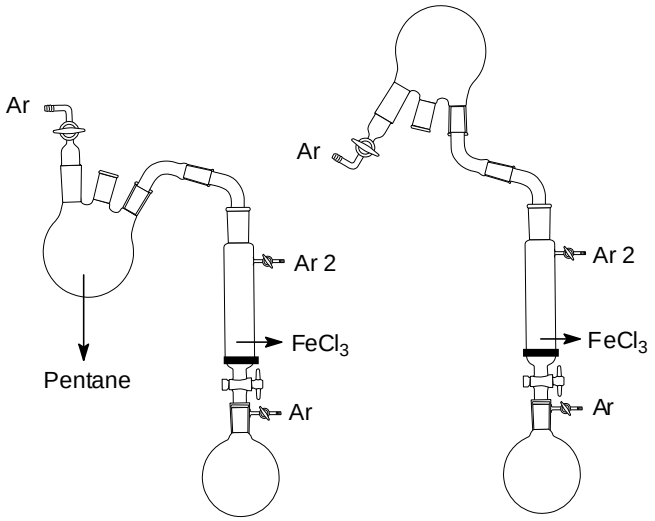

Figure 4-4: Washing of $FeCl_3$ with dry pentane.

4.5 Transfer $FeCl_3$ and storage

After drying the $FeCl_3$ is transferred into a dry and clean *Shlenk*-type storage flask by reversing the set-up. The flask is stored at ambient temperature tightly closed with a stopper and parafilm. When handling correctly and by making sure never air gets into the flask you can keep this $FeCl_3$ for years.

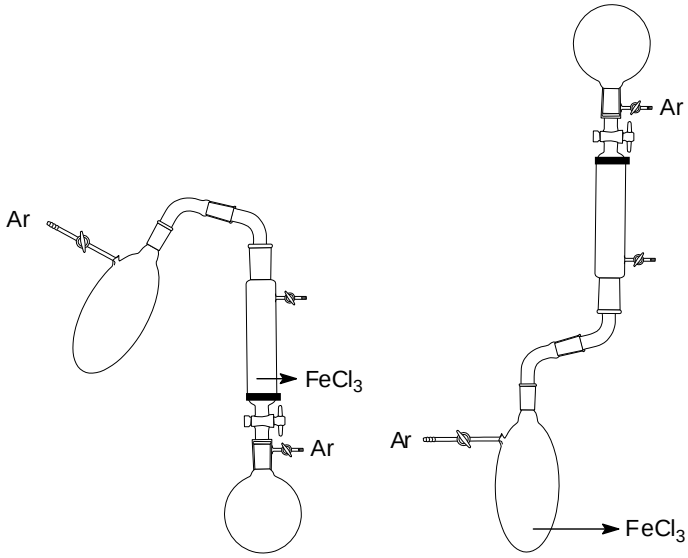

Figure 5-5: Transferring $FeCl_3$ into the storage flask.

4.6 Reference

1. Pray A. R., in: T. Moeller (Eds.), "Inorganic Synthesis" 5, Mcgraw-Hill Book company, New York, **1957**, 153-155.

Summary

Semiconducting polymers could perhaps have the greatest impact upon society through the development of polymer photovoltaic cells for power generation. The demand of energy has increased worldwide, mainly due to the development in areas like Asia and Africa. Currently this demand in energy is satisfied mainly by fossil fuels and nuclear power. However, these energy sources are limited and their use has a serious environmental impact. Therefore research toward renewable energy sources has increased in last decades. Among others, photovoltaics (PVs) offer great technological potential as a renewable, alternative source for electrical energy. Today Si-based solar cells are by far the most dominating type of PVs used and account for 99 % of all solar cells. However, to improve processability, lower manufacturing costs, and create flexibility, solar cells based on conjugated polymeric materials are extensively investigated during the last decade. The work described in this thesis focuses mainly on the design of low band gap polymers and their use in these plastic solar cells. A critical issue for this type of solar cells is the rather narrow absorption of the active layer. Since most of the available conjugated polymers were originally developed for visible-LEDs, they exhibit band gaps > 2 eV. Hence, there is a clear mismatch between the absorption spectrum of these materials and the terrestrial solar spectrum. The latter extends into the near infrared therefore, new low band gap materials with absorption extending to the 700-900 nm (Eg = 1.7 – 1.3 eV) region are needed for efficient photon harvesting.

In **Chapter One** a historical background of conjugated polymers as well as their semiconducting properties are discussed. Also the relation between the chemical structure of the polymer and the band gap is described and an overview of existing thiophene based low band gap polymers is given. Since all polymers were synthesized to serve in

plastic photovoltaic devices, this chapter ends with a brief discussion regarding plastic solar cells and their working principle.

Toward the synthesis of these low band gap polymers, basically two major approaches can be distinguished. The first one is the direct synthesis toward the conjugated polymer *via* oxidative or reductive coupling. The second approach, usually referred to as precursor route, is an indirect way to obtain conjugated polymers. In this approach, a non conjugated precursor polymer is converted into its conjugated form. In **Chapter Two**, a family of 6 polymers based on *bis*-(1-cyano-2-thienyl vinylene)phenylene is synthesized *via* the first approach. The structure consists of a central dialkoxyphenylene core (donor) *p*-disubstituted by two thiophene derivatives (donor) through a cyanovinylene linker (acceptor). The monomers were synthesized in good yields by applying a *Knoevenagel* condensation of a thiophene carboxaldehyde with an aromatic acetonitrile moiety. By changing the thiophene unit we were able to tune the polymers electronic and solubility properties. Moreover, our approach to keep the central core constant leads to a toolbox to create a whole range of monomers, and thus polymers, with different heteroaromatic rings linked to this central core. The polymers are prepared by chemical oxidation of the monomers using $FeCl_3$. Parameters like time and purification of $FeCl_3$ were studied in order to obtain the optimal polymerization conditions leading to soluble, high molecular weight polymers. For future reference, a comprehensive experimental procedure of the purification of $FeCl_3$ is given in the **Appendix**. The influence of the electron donor strength of the thiophene units was studied with UV-Vis absorption spectroscopy and cyclic voltammetry. It is shown clearly that the HOMO energy level decreases due to a decrease of the electron donor strength in the polymer. As a result hereof the band gap increases. In this work we were able to show that changing the substituents on the thiophene unit allows the modulation of the HOMO/ionization potential while changing the substituents on the central core has only little effect on the electronic properties. Efficient charge transfer is demonstrated in blends of the

polymers with PCBM by PL, PIA and LI-EPR measurements. However all solar cells made of the polymers showed only low efficiencies, which is related to the low hole mobilities observed in the pure polymer films. The introduction of a push-pull molecule as side chain is described in order to study the molecular orientation concept for plastic solar cells. Unfortunately, it was impossible to orient the polymer layer between the two electrodes.

A second way to come to processable polymers is the precursor approach, described in **Chapter Three**, which involve the formation of an intermediate non-conjugated, soluble and thus processable, precursor polymer which can be converted into the fully conjugated polymer after processing. The use of such a precursor approach implies the formation of a double bond between the aromatic parts. Based on earlier successful results, of all precursor routes, the dithiocarbamate route has been picked as the method of choice. In the first part of this chapter, the successful synthesis of two particular dithiocarbamate precursor polymers and the corresponding conjugated polymers, poly(3,4-diphenyl-2,5-thienylene vinylene) and poly(3,4-bis(4-butylphenyl)-2,5-thienylene vinylene), is described. The monomer preparation procedures were optimized and several polymerization conditions were studied, including changing the base from LDA to LHMDS. The latter gives rise to higher molecular weight polymers. As a result of the introduction of phenyl substituents, these polymers demonstrate an enhanced thermal stability as compared to PTV. Furthermore, they exhibit significantly improved λ_{max} values as compared to previous reports, indicating its improved purity and lower defect levels. Both polymers have a low band gap (1.7-1.8 eV) and can be reversibly p-doped. Primary solar cell measurements gave promising results.

In the second part, the thiophene unit is replaced by a thiazolo[5,4-*d*]thiazole unit. It is reported that this replacement is effective to reduce the sterical interactions due to the absence of

hydrogen atoms. However the attempt to synthesize this electron poor polymer via the dithiocarbamate precursor route failed.

Despite this last result, the dithiocarbamate precursor route still remains the best approach to synthesize PTV-derivatives and further research in our lab will disclose the scope and limitations of this route.

Samenvatting

Misschien hebben halfgeleidende polymeren wel de grootste impact op onze maatschappij via de ontwikkeling van polymere zonnecellen. De vraag naar energie is immers wereldwijd gestegen, hoofdzakelijk vanwege de ontwikkeling van gebieden zoals Azië en Afrika. Momenteel wordt deze vraag naar energie hoofdzakelijk tegemoetgekomen door het gebruik van fossiele brandstoffen en kernenergie. Nochtans, zijn deze energiebronnen beperkt en hun gebruik heeft een ernstige invloed op het milieu. Als alternatief voor de fossiele brandstoffen bezit de zon de nodige vereisten om door te gaan als ideale energiebron. Ze is gratis, betrouwbaar en onuitputtelijk. Het gebruik van zonnecellen is niet nieuw en vandaag de dag zijn silicium gebaseerde zonnecellen veruit het meest gebruikte type en vertegenwoordigen ze een marktaandeel van 99 %. De productiekost van deze anorganische zonnecellen is echter te hoog voor het gebruik ervan op grote schaal. Een nieuwe klasse van zonnecellen dringt zich dus op. Deze nieuwe zonnecellen zijn gebaseerd op organische halfgeleiders, waaronder geconjugeerde polymeren. Ze zijn potentieel goedkoper, gemakkelijker te produceren en vertonen mechanische flexibiliteit. Een nadeel van de organische zonnecel is echter de eerder smalle absorptieband van de actieve laag. Aangezien de meeste beschikbare geconjugeerde polymeren oorspronkelijk voor LEDs werden ontwikkeld, hebben zij band gaps die groter zijn dan 2 eV. Hierdoor is er een duidelijke mismatch tussen het absorptiespectrum van deze materialen en het emissiespectrum van de zon. Daarom zijn nieuwe low band gap materialen nodig met een absorptieband tot 700-900 nm (Eg = 1.7 – 1.3 eV). Het werk dat in deze thesis wordt beschreven focust hoofdzakelijk op het ontwerpen van low band gap polymeren en hun gebruik in organische zonnecellen

In **Hoofdstuk Een** wordt er een korte historische achtergrond van geconjugeerde polymeren geschetst evenals een bespreking van hun halfgeleidende eigenschappen. Ook wordt de relatie tussen de chemische structuur van het polymeer en de band gap beschreven, gevolgd door een overzicht van de bestaande op thiophene gebaseerde low band gap polymeren. Aangezien alle polymeren gesynthetiseerd worden om te dienen in organische zonnecellen, eindigt dit hoofdstuk met een korte bespreking van plastic zonnecellen en hun werkingsprincipe.

Voor de synthese van deze low band gap polymeren kan onderscheid gemaakt worden tussen twee belangrijke methodes. Een eerste is de directe synthese van het geconjugeerde polymeer via oxidatieve of reductieve koppeling. De tweede werkwijze, die vaak precursor route wordt genoemd, is een indirecte manier om geconjugeerde polymeren te verkrijgen. In deze aanpak wordt een niet geconjugeerd precursorpolymeer omgezet in zijn geconjugeerde vorm. In **Hoofdstuk Twee**, wordt een groep van 6 polymeren, gebaseerd op *bis*-(1-cyano-2-thienylvinyleen)fenyleen, gesynthetiseerd via de eerste methode. De structuur bestaat uit een centrale dialkoxyfenyleen kern (donor) para gesubstitueerd door twee thiofeen derivaten (donor) via een cyanovinyleen link (acceptor). De monomeren werden in goede opbrengsten bereid via een *Knoevenagel* condensatie tussen een thiofeen carboxaldehyde en een aromatische acetonitrile. Door de thiofeen groep te veranderen konden wij de elektronische en de oplosbaarheidseigenschappen van de polymeren regelen. Voorts leidt onze benadering om de centrale kern constant te houden tot een "toolbox" om zo tot een hele waaier van monomeren, en dus polymeren, met verschillende heteroaromatische ringen te komen. De polymeren werden bereid via oxidatieve polymerisatie van de monomeren met $FeCl_3$. Parameters zoals tijd en zuivering van $FeCl_3$ werden bestudeerd om zo de optimale polymerisatieomstandigheden te verkrijgen. Op die manier werden oplosbare en hoog moleculairgewichts polymeren bekomen Voor toekomstige gebruik, wordt een uitvoerige experimentele

procedure van de zuivering van $FeCl_3$ gegeven in de **Appendix**. De invloed van de sterkte van de elektrondonor eigenschappen van de thiofeen eenheden werd bestudeerd met UV-Vis absorptiespectroscopie en cyclische voltammetrie. Er werd duidelijk aangetoond dat de verlaging van de HOMO energieniveaus toe te schrijven is aan een daling van de sterkte van de elektrondonor in het polymeer. Als gevolg hiervan wordt de band gap groter. In dit werk konden wij aantonen dat het veranderen van de substituenten op de thiofeen eenheid de HOMO/ionisatie potentiaal van het polymeer wijzigt, terwijl het veranderen van de substituenten op de centrale kern slechts weinig effect heeft op de elektronische eigenschappen Efficiënte ladingsoverdracht werd aangetoond tussen de polymeren en PCBM door PL, PIA en Li-EPR metingen. Nochtans vertoonden alle zonnecellen die van de polymeren werden gemaakt slechts lage efficiënties. Dit komt waarschijnlijk door de lage ladingsmobiliteit die werd waargenomen in de polymeerfilms. De introductie van een "push-pull"-molecule als zijketen wordt beschreven om het moleculaire oriëntatie concept voor organische zonnecellen te bestuderen. Jammer genoeg, was het onmogelijk om de polymeerlaag tussen de twee elektroden te oriënteren.

Een tweede manier om tot geconjugeerde polymeren te komen is de precursor aanpak, zoals beschreven in **Hoofdstuk Drie**. Deze methode impliceert de vorming van een niet geconjugeerde precursor die oplosbaar en dus verwerkbaar is. Dit precursorpolymeer kan dan in zijn volledig geconjugeerde toestand worden omgezet via een thermische behandeling. Het gebruik van zo een precursor aanpak brengt de vorming van een dubbele binding tussen de aromatische delen met zich mee. Gebaseerd op vroegere succesvolle resultaten werd, van alle precursorroutes, de dithiocarbamate route gekozen. In het eerste deel van dit hoofdstuk, wordt de succesvolle synthese van twee dithiocarbamate precursorpolymeren en hun corresponderende geconjugeerde polymeren, poly(3,4-difenyl-2,5-thienyleen vinyleen) en poly(3,4-bis(4-butylfenyl)-2,5-thienyleen vinyleen) beschreven. De

procedures van de monomeersynthese zijn geoptimaliseerd en verscheidene polymerisatiecondities werden onderzocht, met inbegrip van de verandering van base van LDA naar LHMDS. Deze laatste leidt tot hogere moleculaire gewichten. Het resultaat van de invoering van de fenyl substituenten, is een verbeterde thermische stabiliteit van het geconjugeerd systeem in deze polymeren in vergelijking met PTV. Uit UV-vis metingen bleek dat beide polymeren een lage band gap (1.7 - 1.8 eV) bezitten. Voorts bezitten zij beduidend hogere λ_{max} waarden dan eerder beschreven waarden. Dit wijst op een grotere zuiverheid en minder defecten. Eerste zonnecelmetingen gaven dan ook veelbelovende resultaten.

In het tweede deel, wordt de thiofeen eenheid vervangen door een thiazolo[5.4-*d*]thiazool eenheid. Het is bekend dat deze vervanging de sterische interactie verminderd. Nochtans mislukte de poging om dit elektronarme polymeer via de dithiocarbamaat precursor route te synthetiseren.

Ondanks dit laatste resultaat, blijft de dithiocarbamaat precursorroute nog steeds veruit de beste route om PTV-derivaten te synthetiseren en verder onderzoek in ons laboratorium zal het bereik en de beperkingen van deze route uitdiepen.

List of publications

Colladet K., Nicolas M., Goris L., Lutsen L., Vanderzande D. - Low-band gap polymers for photovoltaic applications.- In: *Thin solid films*, 451/452 (**2004**), p. 7-11.

Henckens A., Colladet K., Fourier S., Cleij T.J., Lutsen L., Gelan J., Vanderzande D. - Synthesis of 3,4-diphenyl-substituted poly(thienylene vinylene) low-band-gap polymers via the dithiocarbamate route.- In: *Macromolecules*, 38:1 (**2005**), p. 19-26.

Vanderzande D., Lutsen L., Henckens A., Colladet K. - Method and preparing derivatives of polyarylene vinylene and method of preparing an electronic device including same. – *Patent* EP1529794.

Colladet K., Muhlbacher D., Lutsen L., Scharber M., Brabec C., Cleij TJ., Gelan J., Vanderzande D. - Soluble low band gap polymers for solar cell applications via oxidative polymerization. In: *Poly. Mater. Sci.Eng.*, 94 (**2006**), p. 426-427.

Colladet K, Lutsen L, Cleij TJ, Gelan J, Vanderzande D - Low band gap polymers via a new and versatile route: The dithiocarbamate precursor route. In: *Poly. Mater. Sci.Eng.*, 94 (**2006**), p.781-782.

Nguyen L., Günes S., Neugebauer H., Sariciftci S., Colladet K., Fourier S., Cleij T., Lutsen L.,Gelan J., Vanderzande D. – Side chain effects on photoinduced absorption and photovoltaic performance of low bandgap thienylene vinylene and phenylene vinylene copolymers. – In*: Eur. Phys. J. Appl. Phys.* 36:3, (**2006)**, 219.

Aguirre A., Janssen G., Goovaerts E., Colladet K., Vanderzande D., Lutsen L. - Optical and EPR spectroscopy in pure and blended films of a novel low band gap polymer. - In: *Eur. Phys. J. Appl. Phys.* 36:3, (**2006)**, 285.

Colladet K., Fourier S., Cleij T., Lutsen L.,Gelan J., Vanderzande D., Nguyen L., Neugebauer H., Sariciftci S., Aguirre A., Janssen G., Goovaerts E. - Low Band Gap Donor-Acceptor Conjugated Polymers towards Organic Solar Cells Applications. – In: *Macromolecules*, 40:1 (**2007**), p 65-72.

Dankwoord

Als je op deze pagina bent geraakt door alle voorgaande te lezen (proficiat daarvoor) zal je begrijpen dat ik ze onmogelijk allemaal heb kunnen schrijven zonder de hulp en inspiratie van anderen, die ik hieronder van harte wil bedanken.

In de eerste plaats wil ik Dirk Vanderzande, mijn promotor, bedanken. Bedankt voor het vertrouwen en de grote mate van vrijheid die je mij geschonken hebt. Ik wil je ook bedanken voor je wetenschappelijke kennis, maar zeker ook voor de toogpraat na het werk en de geweldige zeiltrip (nog een shotje ?).

De twee andere proffen van organische, Jan Gelan en Thomas Cleij verdienen ook een plaats in dit dankwoord. Jan, zonder jou en de financiën van het IUAP project was er niet eens een doctoraat geweest en Thomas, ik zal onze trip naar Atlanta niet licht vergeten. Ik proef de cajun gumbo en de crawfish boil nog steeds.

Peter Adriaensens wil ik bedanken voor het mij wegwijs maken in de wondere wereld van de NMR en Laurence Lutsen, I would like to

thank you for the effort you put in obtaining international projects and for sending our materials worldwide to the people who make devices.

Speaking of devices, a sincere word of thanks goes to the people from other labs who did spectroscopic measurements and made devices from my sometimes "strange" materials. Thanks to the people from the University Antwerp (Aranzazu Aguirre, Griet Janssen and Etienne Goovaerts), Konarka (David Muhlbacher and Christoph Brabec), LIOS (Le Huong Nguyen, Helmut Neugebauer and Serdar Sariciftci) and CEA (Alexandra Apostoluk and Carole Sentein). Without you and your data this thesis would not be the same. I am also very grateful to Marinella Catellani. I learnt a lot about the oxidative polymerization during my stay with you in Milan.

Het zijn niet enkel mensen uit andere labos die hun steentje hebben bijgedragen tot deze thesis. Huguette, bedankt voor de UV en IR metingen. Sofie bedankt voor de CV-metingen, Iris en Veerle voor de GPC analyses, Jan, bedankt voor de opnames van alle massaspectra. Tom, ik vind je elektronen analyses geweldig maar de stank die jij verspreidt verschrikkelijk. Zonder goede technische steun loopt het al snel fout in een labo daarom een speciaal woordje van dank aan Koen voor het fiksen van menig elektronisch probleem en voor de NMR opnames, Jos, de "glassblower", Christel voor de bestellingen en de snoepjes, Sali en de andere MATters voor het paraat houden van de infrastructuur en natuurlijk de femmes fatales van het SBG secretariaat.

Natuurlijk ben ik ook al mijn oude en huidige collega's dankbaar voor de geweldige sfeer in het labo en ver daarbuiten. Anja, Motmans, Hilde, Jos, Roel, Robby, Mael, Wojtek, Iris, Veerle, Liesbet, Zarina, Faty, Raoul, Steven, Wibren, Jérôme, Lien, Ine, Sofie, John, Palmy, Jean, Bert, Jimmy, Endy, Hanne, Joke en Fré, bedankt voor de hulp, de babbel, de voetbalmatchkes, de trips naar kapermolen, de 1 april grappen, de gouden liga, de laboweekendjes, het tooghangen, de lifts,

de bouw- trouw en babyperikelen, de kooksessies en de vele koffies. Dit geldt uiteraard ook voor de collega's van TOES en voor de anorganici.

Het thuisfront mag ook niet vergeten worden, Pa (neen ik kan nog altijd geen zonnecellen thuis op het dak komen leggen), Ma (bedankt voor het achter mijn veren zitten tijdens mijn studies) en Ruben (nog veel succes met uw uitvindingen) bedankt voor de steun. En natuurlijk, mijn vrouwke Inge, bedankt omdat je bent wie je bent… .

Grazie Mille !